



Kaunas University of Technology
Faculty of Mechanical Engineering and Design

Design of Vehicle Speed Enforcement System in Residential Areas
Master's Final Degree Project

Paulius Šatinskis
Project author

Lect. Darius Mažeika
Supervisor

Kaunas, 2023



Kaunas University of Technology
Faculty of Mechanical Engineering and Design

Design of Vehicle Speed Enforcement System in Residential Areas

Master's Final Degree Project

Mechatronics (6211EX017)

Paulius Šatinskis

Project author

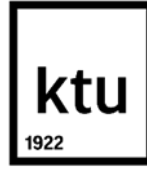
Lect. Darius Mažeika

Supervisor

**Assoc. prof. Rasa Kandrotaitė
Janutienė**

Reviewer

Kaunas, 2023



Kaunas University of Technology

Faculty of Mechanical Engineering and Design

Paulius Šatinskis

Design of Vehicle Speed Enforcement System in Residential Areas

Declaration of Academic Integrity

I confirm the following:

1. I have prepared the final degree project independently and honestly without any violations of the copyrights or other rights of others, following the provisions of the Law on Copyrights and Related Rights of the Republic of Lithuania, the Regulations on the Management and Transfer of Intellectual Property of Kaunas University of Technology (hereinafter – University) and the ethical requirements stipulated by the Code of Academic Ethics of the University;
2. All the data and research results provided in the final degree project are correct and obtained legally; none of the parts of this project are plagiarised from any printed or electronic sources; all the quotations and references provided in the text of the final degree project are indicated in the list of references;
3. I have not paid anyone any monetary funds for the final degree project or the parts thereof unless required by the law;
4. I understand that in the case of any discovery of the fact of dishonesty or violation of any rights of others, the academic penalties will be imposed on me under the procedure applied at the University; I will be expelled from the University and my final degree project can be submitted to the Office of the Ombudsperson for Academic Ethics and Procedures in the examination of a possible violation of academic ethics.

Paulius Šatinskis

Confirmed electronically



Kaunas University of Technology

Faculty of Mechanical Engineering and Design

Task of the Master's Final Degree Project

Given to the student – Paulius Šatinskis

1. Title of the Project

Design of Vehicle Speed Enforcement System in Residential Areas

(In English)

Transporto priemonių greičio kontrolės sistemos kūrimas gyvenamuosiuose rajonuose

(In Lithuanian)

2. Aim and Tasks of the Project

Aim: to design a piezo cable-based vehicle speed enforcement system in residential areas.

Tasks:

1. to compose a road structural element for speed measurement using piezo cables;
2. to conduct the selection of electronic components of the speed control system;
3. to evaluate the control logic for the speed control system;
4. to calculate the designed vehicle speed enforcement system estimate cost.

3. Main Requirements and Conditions

SolidWorks, PVDF copolymer cable, aluminum, silicone, oscilloscope, thermocouple.

4. Additional Requirements for the Project, Report and its Annexes

Not Applicable.

Project author	Paulius Šatinskis <i>(Name, Surname)</i>	<i>(Signature)</i>	2023.02.27 <i>(Date)</i>
Supervisor	Darius Mažeika <i>(Name, Surname)</i>	<i>(Signature)</i>	2023.02.27 <i>(Date)</i>
Head of study field programs	Regita Bendikienė <i>(Name, Surname)</i>	<i>(Signature)</i>	2023.02.27 <i>(Date)</i>

Šatinskis Paulius. Design of Vehicle Speed Enforcement System in Residential Areas. Master's Final Degree Project, supervisor lect. Darius Mažeika; Faculty of Mechanical Engineering and Design, Kaunas University of Technology.

Study field and area (study field group): Production and Manufacturing Engineering (E10), Engineering Sciences (E).

Keywords: Piezoelectric cable; voltage sensitivity; stiffness; bending; compression.

Kaunas, 2023. 68 p.

Summary

Camera-based speed enforcement systems have high costs, and for this reason, these systems are too expensive to be used in residential areas. This study designed a speed enforcement system for residential areas. The speed enforcement system's prototype consisted of three main components: a piezoelectric sensor, a control box, and traffic lights. The control box was equipped with electronic components: relays, programmable logic controller, and analog to digital converters. This study designed piezoelectric sensor construction, in which a piezoelectric cable was installed, and the sensor was constructed from an aluminum profile. This profile was used as a protective element for piezo cable from direct mechanical wear from vehicle tires and helped to attach the cable in the needed position on the road. Performed several voltage sensitivity tests for the designed piezoelectric sensor and tested two types of piezoelectric cables, different types of spacer elements, which helped to position the cable in the aluminum. Therefore, was performed a temperature test at 60°C. The obtained voltage sensitivity results revealed that the highest sensitivity of the piezoelectric sensor construction was obtained when the PVDF copolymer piezoelectric cable was used and when the spacer components were used from two-wire cables with a thermo tube. The mechanical stiffness tests as three-point flexural and compression tests revealed that construction was flexible and withstood 10 t loads. Moreover, the compression test and calculations revealed that the piezoelectric construction withstood 39 MPa compressing pressure, while the heavy truck created 4,3 MPa, static pressure, which was 9 times lower. The designed piezoelectric sensor construction investigation revealed that the sensor operated appropriately, obtained analog signal voltages were from 1 V to 9 V with the maximum vehicle speed of 70 km/h. These experiments were conducted to confirm that the sensor is reliable. In addition, the control logic of the speed enforcement system was evaluated and was calculated the estimated cost of the project prototype, which today's prices were more than twice lower compared with the fixed speed control camera system.

Šatinskis Paulius. Transporto priemonių greičio kontrolės sistemos kūrimas gyvenamuosiuose rajonuose. Magistro baigiamasis projektas, vadovas lekt. Darius Mažeika; Kauno technologijos universitetas, Mechanikos inžinerijos ir dizaino fakultetas.

Studijų kryptis ir sritis (studijų krypčių grupė): Gamybos inžinerija (E10), Inžinerijos mokslai (E).

Reikšminiai žodžiai: Pjezoelektrinis kabelis; įtampos jautrumas; standumas; lenkimas; gniuždymas.

Kaunas, 2023. 68 p.

Santrauka

Kameromis pagrįstos greičio kontrolės sistemos kainuoja brangiai, todėl šios sistemos yra per brangios, kad jas būtų galima naudoti gyvenamuosiuose rajonuose. Šiame darbe buvo sukurta greičio užtikrinimo sistema gyvenamiesiems rajonams. Greičio kontrolės sistemos prototipą sudarė trys pagrindiniai komponentai: pjezoelektrinis jutiklis, valdymo dėžė ir šviesoforai. Valdymo dėžėje buvo sumontuoti elektros komponentai: relės, programuojamas loginis valdiklis ir analoginiai-skaitmeniniai keitikliai. Šio tyrimo metu suprojektuota pjezoelektrinio jutiklio konstrukcija, kurioje buvo sumontuotas pjezoelektrinis kabelis, o jutiklio korpusas pagamintas iš aliuminio profilio. Šis profilis buvo naudojamas, kaip pjezo kabelio apsauginis elementas, kuris apsaugojo nuo tiesioginio mechaninio transporto priemonių padangų pažeidimo, taip pat užtikrino tinkamą pritvirtinimą reikiamoje kelio dalyje. Atlikti keli suprojektuoto pjezoelektrinio jutiklio įtampos jautrumo bandymai ir išbandyti dviejų tipų pjezoelektriniai kabeliai bei skirtingų tipų tarpiklių elementai, kurie padėjo tinkamai pozicionuoti kabelį aliuminio profilyje. Taip pat buvo atliktas temperatūrinis bandymas 60°C temperatūroje. Gauti įtampos jautrumo rezultatai atskleidė, kad didžiausias pjezoelektrinio jutiklio konstrukcijos jautrumas buvo gautas naudojant PVDF kopolimerinį pjezoelektrinį kabelį ir kai tarpiklių komponentai buvo panaudoti iš dviejų laidų kabelio su temperatūriniu vamzdeliu. Mechaninio standumo bandymai, tokie kaip tritaškio lenkimo ir gniuždymo, parodė, kad konstrukcija buvo lanksti ir atlaikė 10 t apkrovas. Be to, gniuždymo bandymas ir skaičiavimai atskleidė, kad pjezoelektrinė konstrukcija atlaikė 39 MPa gniuždymo slėgį, o sunkvežimis sukūrė 4,3 MPa statinį slėgį, kuris buvo 9 kartus mažesnis. Suprojektuotas pjezoelektrinio jutiklio konstrukcijos tyrimas parodė, kad jutiklis veikė tinkamai, gautos analoginio signalo įtampos svyravo nuo 1 V iki 9 V, kai didžiausias automobilio greitis buvo 70 km/h. Šie eksperimentai buvo atlikti siekiant patvirtinti, kad jutiklis yra patikimas. Be to, buvo įvertinta greičio kontrolės sistemos valdymo logika ir apskaičiuota numatoma projekto prototipo šiandienos kaina, kuri buvo daugiau nei du kartus mažesnė lyginant su fiksuota greičio kontrolės kamerų sistema.

Table of Contents

List of Figures	9
List of Tables.....	12
List of Abbreviations and Terms	13
Introduction	14
1. Literature Analysis of Vehicle Speed Enforcement Systems and Related Devices	15
1.1. Review of Speed Enforcement Methods	16
1.1.1. Speed Calming Measures and Speed Bumps	16
1.1.2. Adaptable Speed Bumps.....	18
1.1.3. Speed Enforcement Systems with Cameras	19
1.2. Review of Sensor-Based Systems Used in Traffic Control.....	20
1.2.1. Magnetic Field Sensors for Vehicle Detection.....	20
1.2.2. Piezoelectric Harvesters of Electrical Energy	23
1.2.3. Cement-Based Piezoelectric Sensor System for Vehicle Speed Measurement.....	25
1.2.4. Piezoelectric Cables for Traffic Monitoring.....	27
1.3. Summary of the Chapter.....	30
2. Methodology for Selecting the Design of Piezoelectric Road Structural Element	31
2.1. Selection Method of Piezoelectric Cable Type	31
2.2. Method of Dynamic Load Impact Generation.....	33
2.3. Methodology of Three-Point Flexural and Compression Test.....	34
2.4. Selection of Protective Surface for Selected Piezoelectric Cable	36
2.5. Calculation of the Static Pressure Load from a Vehicle.....	37
2.6. Selection of a Testing Method for Designed Piezoelectric Road Structural Element.....	38
2.7. Summary of the Chapter.....	38
3. Investigation of Speed Enforcement System Road Structural Element and Selection of Electronic Components and Control	39
3.1. Experimental Investigation and Design of Speed Enforcement System Road Structural Element.....	39
3.1.1. Experimental Selection of Piezoelectric Cable Type	39
3.1.2. Experimental Selection of Spacer Structure Type for Piezoelectric Sensor	42
3.1.3. Temperature Impact for Piezoelectric Sensor Sensitivity	43
3.1.4. Completed Construction of Piezoelectric Sensor	45
3.1.5. Three-Point Flexural Bending Test of the Piezoelectric Sensor	46
3.1.6. Compression Test of the Piezoelectric Sensor	47
3.1.7. Actual Test on the Road with the Vehicles	49
3.1.8. Comparison of Designed Piezoelectric Sensor Construction Results with Other Authors ...	53
3.2. Selection of Electronic Components for the Speed Control System Prototype	54
3.2.1. Selection of Analog Input / Digital Output Converter	54
3.2.2. Selection of Traffic Light Element.....	54
3.2.3. Selection of Relay Element for Traffic Light Lamp Switching	55
3.2.4. Selection of Control Unit Module	55
3.2.5. Circuit Prototype of Electronic Components	56
3.3. Control Logic Evaluation for the Speed Enforcement System Prototype.....	57
3.3.1. Main Assumptions for the Speed Control System Logic	58

3.3.2. Operation Algorithm of the Speed Control System Prototype.....	59
3.3.3. Simulation of Code in the Tinkercad Environment.....	60
3.4. Summary of the Chapter.....	61
4. Cost Estimation of the Speed Enforcement System	62
4.1. The Cost Estimation of Each Component	62
4.2. Labor Cost Estimation.....	63
4.3. Summary of the Chapter.....	63
Conclusions	64
Recommendations.....	65
List of References.....	66
Appendices	69
Appendix 1. Detailed Scheme of the Algorithm	69
Appendix 2. Detailed Scheme of the Algorithm (continuation).....	70
Appendix 3. C++ code.....	71
Appendix 4. Electronic Scheme from the Tinkercad Environment.....	74

List of Figures

Fig. 1. Effectiveness of speed calming measures [8]	17
Fig. 2. Different speed bump shapes used on roads [9]	18
Fig. 3. The prototype of an adaptable speed bump with license plate recognition [10].....	18
Fig. 4. Fixed speed camera in Norway [11]	19
Fig. 5. Average speed control system scheme [11].....	20
Fig. 6. Scheme of the components used [13]	21
Fig. 7. The magnitudes of the magnetic field in X position (dashed line is sensor one magnitude, another line is sensor two magnitude) [13]	21
Fig. 8. Measuring system placed on a road [14]	22
Fig. 9. The measuring system located on the road [14]	22
Fig. 10. Piezoelectric transducer layout side view (left) and top view (right) [16].....	23
Fig. 11. Exploded view of a single piezoelectric transducer [16]	24
Fig. 12. The piezoelectric unit from PZT-5H elements (a) and both isometric and top views of piezoelectric harvester box (b) [17].....	24
Fig. 13. Obtained results of open circuit peak voltage with different speeds of the vehicle [17].....	25
Fig. 14. The PMN ceramic cement-based sensor [18]	26
Fig. 15. Placement of the traffic monitoring system in the road (a) top view and (b) side view [18]	26
Fig. 16. Schemes of used piezoelectric sensors: a) PZT ceramics and b) PVDF cable [19].....	27
Fig. 17. Piezo cable for speed evaluation and axle counting [20].....	28
Fig. 18. Output signal from the piezoelectric sensor [20]	28
Fig. 19. Speed enforcement system of piezo cables and camera unit [21].....	29
Fig. 20. The model of the speed measuring system [22].....	29
Fig. 21. Virtual front panel for speed estimation and vehicle type determination [22]	30
Fig. 22. The scheme of piezoelectric speed enforcement system. 1 – Traffic light, 2 – Piezoelectric sensor, 3 – Control box.....	31
Fig. 23. The forces with directions, which affect piezoelectric element: polarization is usually defined as coinciding with Z – the axis, other numbers are the indicators according to the axis 1, 2, 3, also shear directions about each ax 4, 5, 6 [23].....	32
Fig. 24. Scheme of PVDF copolymer cable (left) and PVDF spiral tape cable (right) [24]	32
Fig. 25. Scheme of a drop test device. 1 – Ruler, 2 – Guides for the carriage of mass, 3 – Mass with an accelerometer for dynamic force evaluation, 4 - Table for piezoelectric cables, 5 – Springs for the carriage of mass, the arrow indicates the direction of falling mass [24]	33
Fig. 26. Designed punching device for a drop test for piezoelectric cables (left) and the clamp (right) fitting part. 1 – Guide for a dropping mass, 2 – Aluminum frame, 3 – Mass of 0,5 kg, 4 – Clamp, 5 – Aluminum rectangle profile 20x10x2 mm, 6 – Aluminum profile 30x2 mm, 7 – Rivets	34
Fig. 27. Three-point flexural test scheme [25]	34
Fig. 28. Bending force and deflection diagram [25]	35
Fig. 29. Compressive load and deformation diagram with examples of specimen [26]	35
Fig. 30. Selected aluminum profile for piezo cable protection, raw profile (left) and after cut profile (right).....	36
Fig. 31. Structures for piezo cable stabilization in aluminum profile, structure with silicone and rubber spacer (left), and structure with thermo tube and isolated cable with two wires used as a	

spacer (right). 1 – Piezo cable, 2 – Silicone layer, 3 – Rubber, 4 – Aluminum profile, 5 – Thermo tube, 6 – Isolated cable with two wires	36
Fig. 32. Set-up schematic view of test for piezo cable type selection. 1 – Punching device, 2 – Piezoelectric cable, 3 – Oscilloscope PicoScope3424, 4 – PC, 5 – Thermocouple, 6 – Digital multimeter CHY 24CS LCR.....	39
Fig. 33. Set-up view of the experiment for piezo cable type selection (top). 1 – Punching device, 2 – Piezo cable structure, 3 – Oscilloscope PicoScope3424, 4 – PC, 5 – Thermocouple, 6 – Digital multimeter CHY 24CS LCR. Connection to piezoelectric cable (below left) and cable installation with a fitting part in clamps (below right).....	40
Fig. 34. Captured graphs from oscilloscope by PicoScope6 software. PVDF spiral tape cable voltage (left) and PVDF copolymer cable voltage (right).....	41
Fig. 35. Obtained results from both types of piezoelectric cables	41
Fig. 36. Piezoelectric construction spacer material sample with thermo tube and two-wired cable (left) and another sample with rubber and silicone layer (right)	42
Fig. 37. Set-up schematic view (left) and set-up view (right). 1 – Punching device, 2 – Piezo sensor structure, 3 – Oscilloscope PicoScope3424, 4 – PC.....	42
Fig. 38. Obtained results of the experiment for the selection of piezoelectric sensor spacer material	43
Fig. 39. Set-up schematic view of test for temperature test (left) and set-up (right). 1 – Punching device, 2 – Piezo cable structure, 3 – Oscilloscope PicoScope3424, 4 – PC, 5 – Thermocouple, 6 – Digital multimeter CHY 24CS LCR, 7 – Electric heater HG-1500-CG1	44
Fig. 40. Results of temperature experiment using selected piezoelectric sensor construction	44
Fig. 41. Exploded view of the piezoelectric sensor construction. 1 – Rivet DIN7337 3,2x6, 2 – Bolt DIN7985 M4x6, 3 – Aluminum profile with holes, 4 – Thermo tube, 5 – Cable with two wires, 6 – Piezoelectric cable, 7 – Two aluminum tapes, 10x2, 8 – Nut DIN934 M4, 9 – Aluminum profile without holes	45
Fig. 42. Assembled piezoelectric sensor construction. Isometric view in SolidWorks environment (left) and actual sample for the experiments (middle), the same sample with the visible gap (right).....	45
Fig. 43. Set-up schematic view of the bending test (left) and set-up (right). 1 – Force measuring sensor DBBSTOL – 10 kN, 2 – Specimen of the piezoelectric sensor, 3 – Fixed stands, 4 – Moving stand.....	46
Fig. 44. Obtained results of the three-point flexural bending test, bending force versus displacement.....	46
Fig. 45. Appeared crack in the piezoelectric construction when the ultimate tensile force was reached.....	47
Fig. 46. Set-up schematic view of the compression test with the universal testing machine (left) and set-up view (right). 1 – Force transducer Kraftwufnehmer Typ U5 100 kN, 2 – Upper fixed plate, 3 – Lower moving plate, 4 – Specimen of piezoelectric sensor	47
Fig. 47. Obtained results of compression test, compression force versus displacement.....	48
Fig. 48. Deformed top surface edge of the aluminum profile (marked red)	48
Fig. 49. Fixation of piezoelectric sensors with anchoring screws (marked red) on the road pavement	49
Fig. 50. Set-up schematic view (left) and set-up view (right). 1 – Piezo sensor_1, 2 – Piezo sensor_2, 3 – Oscilloscope PicoScope3424, 4 – PC	50
Fig. 51. Captured graphical result from a car with a speed of 40 km/h	50
Fig. 52. Captured graphical result from a motorcycle with a speed of 40 km/h.....	51

Fig. 53. Captured graphical result from a tractor with a speed of 25 km/h.....	52
Fig. 54. Obtained results from experiments with vehicles, voltage versus velocity	52
Fig. 55. Vector scheme. <i>1</i> – Vehicle tire, <i>2</i> – Piezoelectric sensor construction, <i>a</i> – Dynamic load vector component, <i>b</i> – Static load vector component, <i>a + b</i> – Sum of load vector from a vehicle .	53
Fig. 56. PRECISION 4- 1/2 DIGIT, ADC analog to digital converter [28]	54
Fig. 57. Industrial relay RV8H 1CO DC 24V 6A with spring clamp terminal [31]	55
Fig. 58. Selected PLC modules. <i>1</i> – Power supply module, <i>2</i> – CPU, <i>3</i> – Digital input module, <i>4</i> – Digital output module [32]	56
Fig. 59. Schematic view of the speed enforcement system electronic components and wiring (dashed line). <i>1</i> – Piezo sensor_1, <i>2</i> – Piezo sensor_2, <i>3</i> – Piezo sensor_3, <i>4</i> – Piezo sensor_4, <i>5</i> – Traffic light_1, <i>6</i> – Traffic light_2, <i>7</i> – Controller box.....	56
Fig. 60. Circuit prototype of the electronic components. <i>1</i> – Traffic light, <i>2</i> – Relay, <i>3</i> – PLC, <i>4</i> – Analog-to-digital converter, <i>5</i> – Piezo sensor. Wires: Brown – Phase, Blue – Neutral, Red – Analog signal terminal, Black – Ground, Yellow – Digital input, Green – Digital output.....	57
Fig. 61. Schematic view of the speed enforcement system prototype electronic components and wiring (dashed line). <i>1</i> – Piezo sensor_1, <i>2</i> – Piezo sensor_2, <i>3</i> – Piezo sensor_3, <i>4</i> – Piezo sensor_4, <i>5</i> – Traffic light_1, <i>6</i> – Traffic light_2, <i>7</i> – Controller box, <i>W</i> – is the distance between piezo sensors, <i>L</i> – is the distance between last piezo sensor and traffic light	58
Fig. 62. Simplified scheme of operation algorithm.....	59
Fig. 63. Circuit of the prototype in Tinkercad environment. <i>1</i> – Arduino Uno R3, <i>2</i> – LED lamp as traffic light_1, <i>3</i> – LED lamps as traffic light_2, <i>4</i> – Resistor, <i>5</i> – Analog pushbutton as piezo sensor_1, <i>6</i> – Analog pushbutton as piezo sensor_2, <i>7</i> – Analog pushbutton as piezo sensor_3, <i>8</i> – Analog pushbutton as piezo sensor_4	60

List of Tables

Table 1. Typical properties of the cables [24]	33
Table 2. Cost of each component of the speed enforcement system	62
Table 3. Labor cost for preparing the project and assembling.....	63

List of Abbreviations and Terms

Abbreviations:

PZT – Lead Zirconate Titanate;
PVDF – Polyvinylidene fluoride;
AMR – Anisotropic Magneto Resistance;
PMN – Lead Magnesium Niobate;
DC – Direct Current;
AC – Alternating Current;
CPU – Central Processing Unit.

Terms:

Specimen – that portion of a sample taken for evaluation of some specific characteristic or property.

Buckling – the sudden change in shape (deformation) of a structural component under load, such as the bowing of column under compression or the wrinkling of a plate under shear.

Introduction

Today's quality of life is better than ever because the scientific community has created many innovative inventions and discoveries adapted to today's industry, medicine, and fields of science. As life quality is improved, many enterprises are expanding around the main cities of the countries. Today in developed countries, employed people travel to work by vehicles such as trains, metro, cars, busses, trolleys, and even bicycles or motorcycles. The vehicles driven on the roads create traffic jams and car accidents when people come home from work. Many drivers rush to get from point A to point B as fast as possible, and they do not realize that in traffic, they are not alone, many other people are driving, and many fatal car crashes occur from exceeding the allowed speed limit. In order to avoid fatal car accidents on roads, speed calming measures such as speed bumps, road narrowings, chicanes, and speed tables are used. Although the speed calming measures reduce the speed of vehicles efficiently, the drivers must reduce their speed drastically to drive comfortably through the speed bump. Therefore, it does not matter what the time of the day is, if there are other drivers on the road or not, they still must reduce their speed, and each driving through the speed bump wears out the suspension and brakes additionally. Therefore, many speed enforcement systems with fixed speed and average speed cameras are used in cities. These systems are efficient only in the active field range. The fixed speed camera's field range varies from 50 m to a few hundred meters, while average speed cameras can measure the speed in distances of kilometers. However, the violator, which exceeds the speed limit, can avoid the violation bill by simply waiting on the corner of the road or just turning to another street in the middle of the measuring road section and passing the average speed enforcement system. Many of these systems are used in cities or highways because the government subsidizes those regions for the investigations applied in statistics of fatal car accidents and heavy traffics. However, residential areas are not subsidized as much as cities because there is not much traffic and fatal car accidents. However, fatal car accidents still occur in residential areas, and residents can not feel safe. For this reason, it is almost impossible to acquire expensive speed enforcement systems. This work aims to design a piezo cable-based vehicle speed enforcement system in residential areas, which would have a lower price than a camera-based speed enforcement system that people living in residential areas could afford to purchase and would have low-cost maintenance. Furthermore, this study will suggest a novel speed enforcement system prototype, which will not punish the speed-exceeding violators but will ensure the control of the speed on the road section by switching colors of the traffic light if the speed is exceeded. This research will provide a novel use of a low-cost sensor-based speed enforcement system in residential areas.

Aim: to design a piezo cable-based vehicle speed enforcement system in residential areas.

Tasks:

1. to compose a road structural element for speed measurement using piezo cables;
2. to conduct the selection of electronic components of the speed control system;
3. to evaluate the control logic for the speed control system;
4. to calculate the designed vehicle speed enforcement system estimate cost.

Hypothesis: Novel piezo cable-based vehicle speed enforcement system has low cost and is affordable for residential areas community.

1. Literature Analysis of Vehicle Speed Enforcement Systems and Related Devices

Nowadays, vehicle speed enforcement systems and devices are essential in highway roads, cities, or even residential area roads. Safety on the road depends on many unknown and unpredictable situations, such as slippery roads, poor road visibility at nighttime or daytime, vehicle speed, and the driver's emotional and physical condition. However, all these situations while driving depend on the vehicle's speed. Therefore, exceeding the speed, the vehicle becomes unstable on a slippery road, the driver reacts to an obstacle much slower due to poor visibility, or the driver becomes tired and has less time to reduce speed while the speed is high. Therefore, control of the vehicle's speed on the road is mandatory because the higher the speed, the worse the car accident. Recent research shows that when the vehicle's speed is higher than 30 km/h, the risk of getting fatally injured in a car accident increases exponentially [1]. For example, in Europe, in 2019, 4628 pedestrians were in car accidents compared to 7 years earlier, died 35 000 people [1]. For this reason, automotive manufacturers are producing much safer vehicles and, step by step, increasing vehicle speed control importance on roads for safe driving assurance. Therefore, the relevance of vehicle speed control in our society is crucial.

Although the most straightforward and cheapest method to control the traffic flow and its velocity is to place the speed limit sign on the side of the road, it is insufficient and does not guarantee the desired speed limit [1]. To be sufficient to fulfill a purpose, there are widely used speed control measures divided into two categories: calming speed measures and speed enforcement systems. Road obstacles such as road humps, speed cushions, speed tables, road width restrictions, lane width restrictions, gateways/entry points, and others belong to the category of speed calming measures [2]. Previously mentioned examples are usually installed on the road pavement and kept permanently. Some of these objects on the road are obstacles with low projected heights that vehicles can pass through or drive around. In this case, the driver must reduce the speed to pass through it, which is how the speed is reduced. Speed calming measures are most efficient in low-speed zones at 30 km/h, and these speed controls allow speed reduction from 9 km/h to 10 km/h [2]. Systems such as average speed control, fixed speed cameras, and portable speed cameras belong to the category of speed enforcement systems. These systems are adaptive and can be set to any speed value, which is prohibited from exceeding for drivers. They have a small tolerance, which vehicles can exceed in speed percentage parts. However, when the tolerance value is reached, the penalty bill is sent to the vehicle's owner for the violation because these systems capture each vehicle's number plate each time. The efficiency of the fixed speed camera is noticeable on highway roads, where the speed limit is 120 km/h. 42% of drivers tend to reduce vehicle speed by approximately 30 km/h or even more [3]. Although speed enforcement systems have a higher efficiency on traffic speed control than other previously mentioned traffic calming measures, they are effective in the active working location. Drivers usually reduce the speed near the active camera range, where they can capture the speed, and after that, they usually increase the speed after the active camera range [3]. The investigations [1, 2, 3] prove that speed control systems and devices are reliable and relevant for reducing and controlling traffic flow and speed in needed locations.

Furthermore, atmosphere pollution is directly dependent on CO₂ emissions emitted by vehicles. This topic is relevant because the higher the velocity vehicle reaches, the more fossil fuel it needs to burn and the more pollution particles it emits into the atmosphere. Investigations show that if velocities in the autobahns were reduced to 120 km/h, there would be a 50 % traffic flow rate reduced and a 7,43 % drop in CO₂ emissions in the atmosphere, which is about 9796 tons [4]. If

each vehicle reached 60 km/h speed on the road, it would lead to a 28 % drop in CO₂ emissions [4]. Therefore, investigations show that controlling vehicle speed on the road is one of the key factors in solving the global problem of pollution reduction.

Speed calming measures have a simple construction, and people create novel inventions, for example, there are many modifications of speed bumps. One novel research [5] used a speed bump as a self-powered vehicle and pedestrian warning system. The speed bump was produced from PVC material and anchored on the pavement next to the parking lot. The main idea was that the speed bump would generate electricity each time the vehicle passed. The generated electricity was used to power the warning system with light. It warned pedestrians to stop and look around for vehicles. These speed bumps were also called “energy harvesters.” Another novel research was focused on energy harvesting [6]. This speed bump was created with a slider–crank mechanism, so it helped to convert speed bump vertical movement to rotational movement and to rotate the shaft connected to the generator. Generated electricity was a green energy source that could be used for streetlights.

Moreover, piezoelectric transducers have the potential for wide usage for speed control. Mainly, on the road for vehicle identification are used two types of piezoelectric sensors. They are made from zirconate titanate (PZT), which is a piezoelectric ceramic material, and another type of cable is semi-crystalline plastic polyvinylidene fluoride (PVDF) [7]. These sensors also can be called energy harvesters because they create a voltage when mechanically deformed. It is essential to mention that this phenomenon of piezo ceramics is reversible. When the voltage is supplied to the piezoelectric transducer, it deforms its form. As a result, piezoelectric sensors are embedded into the road pavement.

The speed enforcement system’s novelty and relevance proved that more investigations must be done to solve the drawbacks of the existing speed control systems and devices. For example, speed calming measures such as speed humps installed into the road pavement permanently, all the time damage the vehicle’s chassis, as suspension also brakes, because each time the vehicle must reduce its speed. Also, speed enforcement systems such as fixed speed cameras or average speed cameras are expensive and additional staff are needed to work with data obtained from speed violators. Moreover, speed enforcement systems are usually not used in residential areas, where the speeds are 30 km/h, because there are not many vehicle users, so it is too expensive to maintain these systems in such areas. So, there is a cheaper solution for speed measuring and identification with piezoelectric transducers, but there is a need to design and investigate the cable placement type on the pavement. For this reason, deeper literature analysis must be investigated to understand the methods used in speed measuring and control and to complete the given tasks for this project.

1.1. Review of Speed Enforcement Methods

This section of the chapter will present speed enforcement methods, consisting of speed calming measures and camera-based speed enforcement systems. The advantages and disadvantages of each speed enforcement method will be reviewed, which are broadly used on roads.

1.1.1. Speed Calming Measures and Speed Bumps

The primary method of speed calming is the implementation of physical obstacles on the roads, such as speed bumps, speed tables, chicanes, or road narrowings. Installing speed calming measures in urban areas where many pedestrians are crossing the roads is a systematically controllable way to

reduce driving velocities. The efficiency in vehicle speed reduction by traffic calming measures was researched by N. Distefano and S. Leonardi [8]. This paper evaluated three types of speed-calming measures: speed table, chicane, and road narrowing. They decided to obtain vehicle speed data before and after installing speed calming measures on three streets for investigation. The results of obtained data are shown in Fig. 1. The results showed that chicane and speed tables achieve the highest speed reduction. Speed tables reduced from 40 % to 48 % of average street speed, and the chicane reduced even more than 50 % of average vehicle speed. Road narrowings, about 33 %, achieved a minor change in speed reduction.

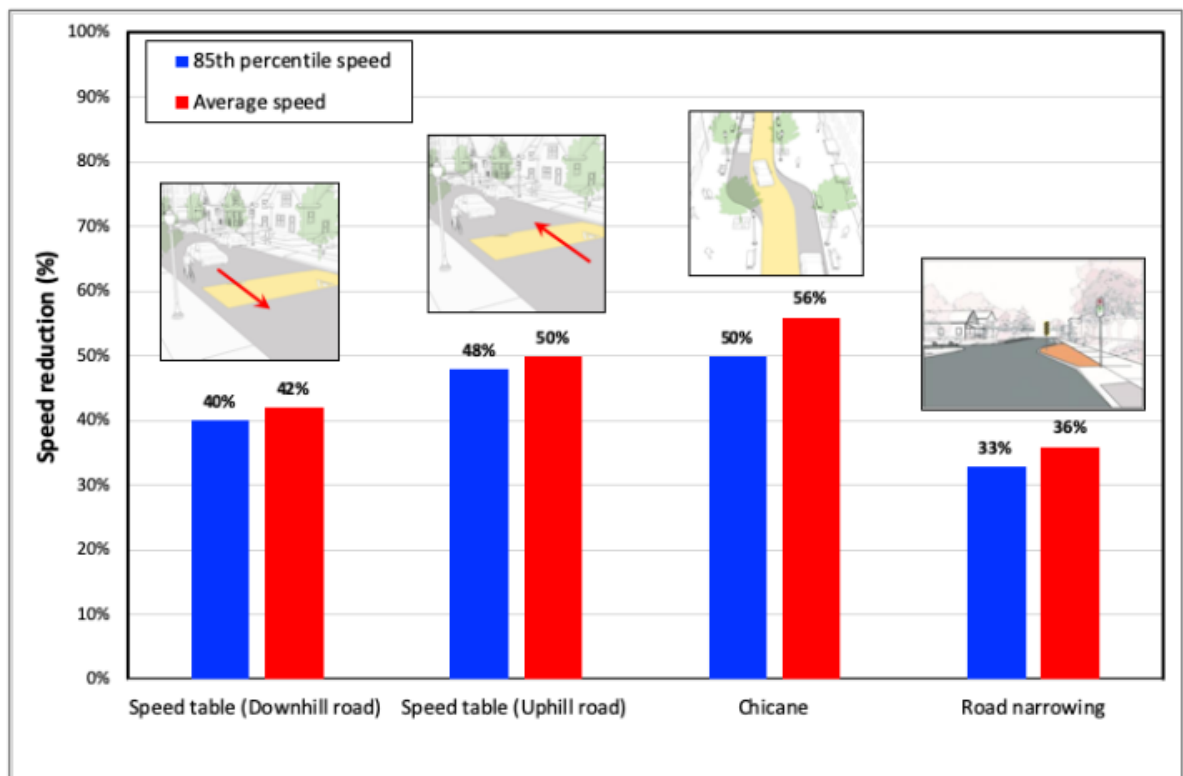


Fig. 1. Effectiveness of speed calming measures [8]

Regarding people getting injured in these streets, percentage values decreased significantly. Speed tables reduced the injured people in that street by 40 %, chicane by 50 %, and road narrowings by 32 % [8]. The results showed that the speed calming devices effectively and efficiently reduce speeds in urban areas.

Another speed-calming measure most frequently used is the speed bump, which is used in residential areas, where the speeds must be kept low to about 30 km/h. Speed bump significantly impacts vehicle velocity reduction and control near schools and other facilities with high pedestrian flow [9]. This speed-calming device helps to reduce the speed effectively because the faster the vehicle drives through it, the more brutal vertical motion is obtained, so the discomfort feeling is created for the driver. Also, the speed bump might damage the vehicle chassis from obtained vertical reaction force motion. Therefore, speed bumps are installed on the road pavement or surface like other speed calming measures. Usually, on road surfaces, speed bumps are used in different shapes (Fig. 2).

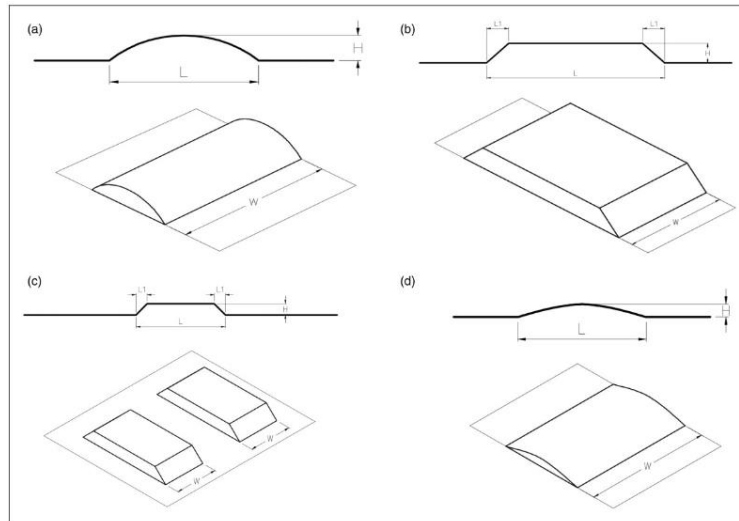


Fig. 2. Different speed bump shapes used on roads [9]

The speed bump shapes are divided into rounded (*a* and *d*) and trapezoidal (*b* and *c*). Usually, rounded shape speed bump L dimension varies from 0,3 to 1,5 m. On the other hand, trapezoidal shape speed bumps L dimension varies from 3,7 to 4,3 m [9]. The smaller the length of the L dimension, the faster through the speed bump vehicle can drive. In this case, the only way to pass through the trapezoidal speed bump with the lowest discomfort in the vehicle is to drive through it at a low speed. On the other hand, the speed bumps can be installed in full-length segments with a distance between them (Fig. 2 *c* and *d*). The latter installation type of speed bump is used for emergency services, that the vehicle could fit in that gap between the segments of a speed bump, and for that, emergency vehicles can drive through the speed bumps at higher velocities [9].

1.1.2. Adaptable Speed Bumps

As previously mentioned, speed bumps are used in slower-traffic roads, in residential areas near the neighborhood of hospitals, at intersections where two roads cross, or in parking lots. These devices help to reduce speed and to reduce accidents in traffic. However, they create discomfort for the passengers and driver while they drive through it, and near the hospitals where many ambulance transport drive through the speed bumps, the patients inside the ambulance vehicle also feel discomfort. There was a proposed solution to this problem by investigating intelligent speed bumps with license plate recognition and adaptable speed bump hardness [10]. The prototype creators presented an adaptable speed bump embedded in the road with springs under it, pressure sensors on the road for speed measuring, and a camera and electromagnetic holder (Fig. 3).



Fig. 3. The prototype of an adaptable speed bump with license plate recognition [10]

The main idea of this project was that vehicle license plate data from emergency service is stored in the server, and when the ambulance drives at high speed through the pressure sensors, the received signals in the controller show the time difference, and the vehicle's speed is calculated. If the speed is exceeded, but there is an ambulance vehicle, the electromagnetic holder will not be activated, and driving through the speed bump will be comfortable and soft. The same situation would appear with any other vehicle but driving and not exceeding the speed limit. The recognition is recorded by a video camera capturing the license plate picture. Obtained letters and numbers from the picture are checked in the database and searched for any match of the emergency vehicle. If any other vehicle drives over the speed limit, the electromagnetic holder is activated, the speed bump position is rigid and stable, and the driver feels the same discomfort as from the regular speed bump.

1.1.3. Speed Enforcement Systems with Cameras

Speed enforcement systems are camera-based systems that take a picture of a vehicle's number plate if the speed is exceeded and send it to the central database, where the fine is created for the vehicle owner. The most often used systems are fixed speed cameras (Fig. 4) and average speed control cameras. Speed control systems are frequently used on city roads and higher-speed roads, so these systems do not reduce the traffic flow because the speed limit is set for the optimum speed of a particular road, and the limit speed can be conveniently changed. Today, fixed-speed cameras have wireless communication, and taken photos are sent to the police database [11]. Fixed cameras are randomly located in the road sections with increased car accident risk, but they are not always active because it is expensive to manage captured data of photos. So, in this case, cameras are chosen in a particular location to be turned on. Nevertheless, drivers do not know which are active, so everyone reduces the speed before every camera [11].



Fig. 4. Fixed speed camera in Norway [11]

Although fixed speed cameras work perfectly fine in their location, where they are installed, and violators are trying to be careful, these systems are inefficient in offset areas where cameras cannot reach the vehicles. Researcher D. Oliveira [12] investigated the efficiency of the speed cameras, and the obtained results show that the cameras are the most efficient in the range of 200 m, and only 60 % of drivers are driving at the same speed as before the camera and after it. Often drivers reduce the speed before the camera's reachable range and during the range. However, after the range, they exceed the speed limit. This phenomenon is called the "kangaroo effect" [12].

More effective systems, such as average speed cameras, are used to reduce the phenomenon problem. The system's working principle is almost the same as a simple speed camera, but this system works with a pair of cameras located in the stretch of the road at a projected distance (Fig. 5).

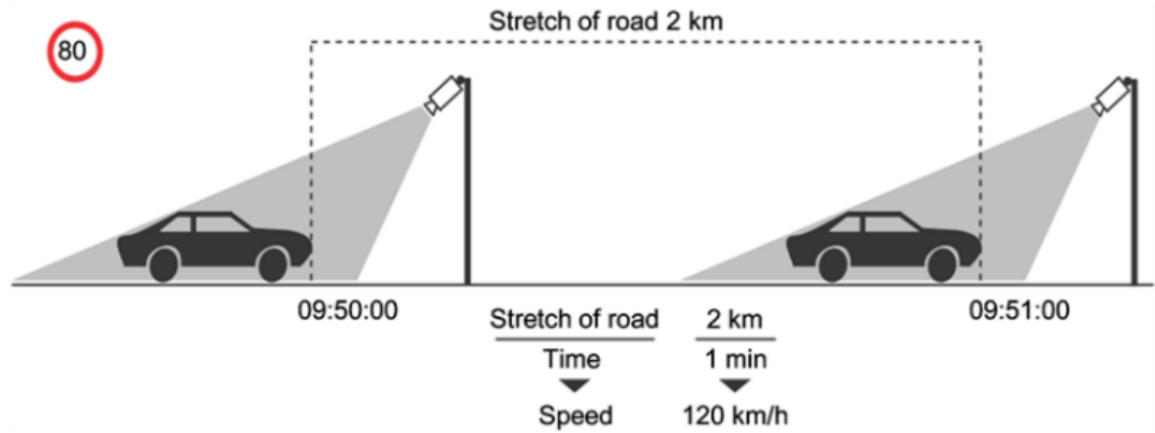


Fig. 5. Average speed control system scheme [11]

These cameras capture every vehicle's license plate picture at the beginning and end of the stretch of the road. The distance between each camera is known, so the start and end of time are captured when the vehicle is detected. The time difference from each camera allows us to evaluate the vehicle's average speed [11]. The average speed control system is effective on closed-area roads with no side roads. If the second camera is not reached, the average speed is not calculated, and the vehicle time duration on a road section is lost. In the situation where the stretch of the road is a closed area without any side roads, every vehicle's speed is evaluated, and every driver maintains the speed limit. Otherwise, vehicle owners who live near and have a side road in the stretch of the road turn, and their captured time data is lost. Drivers who live near or know they must turn in the middle of the road often exceed the speed limit. Moreover, this fact proves that this system has a weak spot.

1.2. Review of Sensor-Based Systems Used in Traffic Control

Previously reviewed speed control measures and systems revealed their advantages and disadvantages. The discomfort effect from speed bumps and the expensive purchase price and exploitation of speed cameras gave a quick start for investigating less expensive and more reliable solutions for traffic control. For this reason, the interest in piezoelectric systems used for traffic control has increased in recent years. Piezoelectric systems in traffic often are used in vehicle determination, classification, vehicle speed measurements, and energy harvesting from traffic motion. This section of the chapter will present sensor-based systems used in traffic control, the types of piezoelectric sensors that generate the signal, and how the piezoelectric transducer is installed on the road.

1.2.1. Magnetic Field Sensors for Vehicle Detection

Traffic monitoring systems comprise several primary elements: the sensor, responsible for signal generation, and the controller, which is programmable and generates the output signal for the traffic light or other traffic control device. In this case, the investigated system consists of the same components. However, the most used types of sensors are magnetic or piezoelectric. The research

of V. Markevičius and other authors [13] investigated anisotropic magnetoresistance sensors (AMR), which are used to detect weak magnetic fields. The operation principle of the AMR sensor is that the sensor captures the Earth's magnetic field, and when the vehicle passes near the sensor, the vehicle's metal chassis distorts the Earth's magnetic field, and this magnetic field distortion allows to define the location of the vehicle. The research [13] presented a basic scheme (Fig. 6) of the components used: two separate AMR sensors, a microcontroller, a distance meter, and a computer.

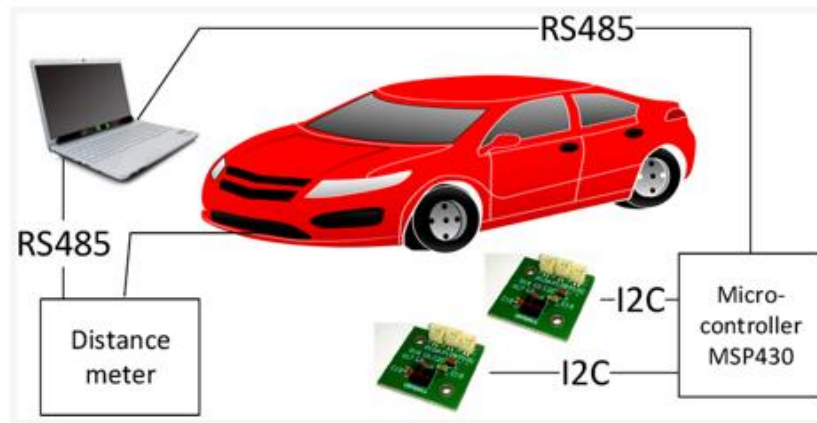


Fig. 6. Scheme of the components used [13]

The experiment investigated how the AMR sensors respond when the vehicle passes near the sensor. The results showed (Fig. 7) that the magnitude of the magnetic field oscillates, with different frequencies and magnitudes, and it is difficult to define which type of vehicle was passing, even the obtained data from the two identical sensors was different, so there was performed a data normalization technique as cross-correlation in order to eliminate the mismatch between two sensors [13]. Figure 7 shows only the X-position magnetic field oscillation. There were also obtained data from Y and Z positions. These research results showed that the Z-position magnetic field had the lowest error. However, the X-position was the most informative position for speed investigation.

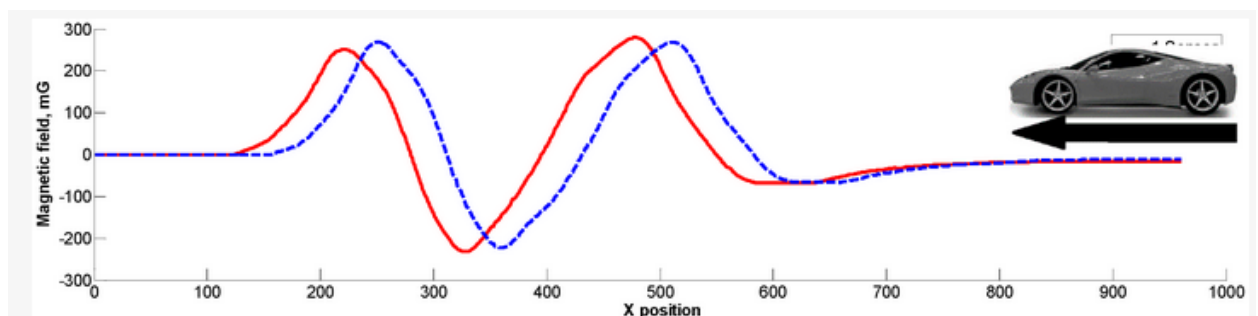


Fig. 7. The magnitudes of the magnetic field in X position (dashed line is sensor one magnitude, another line is sensor two magnitude) [13]

Furthermore, an experiment on the road was investigated for another magnetic field research. There was investigated vehicle speed and length by V. Markevičius and other authors using two AMR sensors [14]. The measuring system (Fig. 8) was developed with PCBs, which were a located microcontroller and AMR sensor. The PCB was on one side of the measuring system and the other side, so the AMR sensors had a 1 m distance between them.

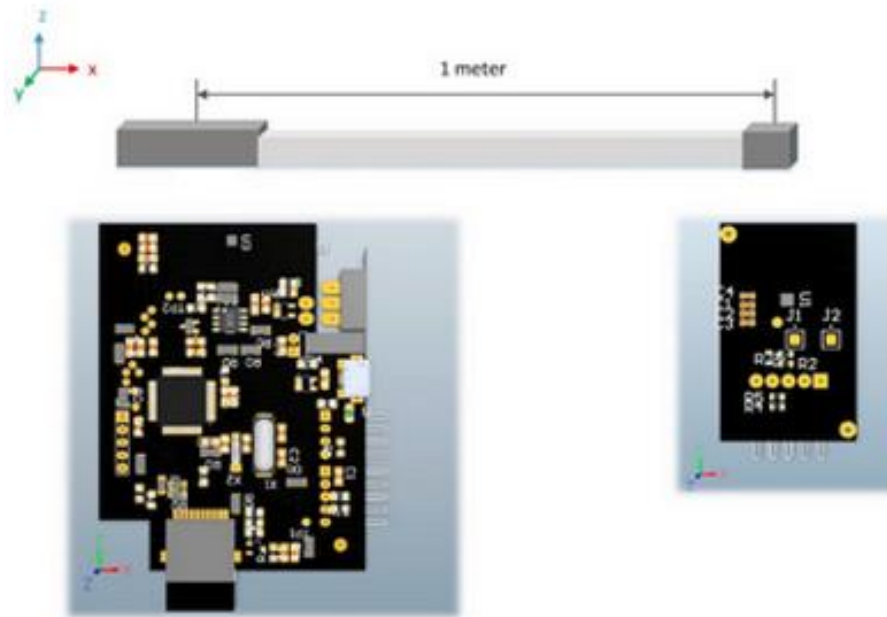


Fig. 8. Measuring system placed on a road [14]

The experiments were conducted in different locations to compare the vehicles' lengths. Previous research [13] decided to use Z component magnitudes of the magnetic field because it has the lowest error. This investigation [14] obtained data from the same Z component magnitudes. Figure 9 shows that the measurement system was placed along the road in the center. However, there were other locations of the system, such as moving it to the left and right for a 30 cm distance, and the results were not affected significantly.

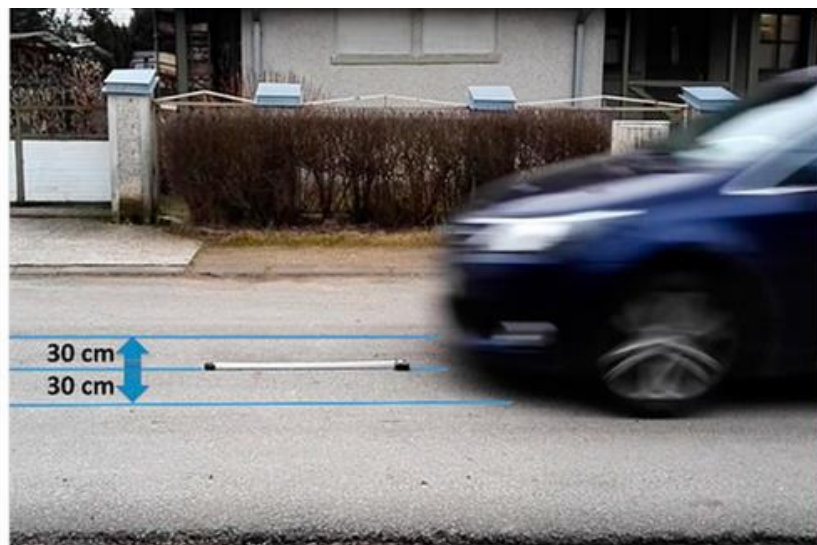


Fig. 9. The measuring system located on the road [14]

As the two AMR sensors were placed at a 1 m distance, the speed evaluation of the vehicle was calculated by taking two magnitudes of the magnetic field signal from one sensor and the other. A time delay between each signal magnitude and the distance between the sensors is known. So, in this case, the vehicle's velocity could be calculated. However, using this system, an autocorrelation function was needed, which had to eliminate the error from obtained data of the AMR sensors

because each time almost the exact dimension vehicle passes near the measurement system, the obtained data between both sensors is different. As a result, there was an estimated maximum error in vehicle length estimation of up to 22 %, which is not as accurate as it should be [14].

1.2.2. Piezoelectric Harvesters of Electrical Energy

Materials such as crystals and ceramics are the raw materials for piezo sensors, and these materials can accumulate electric charge in response to mechanical strain. Also, the previously mentioned phenomenon is called the piezoelectric effect. Moreover, the piezoelectric effect is reversible, the materials, which can generate electric charge while deformed mechanically, can also change their shape while an electric field is applied. Three piezoelectric materials are used: piezo ceramics, thin-film piezo material, and single-crystal material [15]. One of the most popular is zirconate crystal (PZT), piezo ceramic material, and plastic polyvinylidene fluoride (PVDF).

On the roads, many piezoelectric energy harvesters are used, which generate electricity, when the vehicle drives through the sensitive piezoelectric element. In the investigation of Yangsen Cao [16] was designed a piezoelectric transducer, which was embedded in the road pavement (Fig. 10). The holes were drilled to place the piezoelectric element, and these holes were filled with the asphalt mortar. The transducer top was placed near the pavement because the less distance between the vehicle tire and the piezo sensor, the higher the sensitivity. As is shown in the side view (Fig. 10), the piezo transducers were placed 100 m longitudinally distance, and from the top view (Fig. 10), they were placed in two rows for each traffic line. The distances between each transducer longitudinally were 10 cm and laterally 175 cm. Research authors designed this layout as the most effective. Moreover, their results showed that from one piezoelectric transducer, energy was obtained, which was equal to 0,058 J, which was achieved from a single loading value of 0,7 Mpa [16].

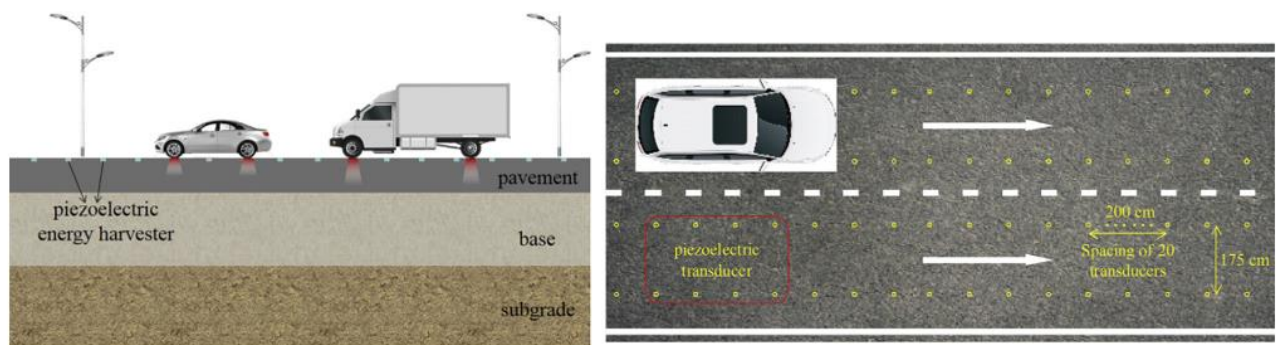


Fig. 10. Piezoelectric transducer layout side view (left) and top view (right) [16]

It is essential to mention that the single piezoelectric element consists of several parts, each of which has its purpose. In the exploded view of the single element (Fig. 11), the main components were displayed: a sealing ring, a squeeze head, a shin, a stop block, another shin, and a base. The sealing ring, squeeze head, and base served as visible structural elements that held everything together. For instance, the squeeze head contained a sensitive piezoelectric ceramic with a diameter of 39.6 mm, and the squeeze head was larger than the ceramic. This design was planned in such a way because the deformation of the piezo ceramics from the pressure was crucial, and a broader area created more pressure for the piezoelectric ceramic.

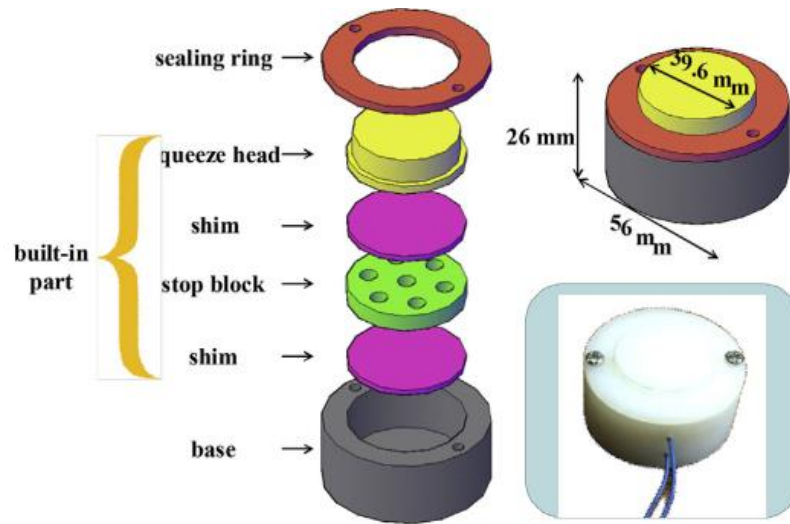


Fig. 11. Exploded view of a single piezoelectric transducer [16]

As more pressure was transferred to the ceramics, more energy was generated within this small component. The referenced study [16] demonstrated that the electric energy output reached an equivalent level of approximately 35 mobile phone batteries' power under daily traffic load.

Another study by H. Yang and other researchers [17] investigated and performed an actual experiment with a piezoelectric harvester. This study investigated the same problem of generating electricity from piezoelectric units installed on the road surface. There was a completed design of a piezoelectric unit (Fig. 12 a) with many stacked together and joined together in parallel piezoelectric ceramics PZT-5H elements. Also, all the piezo elements were wired with internal circuit boards, and everything was sealed and fastened into one flat box (Fig. 12 b). The piezoelectric box was made from nylon, which is well known for high load resistance, and this material is heavily resistant to repeated load shocks. The traveling vehicle's tire dimensions decided the dimensions of the box. Therefore, a square geometric shape was designed with dimensions 30 cm by 30 cm and 8 cm thick [17].

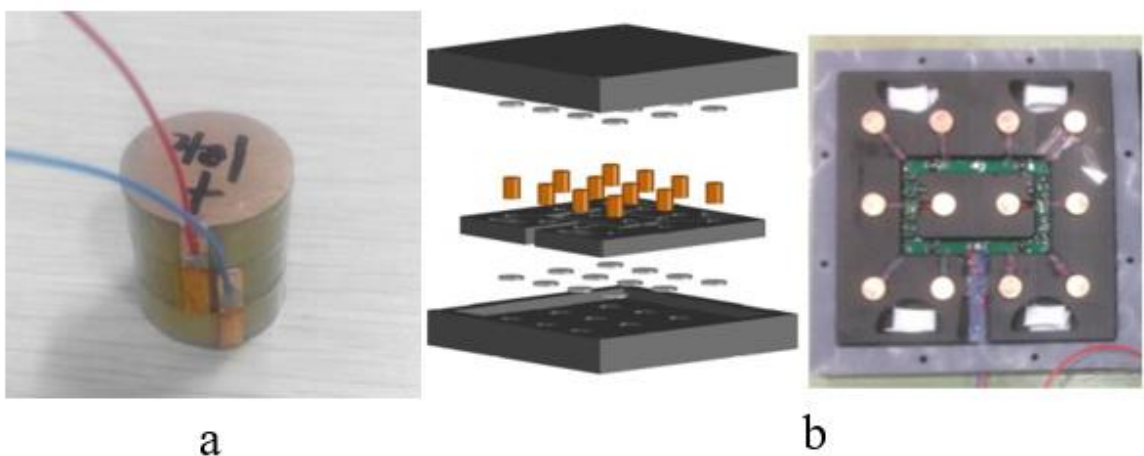


Fig. 12. The piezoelectric unit from PZT-5H elements (a) and both isometric and top views of piezoelectric harvester box (b) [17]

The piezoelectric boxes were embedded into the highway road surface. In one line of traffic, square holes were cut along the road, which was cut each 2,5 m. This distance between each piezoelectric

harvester was decided because it less damages the road construction, and the overall active section of the road was 50 m. Therefore, perpendicular to the traffic direction, the distance between each harvester was 1,875 m. This spacing was selected because the truck and trailer truck axle width is the same spacing [17]. Actual field results showed that (Fig. 13) the lowest obtained open circuit voltage of the designed piezoelectric harvester was 250 V. The higher the vehicle's velocity, the higher the output voltage was reached. The results of two harvester types, F2 and Y10 (Fig. 13), were obtained.

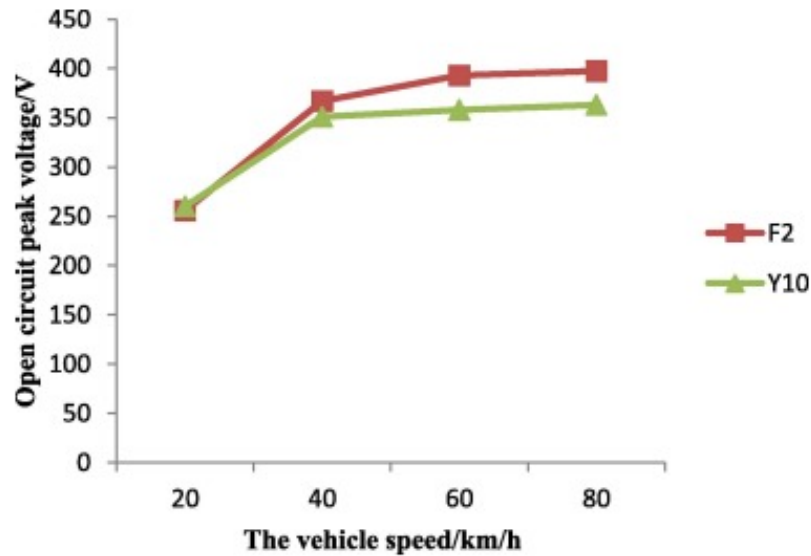


Fig. 13. Obtained results of open circuit peak voltage with different speeds of the vehicle [17]

The highest voltage peak was 400 V, but the voltage increase differed insignificantly between vehicle speeds of 50 / 80 km/h. The piezoelectric ceramics PZT5-H reached its peak voltage at 80 km/h. From these results, a trend line can be summarized that faster speeds than 80 km/h do not generate more voltage.

1.2.3. Cement-Based Piezoelectric Sensor System for Vehicle Speed Measurement

Monitoring could be used for traffic as an alternative to piezoelectric sensors, cement-based piezoelectric composite. The investigation by J. Zhang and his team [18] was performed with this kind of piezoelectric sensor. The main idea was to create a highly effective system that could detect traffic flow, calculate the speed of the vehicles and perform a weight-in-motion measurement. The latter measurement evaluated the vehicle's weight that passed through the sensors. It is vital to weigh and store the data of the vehicles because heavy vehicles on the road damage the road surface in time, and it costs a vast amount of investments for road reconstruction, and the damaged road is also dangerous for drivers.

In this investigation [18], the main component of a road monitoring system was cement-based piezoelectric sensor, which was fabricated by combining the active phase of PMN ceramic and sulfoaluminate cement, which is the passive phase. This combined composite sensor with cement and PMN ceramic have a higher piezoelectric voltage output and better acoustic properties using concrete materials. This traffic monitoring sensor is relatively smaller than piezoelectric harvesters with PZT elements. Its diameter is 45 mm and 30 mm in height (Fig. 14). The composite of epoxy-cement has a silver coating to prevent electromagnetic interference.

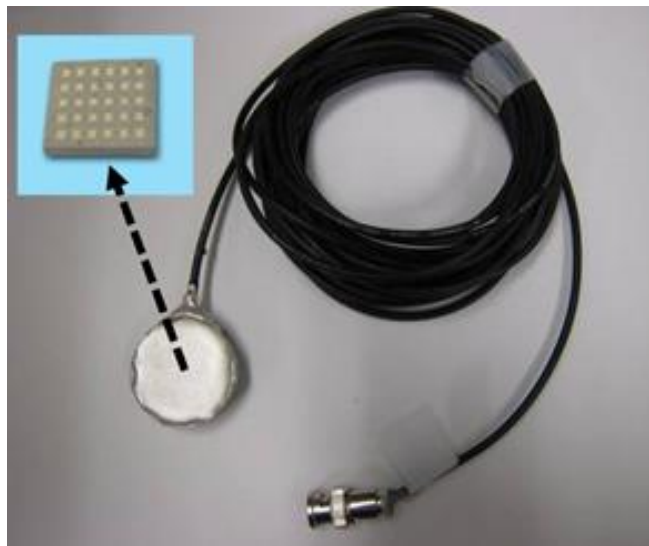


Fig. 14. The PMN ceramic cement-based sensor [18]

A reinforced concrete beam was designed to investigate the speed measuring system in actual traffic conditions, which in this study [18] is named as weigh-beam (Fig. 15 a). The layout of the weigh-beam was perpendicular to the traffic heading direction, and they were embedded in the road surface, which had a distance of 4 m between each of them, and their length was only half the width of the road line. Underneath the reinforced concrete beam, the piezoelectric sensor (Fig. 15 b) had to be prepared for the concrete foundation. The reinforced concrete beam was placed equally with the road pavement height, which helped to prevent the weigh-beam from being pulled out if a vehicle suddenly began to brake.

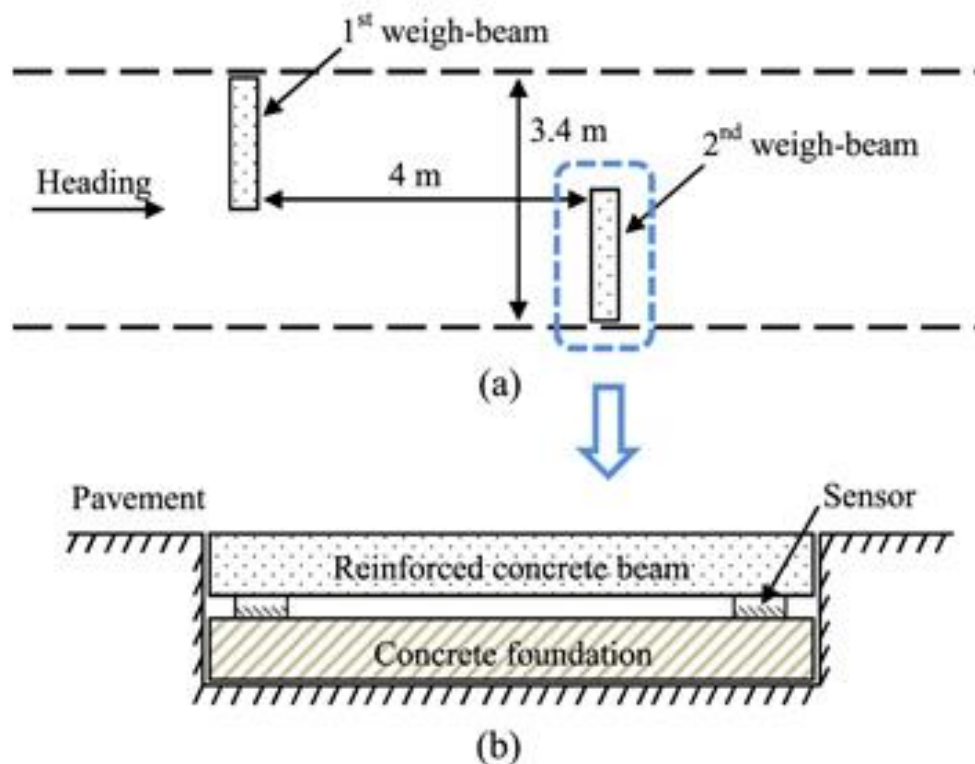


Fig. 15. Placement of the traffic monitoring system in the road (a) top view and (b) side view [18]

The study [18] experimented with a truck weight of 10 tons, with different speeds of 20 km/h, 40 km/h, 60 km/h, and 70 km/h. The results showed that the higher the truck velocity, the higher the sensor output voltage, and with the 70 km/h speed, a 0,3 V output voltage signal was reached. Each weigh-beam generated a separate signal when the vehicle passed through it, and the times when the axle hit the active sensor zone were captured. The distance between each weigh-beam was known, so evaluation of the vehicle's speed was possible.

1.2.4. Piezoelectric Cables for Traffic Monitoring

Another type of piezoelectric material widely used in traffic monitoring is polyvinylidene fluoride (PVDF) piezoelectric cable. This piezoelectric cable was compared with PZT ceramics in research by I. Fina and others [19]. This research aimed to demonstrate the use of piezoelectric sensors on roads, which could be able to classify cars and other vehicles. In their work, they decided to use piezoelectric ceramics (Fig. 16 a) and PVDF cable (Fig. 16 b). PZT ceramics were fixed on a metal plate, and an electrode was attached to the top of the sensor; the PVDF cable did not need any extra attachments. Both sensors were directly placed on the road surface with waterproof cloth tape, protecting both sensors from moisture.

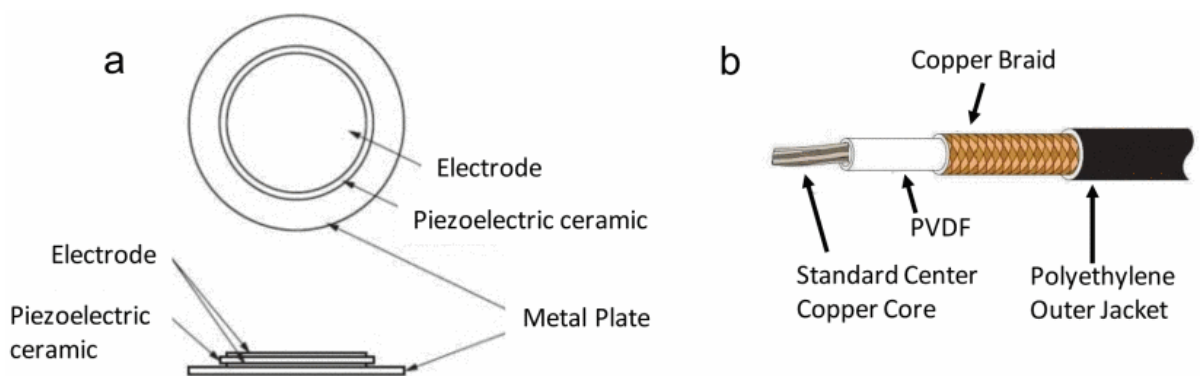


Fig. 16. Schemes of used piezoelectric sensors: a) PZT ceramics and b) PVDF cable [19]

The results showed that PZT ceramics failed rapidly because the welding broke when vehicles passed the PZT sensor. In contrast, PVDF showed great results because the cable was flexible and was not damaged by the impact of the vehicle's generated load. Moreover, the cable was placed for six months on the road, and no severe damage was noticed [19]. This research proves that although PZT ceramics are way more sensitive and generate more voltage than PVDF cable, this sensor fails in time from generated dynamic forces. So, the PZT material is not as reliable as the PVDF cable.

One research by C. Leung and his team investigated the use of piezoelectric cables in aircraft taxiways to classify the aircraft and measure its velocity [20]. The piezoelectric cable was placed in the road pavement (Fig. 17), and a unique long groove was made perpendicular to the road. The groove was made 19 mm deep and 19 mm in height. Plastic standoff parts were placed as supports to hold the cable in place. The cable was placed near the top of the road pavement around 7 mm to the top of the road. The principle of this speed measuring system is that when the aircraft tire passes through the created groove with piezo cable, it stresses the plastic standoff part, and this part deforms its shape. As a plastic standoff holds the piezo cable, the cable is also deformed under the same stress. In this case, the output signal generates the voltage for the controller from the piezoelectric cable.

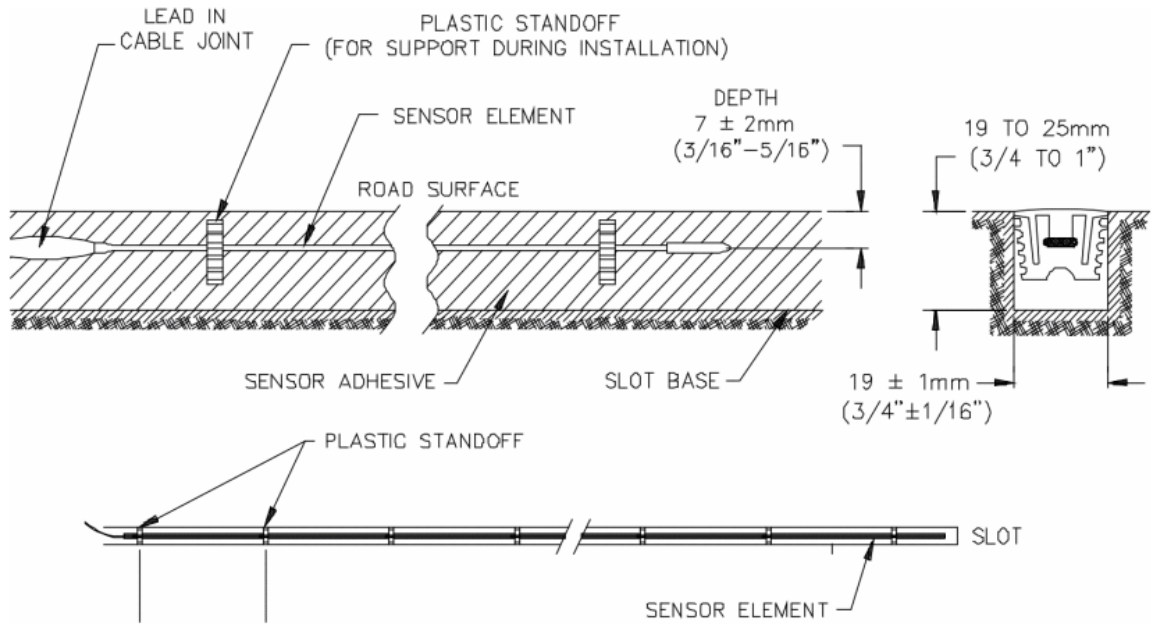


Fig. 17. Piezo cable for speed evaluation and axle counting [20]

This research results from [20] show that placed piezo cable in the created groove generates 496 mV in output (Fig. 18). Having in mind that cable is not directly deformed from the aircraft tire, but it is deformed through the plastic part and the cable by itself is 7 mm placed under the pavement, the deformation from the tire is absorbed, and the magnitude of the acting force is weak. Therefore, from the results (Fig. 18), it is clear that the signal is weak and not even reaching 1 V.

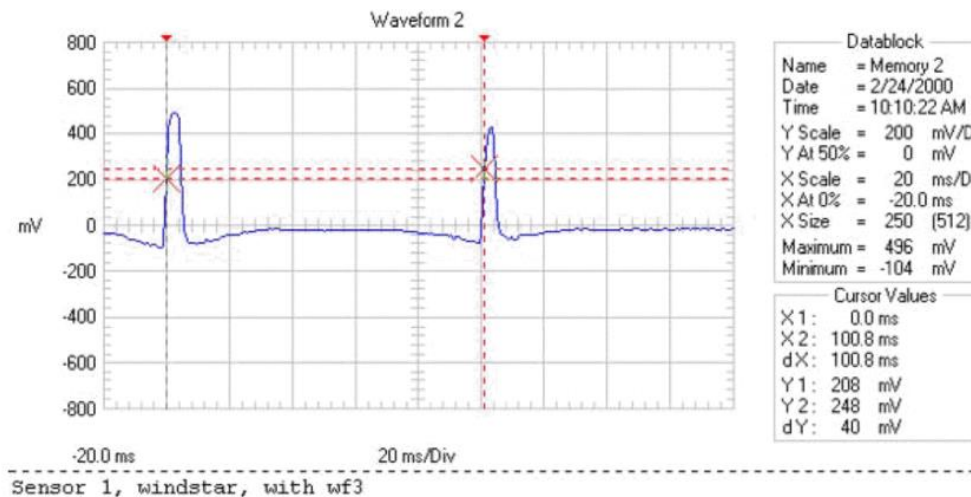


Fig. 18. Output signal from the piezoelectric sensor [20]

Many countries use speed cameras, but the Norwegian country currently uses 250 automatic operating speed enforcement systems based on piezoelectric cables [21]. In the study of T. Haugen and his team [21], they described placing two piezoelectric cables (Fig. 19) in the road, perpendicular to the driving direction, at 25 mm depth. Moreover, this system consists of a camera unit (Fig. 19) and a data logging unit. When the vehicle passes through the cables, the piezo cable is deformed, and a voltage signal is created, which receives the data logging unit. This unit calculates the speed from passing vehicles by the captured time difference when the vehicle axle hits the first

piezo cable and the second one, and the distance between each piezo cable is known (3 m). If the passing vehicle exceeds the speed limit, the camera unit takes the picture, and the speed violation is sent to the driver.



Fig. 19. Speed enforcement system of piezo cables and camera unit [21]

The typical speed measuring system was researched by B. Gonzales and others [22]. The investigated vehicle speed measuring system (Fig. 20) consisted of two independent piezoelectric cables, (1) and (2), with a distance between them of 5 m. They were placed in one traffic lane across the road 3,4 m. Magnetic sensor (3) was used to determine changes in the magnetic field compared to Earth’s naturally created magnetic field. The changes in the magnetic field are created when the metallic masses as vehicles pass near the magnetic sensor, and the changes are obtained in three axes – X, Y, Z. These sensors were also called magnetoresistive sensors, which were also used in the previously mentioned research by V. Markevičius [13]. This system also had a camera for visual inspection of the vehicles and electronic cabinet, where all the cable layout and the controller were placed.

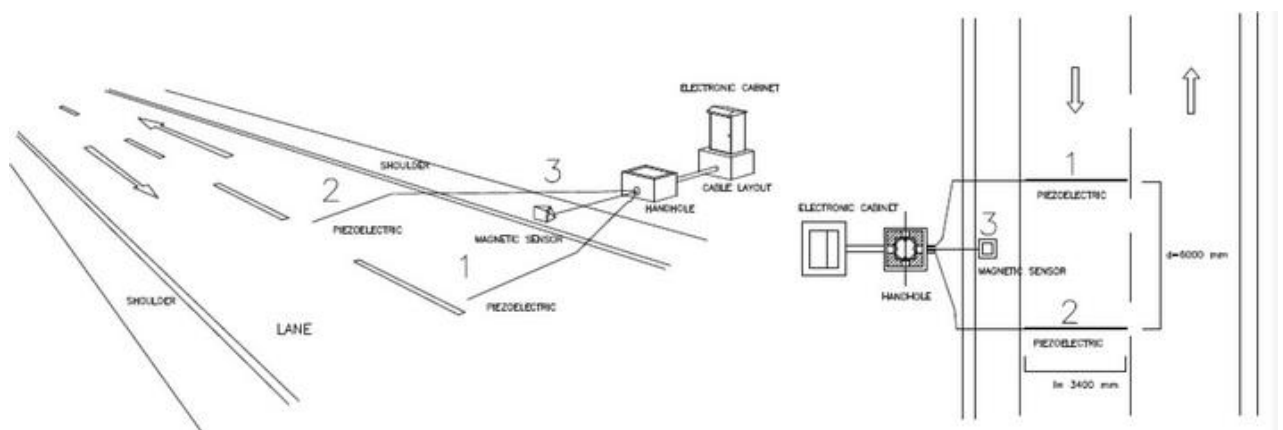


Fig. 20. The model of the speed measuring system [22]

This investigation decided to use PVDF piezoelectric cables with spiral wrap, placed non-intrusively on the road pavement and protected with Pro-Tech-branded cable protection. This system was created not only for vehicle speed calculation but also for vehicle type classification. From obtained signal from piezo cables, the distance between the vehicle axles, for confirmation of the vehicle type, the camera takes a picture of the vehicle [22]. The software was created with the LabVIEW program, where the virtual front panel was created (Fig. 21).

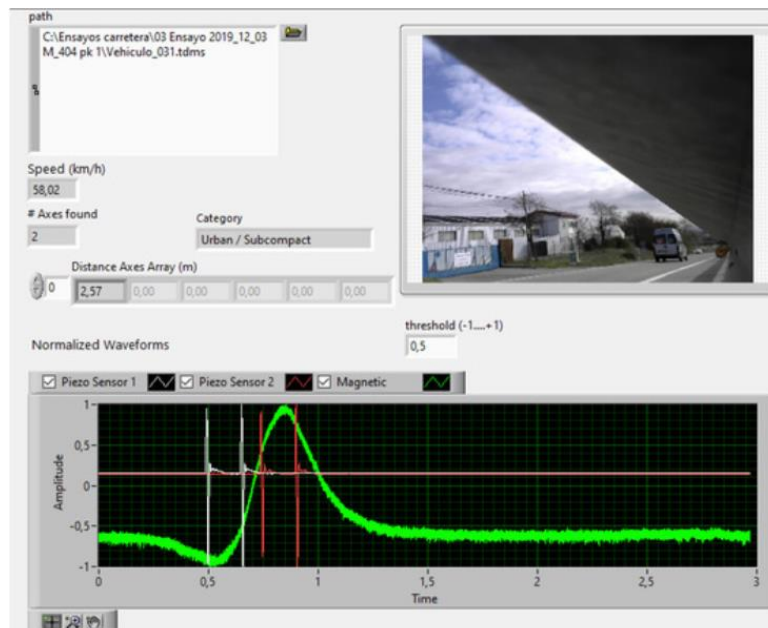


Fig. 21. Virtual front panel for speed estimation and vehicle type determination [22]

The virtual front panel software calculated the vehicle's speed and distance between the axles. It also determined how many axles were captured and defined the type of vehicle. The obtained voltage amplitudes from the piezo cables were normalized to ± 1 V [22].

1.3. Summary of the Chapter

Although speed calming measures are effective, sustainable, and cheap, they damage the vehicle's suspension and other chassis joints. Also, it reduces traffic speed on that road because everyone must reduce their speed. For emergency transport, there is also an inconvenient situation because it is a permanent object on the road, and like everyone, the emergency vehicle must reduce the speed, and there is a higher probability of a car accident from hard braking. Speed measuring systems, such as fixed speed cameras and average speed cameras, are expensive because the used components have a high cost, and the obtained data from the cameras must be evaluated and the penalty bills sent. Also, in the literature review were presented sensor-based systems with a sensitive sensor for traffic monitoring and control, which created an analog input signal for the controller. The sensors presented in the literature review were several types: anisotropic magnetoresistive sensors (AMR), piezoelectric sensors as piezo zirconate crystal (PZT), which is also called piezo ceramic material, the active phase of PMN ceramic with sulfoaluminate cement and plastic polyvinylidene fluoride (PVDF) piezoelectric cable. The major drawback of the magnetoresistive sensor was its lack of accuracy, so it was not easy to capture the time difference. The piezoelectric ceramics have a high output of generating a signal, and even from that, generating electricity for the streetlights is possible. However, they are sensitive to high dynamic impacts from the vehicles, and the sensor fails in time. Piezo sensors with cement are durable. However, they have low sensitivity compared with the piezo cables. PVDF piezoelectric cables have lower sensitivity than the PZT. However, they are reliable because they are flexible, waterproof, and they still work correctly after many dynamic load cycles. However, there is a lack of investigation about the installation of the piezo cable on the road, what protective layer was used for the cables, and how to increase the sensitivity of such a sensor. So, in further investigation, this study will present the speed enforcement system design using piezoelectric cables and other components.

2. Methodology for Selecting the Design of Piezoelectric Road Structural Element

After an analyzed literature review of the speed enforcement systems, it is essential to decide the optimal system that could be used in residential areas because in other areas such as cities or countryside, innovative, adaptable speed enforcement cameras are used as fixed or average speed enforcement cameras. Those systems are installed on those roads because the traffic load rate is high, and there are many fatal car accidents, so the government invests a high budget in protecting as many people as possible from fatal injuries. Speed enforcement cameras require high technologies, databases, and personnel to maintain them. Therefore, the mentioned systems cost a severe amount of money and resources. However, there are lower speed limits in residential areas, and there is not much traffic. For this reason, high-tech systems are not used in residential areas. Instead, there are speed bumps or other speed calming measures. Latter devices, which are often used in residential areas, damage vehicle suspension, and brake systems. The traffic speed is slowed down, and the speed bumps are easily disassembled or damaged. So, another solution is needed, which would be cheaper than speed enforcement cameras, worth investing in, and reliable.

This study will investigate sensor-based piezoelectric speed enforcement system prototype (Fig. 22), in which sensors would be piezoelectric cables (2), the signal data would be obtained by the controller (3), and there would be used a traffic light (1) to force the drivers to keep the speed limit and not exceed it.

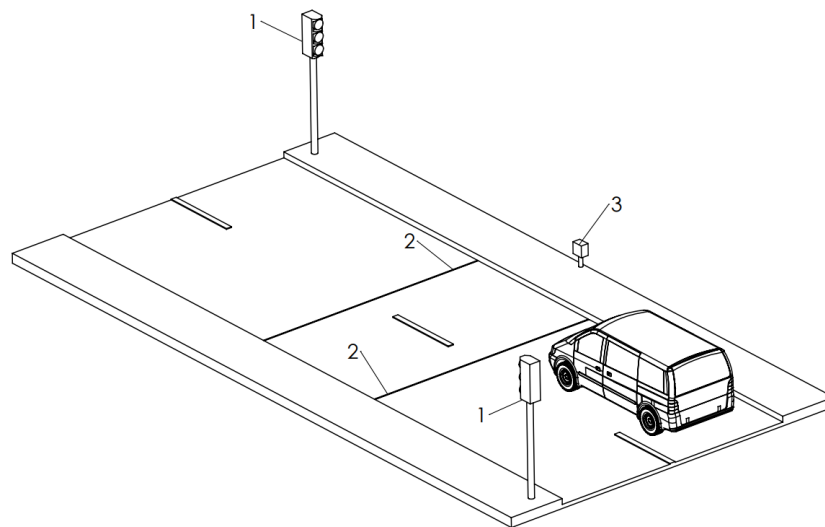


Fig. 22. The scheme of piezoelectric speed enforcement system. 1 – Traffic light, 2 – Piezoelectric sensor, 3 – Control box

2.1. Selection Method of Piezoelectric Cable Type

A sensor will be used as a piezoelectric material from the previous overview of the investigated speed enforcement system. The piezoelectric sensor was chosen because for this sensor is not needed an external energy source like other types of sensors such as inductive, capacitive, and magnetic. It is an advantage that creates less complexity for electrical wiring circuits. The literature review mentioned that the most used piezoelectric materials are zirconate crystal (PZT) and plastic polyvinylidene fluoride (PVDF) piezoelectric cables. Piezoelectric materials correspond to stress, which is applied in the same direction as d_{33} . The d_{33} is an essential indicator of piezoelectric material, which indicates suitability for strain-dependent applications, and this is a piezoelectric

charge constant. The polarization is induced in direction (3), parallel to the direction in which the piezoelectric element is polarized. The coordinate system and polarization are shown in Fig. 23 [23].

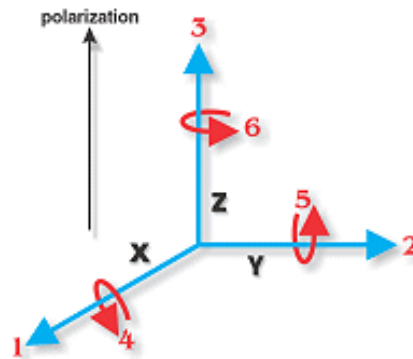


Fig. 23. The forces with directions, which affect piezoelectric element: polarization is usually defined as coinciding with Z – the axis, other numbers are the indicators according to the axis 1, 2, 3, also shear directions about each ax 4, 5, 6 [23]

The d_{33} coefficients were compared in research [19], and this research claimed that the d_{33} direction of the coefficient of PZT ceramic element varied from $200 \cdot 10^{-12}$ C/N to $600 \cdot 10^{-12}$ C/N comparing the PVDF copolymer cable d_{33} coefficient was around $30 \cdot 10^{-12}$ C/N. From these coefficients can be seen the difference in electric charge generation. The PZT ceramic generates from 6,6 to 20 times more charge than the PVDF copolymer cable, applying the same amount of stress. This fact justifies why PZT ceramics are often used as electric energy harvesters. However, ceramics is a brittle material, and due to the high dynamic impact might fail. This study decided to use PVDF copolymer cable because it is flexible and reliable. The research [19] has proven that piezoelectric cable can withstand many impact iterations without damage.

The piezoelectric cable can be manufactured with the same piezoelectric polymer but with a different type of coating. There are two different coatings of polymer: coating with solid, extruded polymer, or counter-wound double polymer spiral wrap [24]. Both piezoelectric cable types are defined as high-sensitivity components shown in Fig. 24.

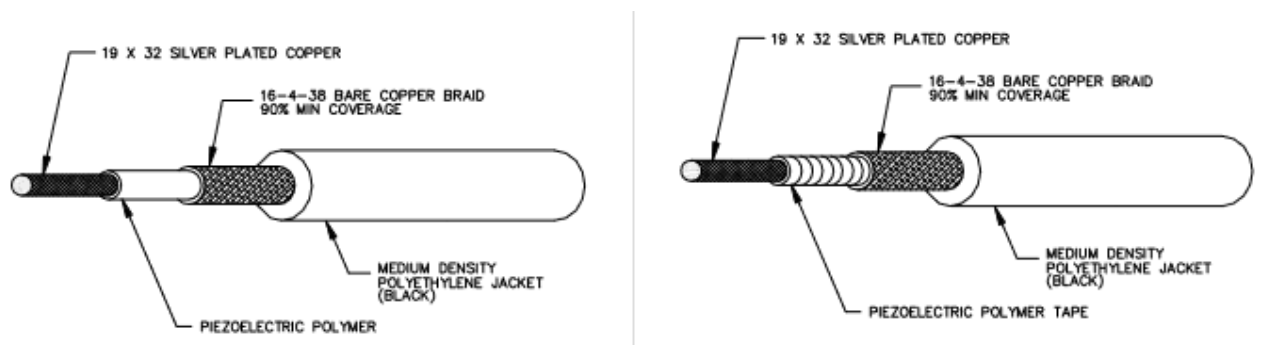


Fig. 24. Scheme of PVDF copolymer cable (left) and PVDF spiral tape cable (right) [24]

Both of the cables are made in the central core of silver-plated copper, then in the outer of that wire is extruded copolymer or in other cable type is the polymer tape and on top of this layer is placed on both of the cable types copper braid and the outer shield black polyethylene jacket. Typical properties of current cables are listed in Table 1.

Table 1. Typical properties of the cables [24]

Cable Characteristics	Solid Copolymer	Spiral Wrap
Diameter	$2,8 \pm 0,1$ mm	$2,6 \pm 0,1$ mm
Capacitance	650 ± 150 pF/m	950 ± 150 pF/m
Dissipation factor	0,015 @ 1 kHz (1 m)	0,016 @ 1 kHz (1 m)
Sensitivity	20 ± 5 pC/N @ 0,1 N	20 ± 5 pC/N @ 0,1 N
Weight	17 kg/km	(TBC)
Tensile strength	>200 N	>200 N

Both cable characteristics are almost the same. The main difference is in the diameter. The copolymer cable has a slightly wider outer diameter than the spiral wrap cable. However, spiral wrap cable capacitance and dissipation factor are slightly higher than copolymer cable.

2.2. Method of Dynamic Load Impact Generation

Piezoelectric cables do not store the electric charge. If the cable is deformed slightly and the load is static, only slightly increasing, there is no noticeable voltage difference in output. However, as the dynamic load is applied to the piezoelectric sensor, the voltage amplitude drastically increases and rapidly decreases. Piezo cable sensitivity is determined according to a methodology written in the paper [24]. The drop test method is used to define the sensitivity of the piezo cables itself. In the study [24], the drop test was performed with a device with a falling mass of 2 kg, which was dropped from heights up to 700 mm. The scheme of the drop test device is shown in Fig. 25.

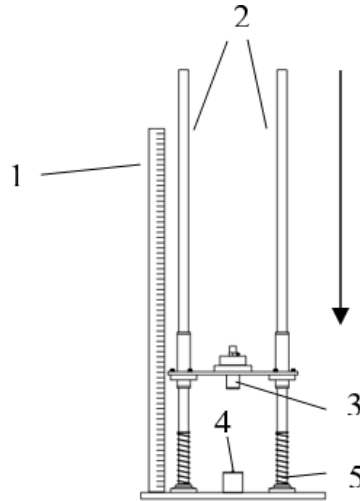


Fig. 25. Scheme of a drop test device. 1 – Ruler, 2 – Guides for the carriage of mass, 3 – Mass with an accelerometer for dynamic force evaluation, 4 - Table for piezoelectric cables, 5 – Springs for the carriage of mass, the arrow indicates the direction of falling mass [24]

The falling mass object creates different dynamic impact forces from different heights, generating analog voltage signals in the piezoelectric cable. This study will perform a drop test with the homemade punching device shown in Fig. 26. The device is 450 mm high, 145 mm wide, and 155 mm long. This device is created mainly from four pieces and has guide (1) for a dropping mass. Also, there is the aluminum frame (2), which holds the mechanical hand vise clamp (4) and the mass (3) together. The mass weight is 0,5 kg, and the maximum height from which it could be

dropped is 200 mm. As mentioned before, this device has a mechanical hand vise clamp, making it uncomfortable to place the piezo cable. For this reason, a fitting part was created (Fig. 26), made from three parts of rectangular aluminum profiles 30x10x2 mm (5) and flat aluminum profile 30x2 mm (6) to hold all three separate rectangular parts together. Everything was riveted together with aluminum rivets (7).

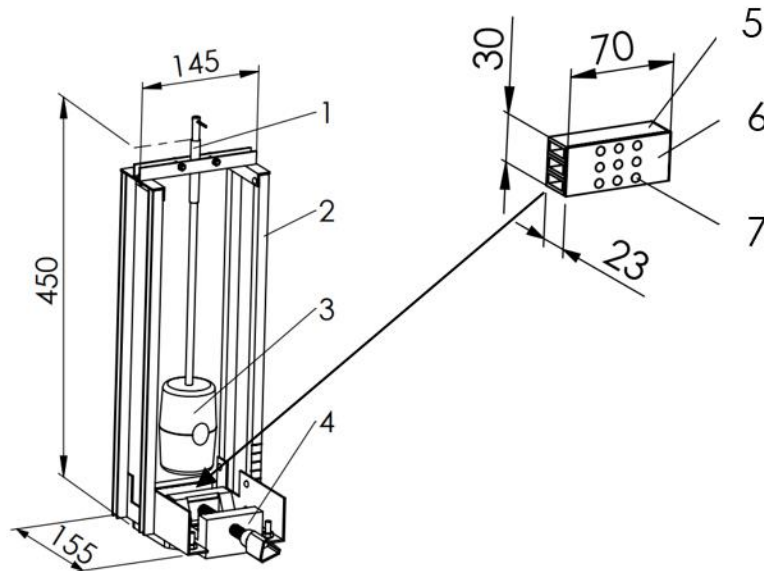


Fig. 26. Designed punching device for a drop test for piezoelectric cables (left) and the clamp (right) fitting part. 1 – Guide for a dropping mass, 2 – Aluminum frame, 3 – Mass of 0,5 kg, 4 – Clamp, 5 – Aluminum rectangle profile 20x10x2 mm, 6 – Aluminum profile 30x2 mm, 7 – Rivets

2.3. Methodology of Three-Point Flexural and Compression Test

The bending flexural test is often applied to brittle or ductile materials such as stainless steel tools and hard metals to determine the bending properties of materials. The flexural test allows us to obtain deflection, modulus of elasticity, and flexural strength [25]. The sample, also defined as a specimen (Fig. 27), is placed between the two supporting pins at a certain distance, undermined the specimen, and the loading pin is above the specimen in the center. Then, the load is applied to the loading pin, and the specimen is bent.

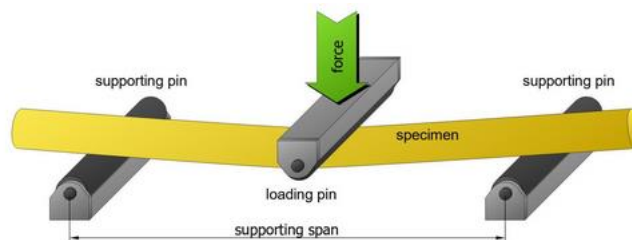


Fig. 27. Three-point flexural test scheme [25]

With a three–point flexural test can be determined yield and tensile force boundaries. The yield force defines the force value, and when it is applied to the specimen, the sample is in the elastic deformation state. After the yield force is unloaded, the sample must return to its original state and not be left with any deformation. However, when the applied force value is higher than the yield force, after unloading the force from the sample, there is left deformation, and the specimen is in the

plastic state and cannot return to its original state. As the load force increases, the plastic deformation also increases and reaches the tensile force value, which is the maximum for the material. After reaching tensile force, ductile materials still have plastic deformation but do not break. However, brittle materials break at their tensile force limit and do not have further plastic deformation.

Moreover, from the three-point flexural test, bending force and deflection diagram (Fig. 28) (flexural yield strength) are obtained. In this diagram, F_y is the yield force and F_{max} is the tensile force. Therefore, this diagram allows to determine the force limits where the elastic deflection ends and the plastic deflection limit.

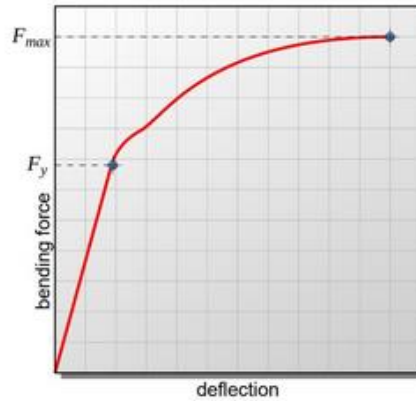


Fig. 28. Bending force and deflection diagram [25]

The compression test's primary goal is determining the material's response when a compressive force is applied to brittle or ductile material. During this test, compressive yield force, tensile force, or elastic modulus can be determined. An essential factor during the compression test is the buckling of the specimen. The buckling happens when the specimen's height is too long. Therefore, the specimen dimensions must be selected according to the specific length and diameter ratio, $L/D < 2$, when the specimen is a round rod [26]. The compressive load and deformation of a material diagram are shown in Fig. 29.

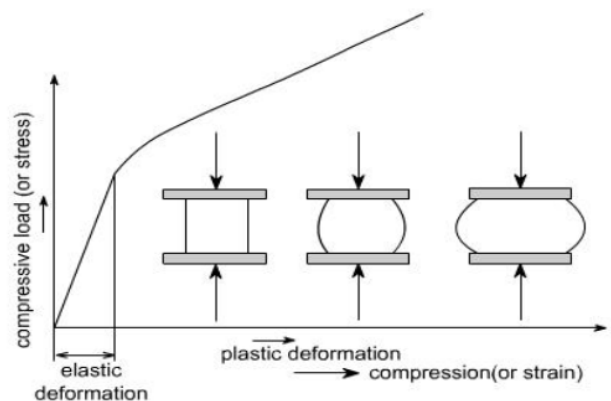


Fig. 29. Compressive load and deformation diagram with examples of specimen [26]

As previously mentioned, bending force and deflection diagram, the compressive load and deformation diagram also have elastic deformation boundaries. When the yield force reached and removed the yield force, the specimen's geometric shape returns to the original state. There is also a

plastic deformation boundary, where the tensile force is reached, and when the force is decreased, the specimen is permanently deformed.

2.4. Selection of Protective Surface for Selected Piezoelectric Cable

The piezoelectric cables can not be placed on the road without any protective structure because the outer layer of the piezo cable would rapidly wear out, and the cable as a sensor would be damaged permanently. Therefore, a protective structure for the sensor must be used because it would stabilize the sensor on the road, and the vehicle's tire would not directly touch it. Research [22] from the literature review proposed using Pro-Tech-branded cable protection, in which the cable was inserted and installed this structure on the road surface. The solution's advantage is that the sensor's sensitivity is high because almost direct stress from a vehicle tire is applied. However, it is an unreliable and not last long solution because the wear of the elastic protective material due to a friction force is rapid. Another research [20] suggested cutting the road surface and installing the cable with plastic holding parts. This method protects the cable from mechanical wear. However, the obtained signal from the sensor is unreadable, and the controller, without an extra voltage amplification device, could not sense a low voltage amplitude signal. Therefore, this study will use an aluminum alloy Al 6063-T6 profile, which could hold the piezo cable in place. However, the raw profile geometry was not acceptable. It had high edges, so the profile (Fig. 30) was cut along and narrower.

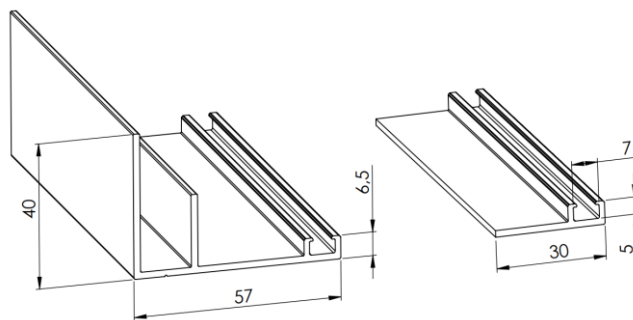


Fig. 30. Selected aluminum profile for piezo cable protection, raw profile (left) and after cut profile (right)

The piezoelectric cable will be placed along the profile length in the “U” channel. The “U” channel's inner dimensions are shown in Fig. 30 (right). The piezoelectric cable's outer diameter is only 2,8 mm, so if it is just placed along the channel, it is loose and not above the profile edges. For this reason, will be used a spacer material, which would lift the cable, but there is also a need to stabilize the cable. Two options for stabilizing the profile channel are whether to use a silicone or thermo tube. Both examples of structures are shown in Fig. 31.



Fig. 31. Structures for piezo cable stabilization in aluminum profile, structure with silicone and rubber spacer (left), and structure with thermo tube and isolated cable with two wires used as a spacer (right). 1 – Piezo cable, 2 – Silicone layer, 3 – Rubber, 4 – Aluminum profile, 5 – Thermo tube, 6 – Isolated cable with two wires

For the experiment of piezoelectric sensor structure selection will be prepared two aluminum (4) samples, of which one (Fig. 31 left) will have installed piezo cable (1) with rubber spacer (3) and silicone layer (2). Another sample (Fig. 31 right) piezoelectric cable (1) will be installed with an isolated cable with two wires (6). It will also be used as a spacer and thermo tube (5).

2.5. Calculation of the Static Pressure Load from a Vehicle

Designed piezoelectric sensors must withstand huge loads from driving vehicles through the sensor. In residential areas where the vehicle traffic is low, often are met light category vehicles, which mass below 3,5 t. The heaviest vehicles in residential areas, which could drive through these roads, are tractors with trailers, or rubbish trucks, which clean rubbish bins. A rubbish truck's mass can reach up to 26 t while fully loaded with rubbish [27]. Mostly these trucks have three axles, which means there are six wheels. This means that approximately one tire load to the road pavement is about 4,3 t, which is 4300 kg. The truck one tire [27] dimensions are 315/80 22,5, which means the tire's width is 318 mm. The static load force is calculated using Eq 1.

$$F_{static} = m \cdot g \quad (1)$$

where: m is mass by which one is loaded tire (kg); g is the acceleration due to gravity (m/s^2).

$$F_{static} = 4300 \cdot 9,81 = 42183 \text{ N}$$

This study uses an aluminum profile as a protection for the piezoelectric cable and also allows installing the cable correctly into the “U” channel and fixing the whole construction on the road pavement. The construction must have enough stiffness to withstand the load pressure from the worst case, the heaviest truck tire acting static pressure. As the tire width of the truck is 318 mm, which is 0,318 m, and the aluminum profile width is 30 mm, which is 0,03 m, the total surface area into which the load pressure is applied can be calculated using Eq 2.

$$S_{area} = tw \cdot pw \quad (2)$$

where: tw is the width of the tire (m); pw is the width of the profile (m).

$$S_{surface} = 0,318 \cdot 0,03 = 0,01 \text{ m}^2$$

The normal stress applied to the truck tire's aluminum profile is calculated using Eq 3.

$$\sigma_{normal} = \frac{F_{static}}{S_{surface}} \quad (3)$$

where: F_{static} is static load force from tire (N); $S_{surface}$ is the total surface area in which the load is acting from the truck tire (m^2).

$$\sigma_{normal} = \frac{42183}{0,01} = 4218300 \text{ Pa} = 4,218 \text{ MPa}$$

The obtained value is the normal stress on the aluminum profile when the truck drives through it. The calculated normal stress value is the value that piezoelectric sensor construction must withstand and must not disintegrate.

2.6. Selection of a Testing Method for Designed Piezoelectric Road Structural Element

The selected structure of piezoelectric cable will be used for further investigation, and this component also can be called a piezoelectric road structural element. In order to achieve accurate signals from this sensor, it is essential to perform actual experiments on a road with a vehicle passing through the sensor. For example, the investigation of a speed enforcement system with piezoelectric cables [22] placed the sensors on the road with a 6 m distance between the sensors, the sensors were tested on the asphalt surface, the piezoelectric cables were not embedded into the road surface but just placed on the road. A similar experiment will be performed in this study, but the distance between the sensors will be 4 m. The selected road structural element with a piezoelectric cable will be placed on the road and anchored to the asphalt pavement.

2.7. Summary of the Chapter

Overall, this chapter presented the methodology of the designed speed enforcement system prototype, briefly explaining this system's main components. The main component essential to the design was piezoelectric sensor construction. The piezoelectric effect principle was explained and presented mainly using piezoelectric cable types. In order to achieve voltage in the output of the piezo cable, the drop test method was considered, and the punching device was designed. This device generates a constant dynamic load, from which the analog signal voltage would be possible to obtain. Three-point flexural and compression test methods were also presented, and their importance in properly defining mechanical properties for the designed piezoelectric sensor construction. The construction presented in the methodology was made from aluminum Al 6063 T6. Therefore, it presented two different types of installation methods for the piezoelectric cable in the aluminum construction, presented the spacer types, one of them was two-wire cable and thermo tube, another one was silicone and rubber. The calculation method of generated pressure to the sensor construction of the heaviest possible vehicle, which might drive through the sensor construction, was presented. The testing method of the piezoelectric sensor construction was selected on the actual road and was presented with its importance.

3. Investigation of Speed Enforcement System Road Structural Element and Selection of Electronic Components and Control

This chapter will provide an experimental investigation of the piezoelectric road structural element and will be evaluated the performance of the sensor under real road conditions with vehicles. Additionally, will be discussed the selection of electronic components for the prototype of the speed enforcement system and presented the control logic of the designed system prototype.

3.1. Experimental Investigation and Design of Speed Enforcement System Road Structural Element

This section of the chapter will present obtained results from the designed piezoelectric sensor construction. In addition, there will be evaluated obtained voltage output sensitivity results. This section of the chapter will also present experimental research results and calculations for selected construction components and determine the strength limits of the piezoelectric structural road element.

3.1.1. Experimental Selection of Piezoelectric Cable Type

In order to define which piezo cable type has higher sensitivity was used a drop test, with a designed punching device. The voltage measurement of the cable is the sensitivity measurement object because the controller, which must operate the speed control system, will be using analog signals of voltage amplitude. So, the higher the cable voltage with the same punching device conditions, the higher sensitivity. The set-up schematic view of the components which were used during the experiment for the piezo cable selection is shown in Fig. 32. For the experiment punching device (1) was used, piezo cable (2), one sample of piezo cable was PVDF copolymer cable and another one PVDF spiral tape cable. Also, there was used oscilloscope (3) model PicoScope3424, PC (4), thermocouple (5), and digital multimeter (6).

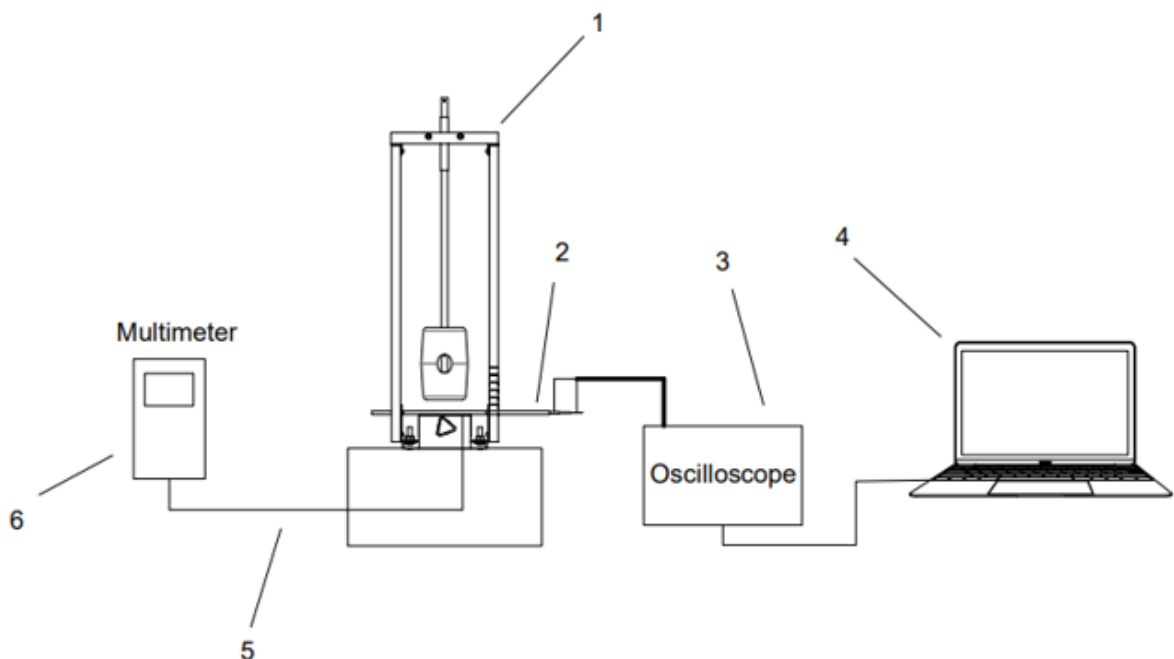


Fig. 32. Set-up schematic view of test for piezo cable type selection. 1 – Punching device, 2 – Piezoelectric cable, 3 – Oscilloscope PicoScope3424, 4 – PC, 5 – Thermocouple, 6 – Digital multimeter CHY 24CS LCR

The set-up view of the experiment is shown in Fig. 33. The first steps started from a falling mass of 0,5 kg, which was in the punching device (1). The mass fell from different heights, from 10 mm to 100 mm height. Piezoelectric cable fitted on the fitting part (Fig. 26), which was fixed with clamps of the punching device (1) (Fig. 33). When mass fell, it punched the piezo cable (2), and after the impact, the piezoelectric cable was deformed, and the voltage was generated between piezo cable two contacts: silver plated copper and bare copper braid (Fig. 24). Oscilloscope (3) was connected with one channel cable to those piezoelectric contacts (Fig. 33). In the PC (4) was already installed software PicoScope 6, where the obtained voltage amplitude and time duration of the obtained signal was captured in a graph. The multimeter (6) indicated the piezoelectric cable temperature at which it was operating. The room temperature was measured with thermocouple (5). The temperature at which the experiment was performed was 21 °C.

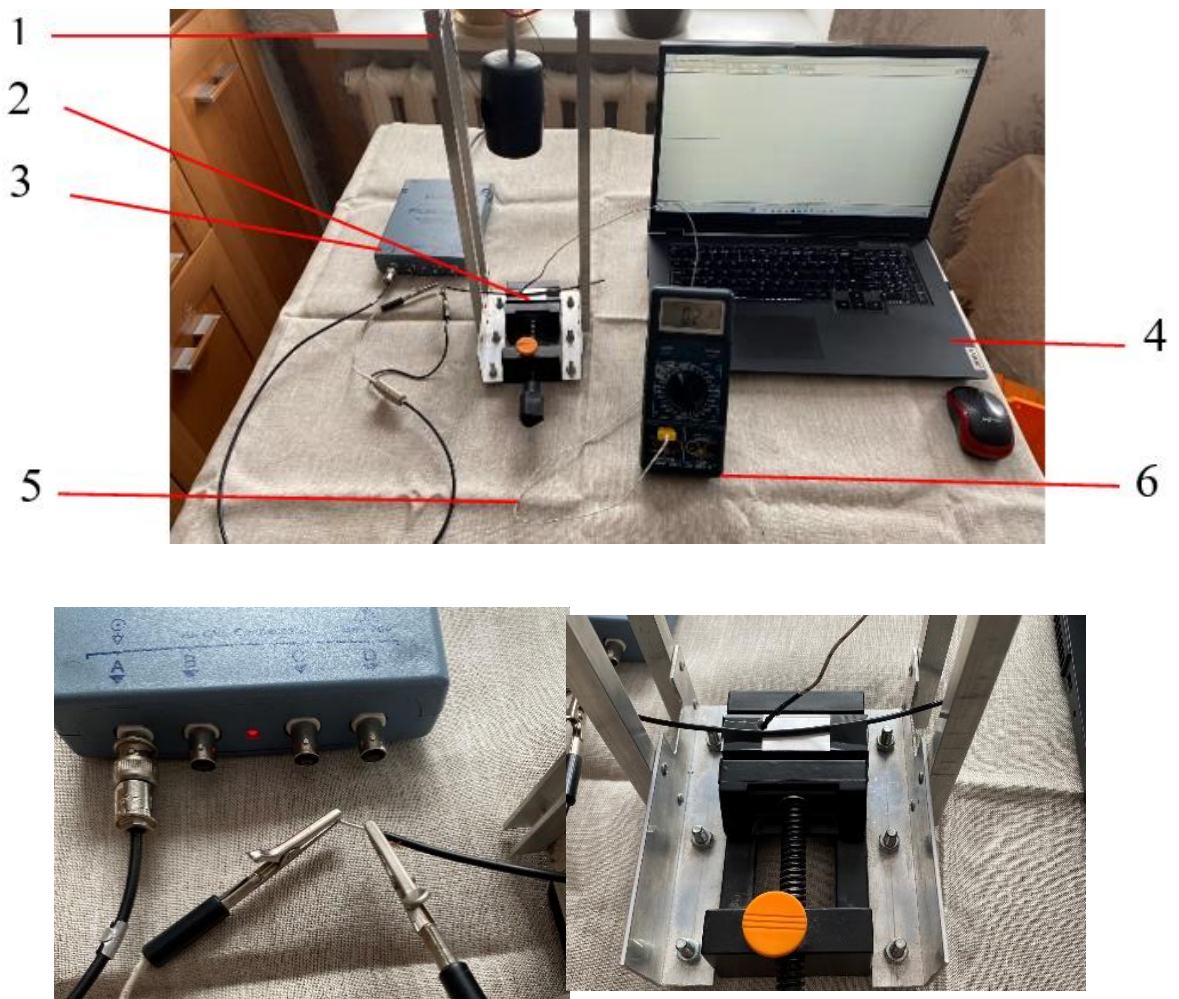


Fig. 33. Set-up view of the experiment for piezo cable type selection (top). 1 – Punching device, 2 – Piezo cable structure, 3 – Oscilloscope PicoScope3424, 4 – PC, 5 – Thermocouple, 6 – Digital multimeter CHY 24CS LCR. Connection to piezoelectric cable (below left) and cable installation with a fitting part in clamps (below right)

The results were captured in the picture format, showing each experiment iteration measured voltage amplitudes and time durations. Figure 34 (left) shows the PVDF spiral tape cable voltage and (right) PVDF copolymer cable voltage. The first iteration of the test was performed when the mass fell from 10 mm height.

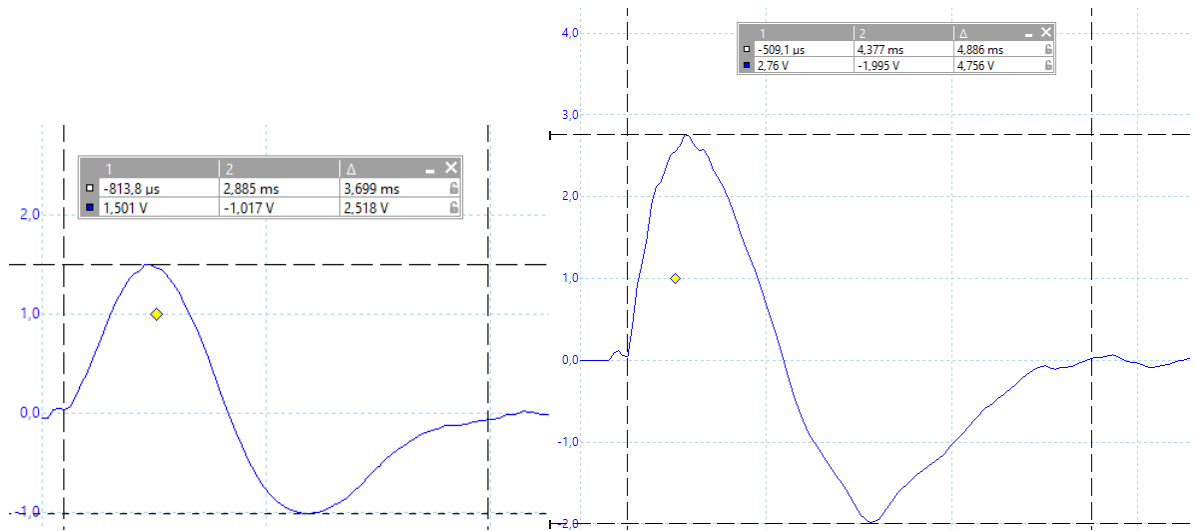


Fig. 34. Captured graphs from oscilloscope by PicoScope6 software. PVDF spiral tape cable voltage (left) and PVDF copolymer cable voltage (right)

Other test iterations were performed with the same falling mass but with heights varying from 20 mm to 100 mm. Obtained results are shown in Fig. 35.

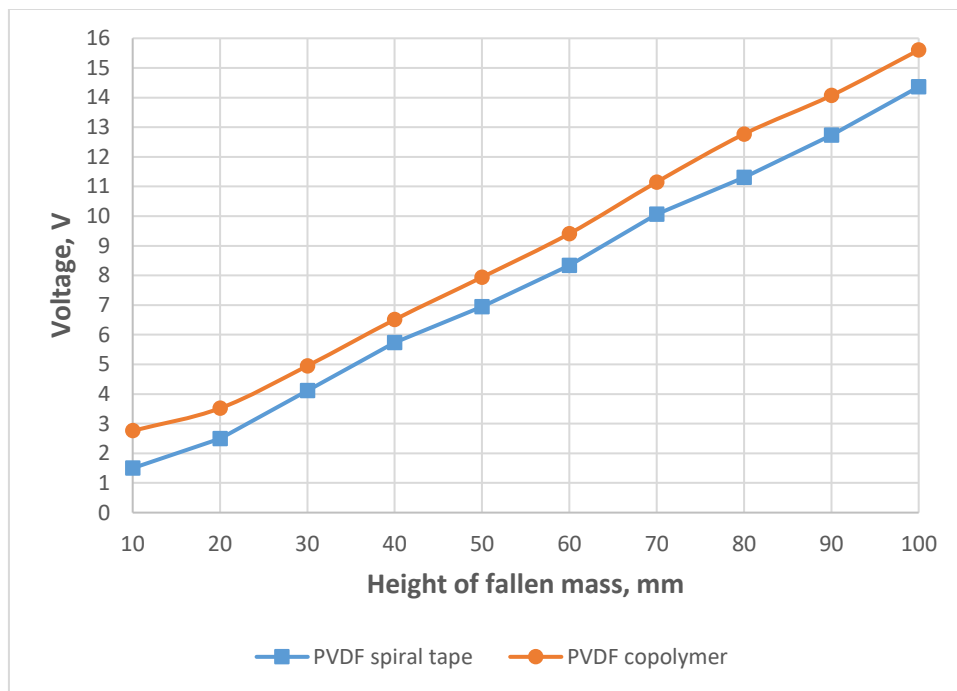


Fig. 35. Obtained results from both types of piezoelectric cables

Obtained results revealed that a PVDF copolymer cable has a higher analog signal voltage than a PVDF spiral tape cable. With each trial of the experiment, the copolymer cable generated a 1 V higher amplitude than a spiral tape cable with the same conditions, where the height of the falling mass generated the same dynamic force. Table 1 presents the specifications of both cables, and the sensitivity of electric charge from 1 N force is around 20 ± 5 pC/N and the same value for both cables. The graph (Fig. 35) shows that both cables have almost a linear dependence on the acting load. However, obtained results with voltage amplitudes show higher sensitivity by PVDF copolymer cable. For the reason of higher sensitivity of voltage, for further tests was used PVDF copolymer cable type.

3.1.2. Experimental Selection of Spacer Structure Type for Piezoelectric Sensor

The aluminum profile (Fig. 30) was presented in the methodology part, which was used as the construction part of the piezoelectric sensor. The aluminum profile has a “U” channel, which was convenient for installing the piezo cable. However, the “U” channel was too broad and deep to insert the piezoelectric cable directly. For this reason, a methodology proposed a few types of installation. Piezoelectric installation type with the rubber and silicone layer and another type with two-wired cable and a thermo tube. The rubber and the silicone are elastic and might absorb a high dynamic load so that the cable might generate less voltage signal. This experiment aimed to evaluate the sensitivity of each installation type of piezoelectric cable with different spacer materials in the aluminum profile. Samples of the construction are shown in Fig. 36.



Fig. 36. Piezoelectric construction spacer material sample with thermo tube and two-wired cable (left) and another sample with rubber and silicone layer (right)

The piezoelectric spacer material construction sample on the left side was made of a thermo tube and two-wired cable. Therefore, the sample on the right was made of rubber and silicone. The set-up schematic view and the set-up view are shown in Fig. 37.

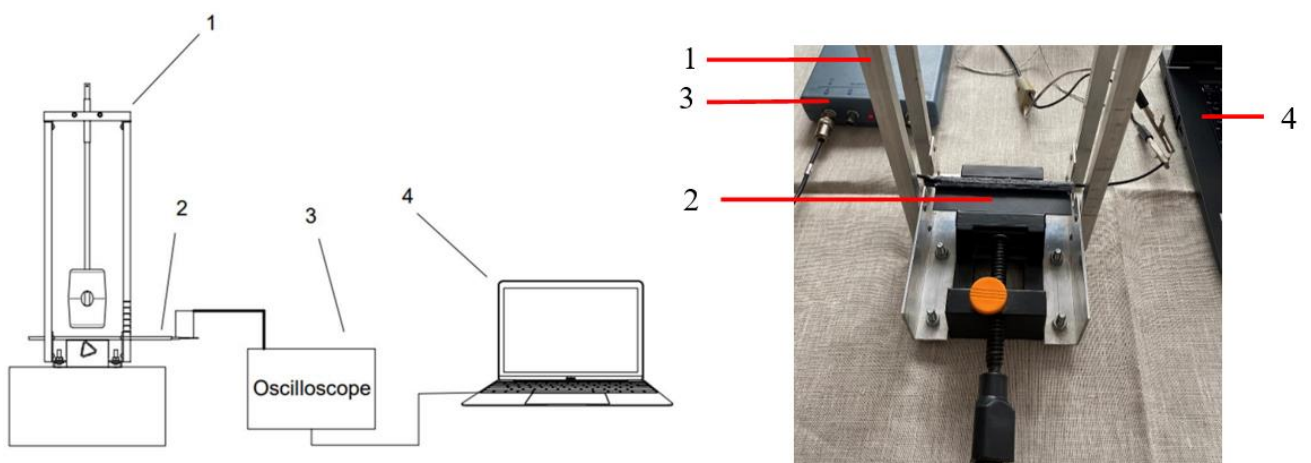


Fig. 37. Set-up schematic view (left) and set-up view (right). 1 – Punching device, 2 – Piezo sensor structure, 3 – Oscilloscope PicoScope3424, 4 – PC

For this test, was used designed punching device (1), piezo cable spacer material structure (2), oscilloscope PicoScope3424 (3), and PC with the software PicoScope 6 (4). The mass of the punching device (1) was released ten times for one sample of spacer material to test. The heights from which mass was released were from 10 mm to 100 mm. The room temperature at which the experiment was performed was 21 °C. The obtained results are graphically shown in Fig. 38.

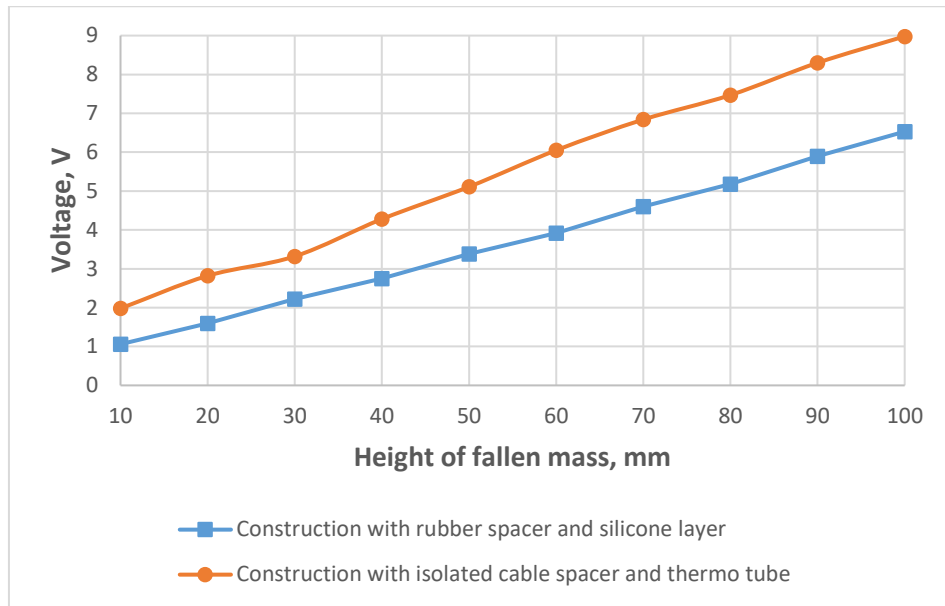


Fig. 38. Obtained results of the experiment for the selection of piezoelectric sensor spacer material

The obtained results indicated that each punching load from different heights gave a specific amount of voltage increment from a piezoelectric cable. This experiment showed that the sensitivity decreased, compared to the previous experiment, because of the cable type selection experiment (Fig. 35), then obtained 2,76 V voltage from a 10 mm fallen mass height with PVDF copolymer cable, and from this experiment results (Fig. 38) the obtained voltage from the same height is 1,06 V with rubber and silicone and 1,98 V with two-wired cable and thermo tube spacer. This phenomenon happened because the piezoelectric cable had a protective layer above the cable. In one sample, it was a silicone layer, and another one was a thermo tube. Therefore, below the piezoelectric cable, the load from the falling mass was absorbed by a rubber spacer in one sample, and in the other, it was absorbed by a two-wire cable. These construction elements absorbed load and acted as a spring. Therefore, some amount of load did not affect the cable, and less deformation was generated.

The experiment results revealed higher sensitivity from the piezoelectric sensor construction, using a two-wire cable and thermo tube. Therefore, the latter spacer material construction was around 56 % more sensitive than a construction with a rubber and silicone layer because the rubber is elastic material and absorbs a vast amount of applied load, and for this reason, piezoelectric cable was less deformed, the less voltage was obtained. For this reason, piezoelectric sensor construction with a two-wire cable and a thermo tube will be used for further investigation.

3.1.3. Temperature Impact for Piezoelectric Sensor Sensitivity

In the summertime, the temperature of the asphalt increases up to 60°C. In order to find out if the piezo cable structure can operate at such temperature, was performed, an experiment which a set-up schematic view is shown in Fig. 39. There was used designed punching device (1), a piezo sensor structure with two-wire cable, and thermo tube (2), oscilloscope PicoScope3424 (3), PC (4), thermocouple (5), digital multimeter (6) and electric heater HG-1500-CG (7). An electric heater (7) increased the temperature to 40°C, 50°C and 60°C. The digital multimeter (6) with thermocouple (5) allowed to capture the temperature reading reached at the time. With the oscilloscope (3), was measured the voltage output from the piezo sensor structure.

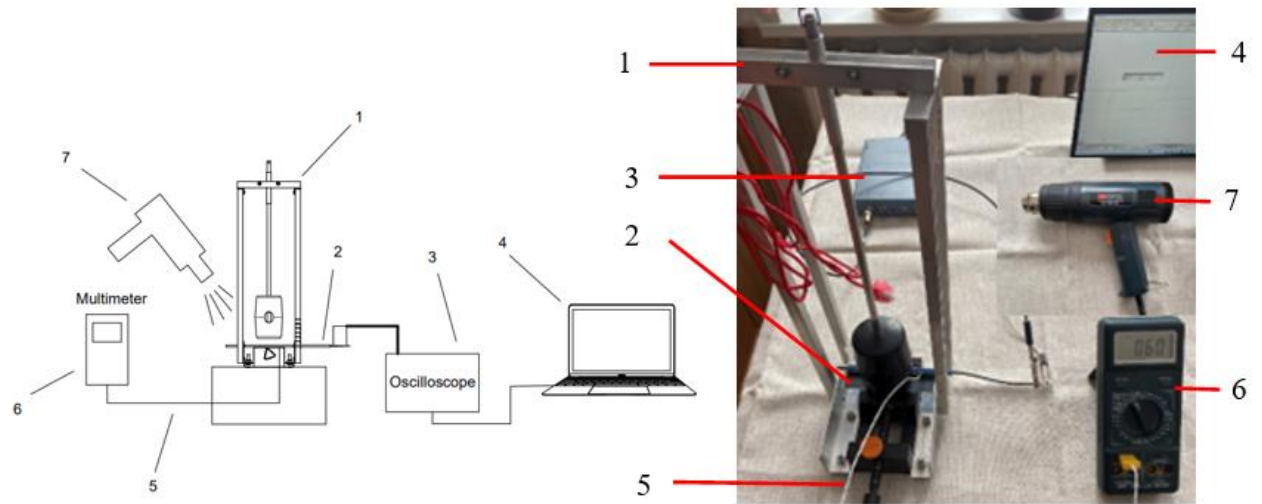


Fig. 39. Set-up schematic view of test for temperature test (left) and set-up (right). 1 – Punching device, 2 – Piezo cable structure, 3 – Oscilloscope PicoScope3424, 4 – PC, 5 – Thermocouple, 6 – Digital multimeter CHY 24CS LCR, 7 – Electric heater HG-1500-CG1

The mass of the punching device was released from 10 to 50 mm heights. At first, the sample of piezoelectric sensor construction was heated to 40°C, then measured the voltage from the sample. Next, the procedure was repeated with different heights of the mass. After the measurement's first iteration, the sample was heated to 50°C and later to 60°C. The obtained results revealed that the sensitivity of the piezoelectric sensor construction dropped due to the depolarization effect in higher temperatures. The graphic difference of voltage drop by different temperatures is shown in Fig. 40.

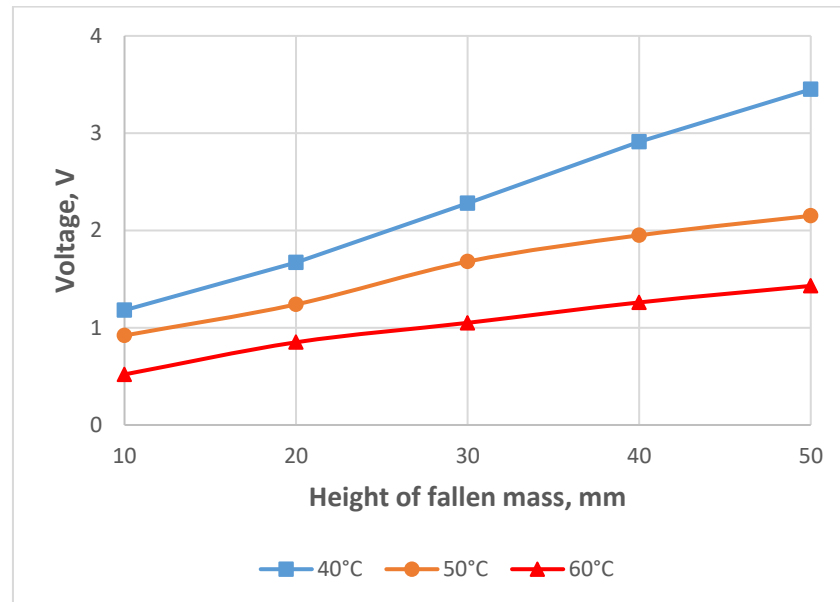


Fig. 40. Results of temperature experiment using selected piezoelectric sensor construction

The results showed that even at 60°C, the temperature of the piezoelectric sensor generates 0,52 mV at the lowest dynamic load impact. This means that in a natural environment at this temperature, the generated voltage output signal is enough to sense the signal for the controller, and the speed control system with this sensor would operate well even at 60°C. Furthermore, from obtained voltage and temperature curves, the difference was spotted that each increase of 10°C reduced the voltage output amplitude around 0,5 – 1 V with the same load.

3.1.4. Completed Construction of Piezoelectric Sensor

After performing previous experiments, there was essential to investigate mechanical properties such as construction stiffness when the load is acting on the construction. In order to investigate the stiffness of the construction, it was decided to use a double-sided aluminum profile, which would surround and protect the piezoelectric cable from the top, bottom, and sides. The exploded view of the piezoelectric sensor construction is shown in Fig. 41.

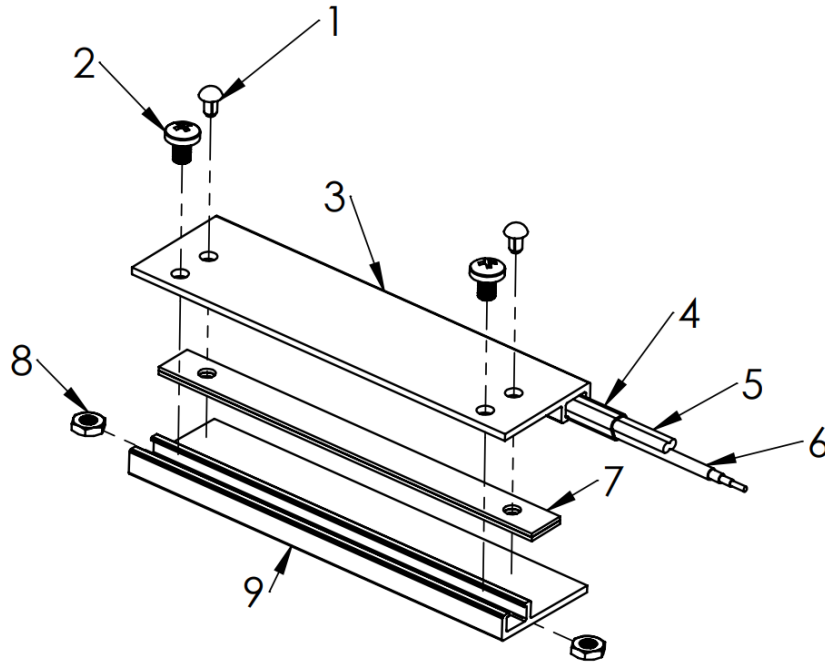


Fig. 41. Exploded view of the piezoelectric sensor construction. 1 – Rivet DIN7337 3,2x6, 2 – Bolt DIN7985 M4x6, 3 – Aluminum profile with holes, 4 – Thermo tube, 5 – Cable with two wires, 6 – Piezoelectric cable, 7 – Two aluminum tapes, 10x2, 8 – Nut DIN934 M4, 9 – Aluminum profile without holes

The previous thermal experiment used piezoelectric sensor construction with an aluminum profile (3), thermo tube (4), and two-wire cable (6). For the construction, was added aluminum profile (9), two aluminum tapes 10x2 (7), bolts DIN7985 M4x6 (2), aluminum rivets DIN7337 3,2x6 (1), and nuts DIN934 M4 (8). Assembled piezoelectric sensor construction is shown in Fig. 42.

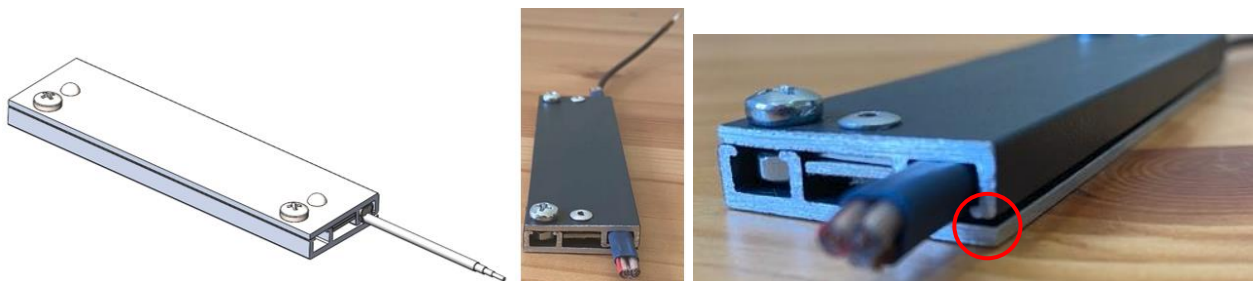


Fig. 42. Assembled piezoelectric sensor construction. Isometric view in SolidWorks environment (left) and actual sample for the experiments (middle), the same sample with the visible gap (right)

The assembled sample for further experiments had a small gap (Fig. 42) between the top and bottom aluminum profiles, which was essential to increase the sensitivity of the piezoelectric sensor because when the vehicle passed through this sensor construction, the compressive force would deform the piezo cable directly by this gap.

3.1.5. Three-Point Flexural Bending Test of the Piezoelectric Sensor

Designed piezoelectric sensor for speed enforcement system will be used on the road. Therefore, defining the maximum bending force which could withstand sensor construction in elastic deformation boundaries is essential. This experiment aims to determine how much pavement can be deformed because most asphalt roads have deformed surfaces from tires along the road. The more deformed the road, the more will bend the piezoelectric sensor. The set-up view of three-point flexural bending test is shown in Fig. 43.

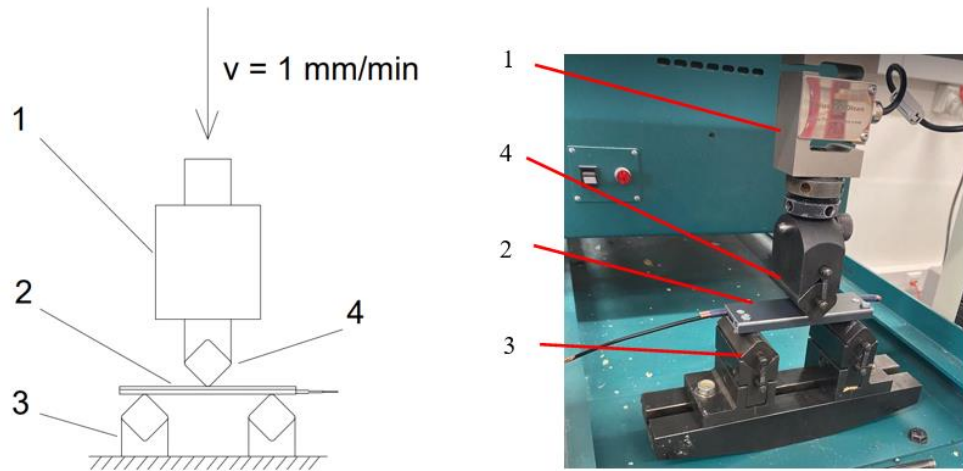


Fig. 43. Set-up schematic view of the bending test (left) and set-up (right). 1 – Force measuring sensor DBBSTOL – 10 kN, 2 – Specimen of the piezoelectric sensor, 3 – Fixed stands, 4 – Moving stand

The universal testing machine Tinius Olsen H10KT was used for the three-point flexural bending test. Fixed stands (3) and moving stands (4) were used to perform the three-point flexural bending test. The distance between fixed stands (3) was set to 85 mm. As a specimen for this test, a piezoelectric sensor was used 110 mm long (2). The bending test was performed in the weakest spot of the construction, where no bolts or rivets were placed. The force was measured by a force sensor DBBSTOL – 10 kN (1). The maximum load range was set to 10 kN, the displacement range of the moving stand (4) was set to 25 mm, and the approach speed v was set to 1 mm/min. Obtained results of the three-point flexural bending test are shown in Fig. 44.

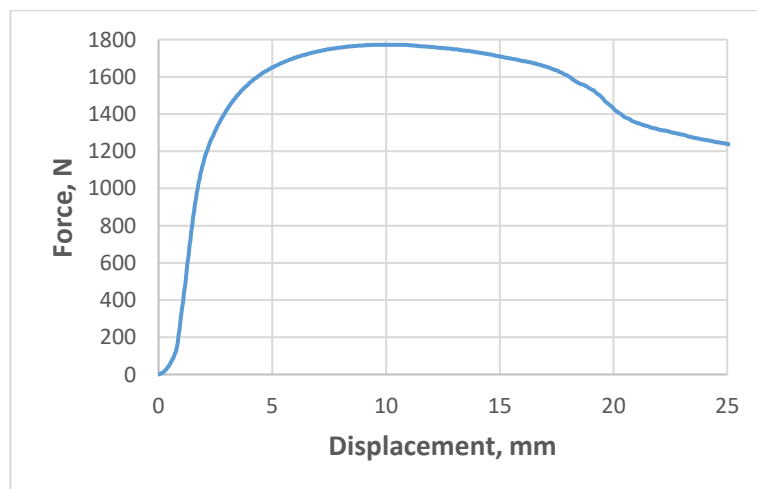


Fig. 44. Obtained results of the three-point flexural bending test, bending force versus displacement

Obtained bending test results revealed that piezoelectric sensor construction reaches yield strength when the bending force is 1366 N. Reached maximum allowable bending displacement in the elastic range was 2,6 mm. The maximum reached the tensile force of the bending was 1774 N when displacement was 10 mm. When the piezoelectric sensor's construction reached the ultimate tensile force, it cracked in the middle (Fig. 45), and then the construction gave up on resistance, and the bending force started to decrease.

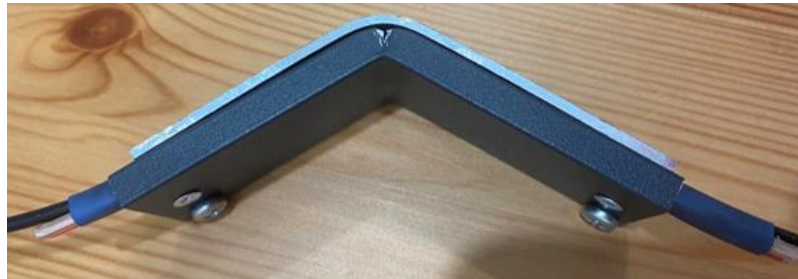


Fig. 45. Appeared crack in the piezoelectric construction when the ultimate tensile force was reached

The construction of the piezoelectric sensor can be a maximum bent of 2,6 mm while the length of the construction is 110 mm. Therefore, the construction is elastic, and when the load is unloaded, the construction comes back to the original geometric shape. As the piezoelectric sensor constructions would be 6 m long, the bending test showed that these constructions would be flexible and could be adapted to uneven road surfaces. However, the pavement of the road must be rigid and without any cracks because the piezoelectric sensor's construction cannot hold high loads when bent, especially when this construction is long.

3.1.6. Compression Test of the Piezoelectric Sensor

The designed piezoelectric sensor construction must withstand load from various types of vehicles and not break. Therefore, the maximum normal stress value from the rubbish vehicle was calculated in the methodology. The piezoelectric sensor must withstand much higher loads because when the vehicles pass the sensor, they will create much higher dynamic loads, in this case, normal stresses. For this reason, a compression test was performed for the designed piezoelectric sensor construction, which set-up view is shown in Fig. 46.

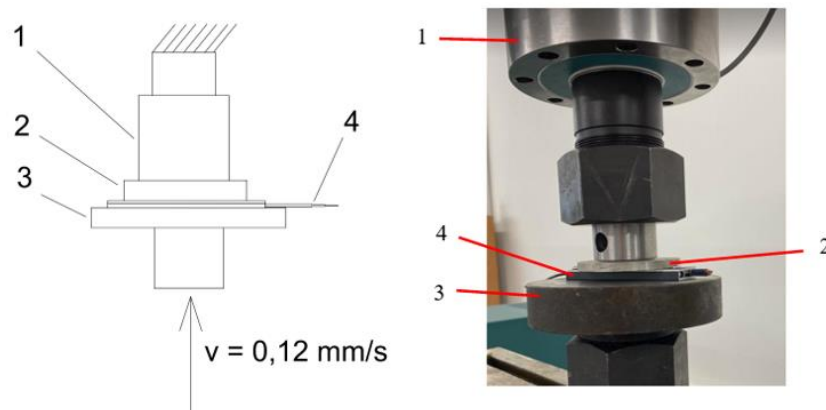


Fig. 46. Set-up schematic view of the compression test with the universal testing machine (left) and set-up view (right). 1 – Force transducer Kraftwufnehmer Typ U5 100 kN, 2 – Upper fixed plate, 3 – Lower moving plate, 4 – Specimen of piezoelectric sensor

The compression test was performed with a universal testing machine with a separate updated force transducer Kraftwufnehmer Typ U5 100 kN (1), connected to the separate controller Spider 8. The upper plate for compression (2) was fixed, lower plate (3) was moving and compressing the specimen (4). The lower plate (3) speed during the test was 0,12 mm/s. The obtained results are shown in Fig. 47.

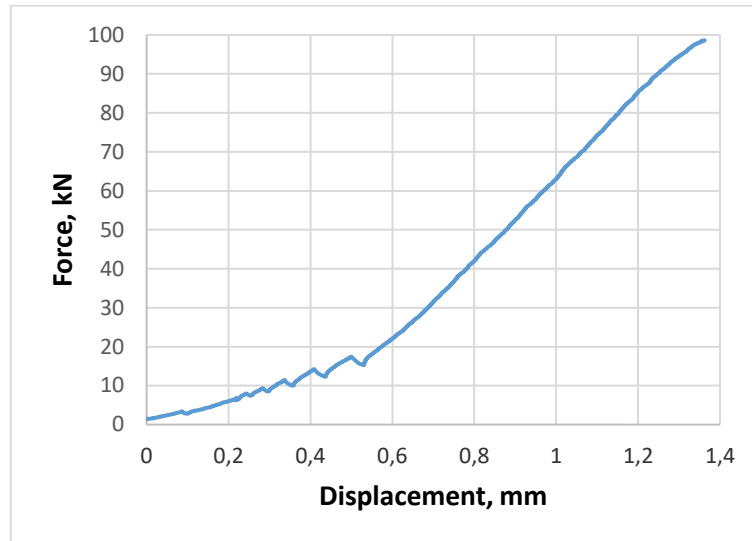


Fig. 47. Obtained results of compression test, compression force versus displacement

The obtained results from the compression test revealed that the piezoelectric sensor construction was strong enough to withstand 98 kN of compressive force, the sensor top profile was deformed a little bit, and it was barely visible deformation shown in Fig. 48.



Fig. 48. Deformed top surface edge of the aluminum profile (marked red)

From the results graph (Fig. 47) were obtained the visible compressive force increasements and decreasements in displacement range from 0 mm to 0,55 mm, which was the closing of the gap between two aluminum profiles, this gap was presented in Fig. 42. When the gap was closed, then started the compression of the whole aluminum construction. The total displacement of aluminum construction was 0,81 mm, where the acting compressive force was approximately 98 kN. Since the universal testing machine could compress the specimen to 100 kN, in order to not overload the machine, the compression test was stopped until 98,584 kN force was reached. Obtained results (Fig. 47) revealed that near the end of the experiment, the graph started to change its shape from linear to curve, and the force slightly decreased.

The surface area, which was acting as compressive yield force, was equal $S_{compr} = 2,496 \cdot 10^{-3} m^2$. The normal stress from the upper fixed plate (Fig. 46) can be calculated using Eq. 4.

$$\sigma_{compr} = \frac{F_{compr}}{S_{compr}} \quad (4)$$

where: F_{compr} is acting load from upper fixed plate to piezoelectric sensor construction (N); S_{compr} is surface area, in which was acting force from the upper plate (m²).

$$\sigma_{compr} = \frac{98584}{2,496 \cdot 10^{-3}} = 39496794,9 \text{ Pa} = 39,497 \text{ MPa}$$

From calculations of the methodology part, it was essential to ensure that the designed piezoelectric sensor construction could have enough stiffness to withstand normal stresses from the truck, which were equal to $\sigma_{normal} = 4,218 \text{ MPa}$. Divided σ_{compr} from σ_{normal} was obtained a coefficient of 9,36, which showed that the designed construction could withstand nine times heavier load than it could be created from the static force of the rubbish truck. Potentially this construction can withstand dynamic forces from these vehicles also. As the piezoelectric sensor held and was not broken with the load up to 10 t, then it means that it could withstand the heavy loads from a truck tire such as a rubbish truck.

3.1.7. Actual Test on the Road with the Vehicles

In order to realize how designed piezoelectric construction behaves in the actual environment, the abandoned road was found, where simulated actual environmental conditions. For the experiment was essential to create previously presented piezoelectric sensor construction that would be 2 m long. Two identical pieces of sensor constructions were made, fixed on the road with a distance of 4 m between each piezoelectric sensor. The fixation on the road pavement was assured with anchoring screws M5x40 with nylon tubes, shown in Fig. 49.



Fig. 49. Fixation of piezoelectric sensors with anchoring screws (marked red) on the road pavement

The distance between each anchoring screw in the piezoelectric sensor construction was approximately 150 mm. Furthermore, to obtain the designed piezoelectric construction voltage sensitivity was essential during this experiment. The used components' set-up is shown in Fig. 50.

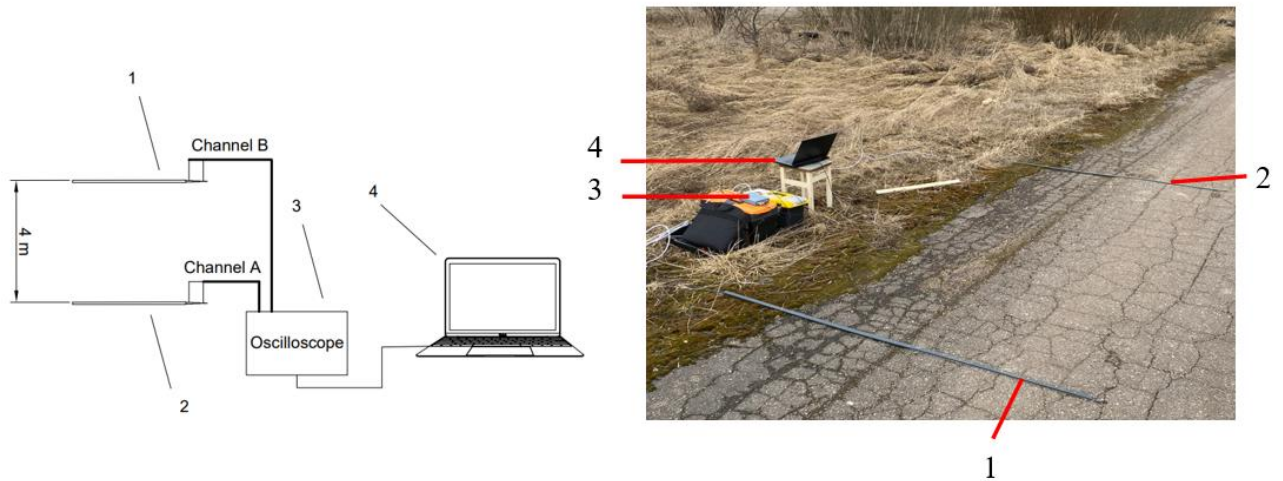


Fig. 50. Set-up schematic view (left) and set-up view (right). 1 – Piezo sensor_1, 2 – Piezo sensor_2, 3 – Oscilloscope PicoScope3424, 4 – PC

The previously mentioned piezo sensors (1) and (2) were installed at a distance of 4 m. Both piezo sensors were connected to channels A and B in oscilloscope PicoScope3424 (3). The oscilloscope (3) was connected to the PC (4) in order to read and save obtained data with voltage amplitudes from both sensors (1) and (2).

In this experiment, three types of vehicles participated: car, tractor, and motorcycle. Each vehicle hit the piezoelectric sensor with only one wheel per axle because the installed sensor construction was only 2 m long. The experiment was performed by driving at different speeds and increasing the speed by 10 km/h each time. As a result, the car and motorcycle data were recorded from 10 km/h to 70 km/h. However, the tractor could not reach high speeds, so it was asked to drive at the maximum possible speed. The obtained results were captured with the software Picoscope6, and captured example of the car is shown in Fig. 51.

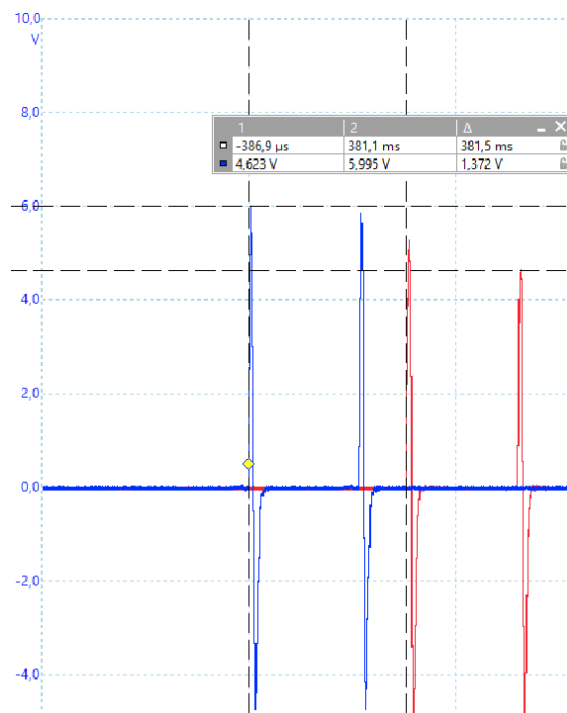


Fig. 51. Captured graphical result from a car with a speed of 40 km/h

The captured analog voltage result from a car's blue color graph was from channel B and the red graph was from channel A. Almost all voltage amplitudes were equal because the car tires were the same size, and the air pressure in the tires was almost equal. The voltage difference of 1,372 V was due to the uneven road pavement surface. These pavement deflections were copied by flexible sensor construction and affected the sensitivity of the sensors. For this reason, channel A (red graph) output voltage was slightly decreased. The graph (Fig. 51) obtained the time difference when the first axle hit the sensor_1 and sensor_2 (Fig. 50), which was equal to 381,5 ms. Therefore, the vehicle's speed from analog voltage signals can be calculated using Eq. 5.

$$v = \frac{s}{\Delta t} \quad (5)$$

where: s is the distance between the piezoelectric sensors (m); Δt is the time difference, which was started to calculate when the first axle hit the piezo sensor and stopped calculation of the time when again the same axle hit the second piezo sensor (s).

$$v = \frac{4}{0,382} = 10,471 \frac{m}{s} = 37,696 \frac{km}{h}$$

Obtained result example of the motorcycle is shown in Fig. 52.

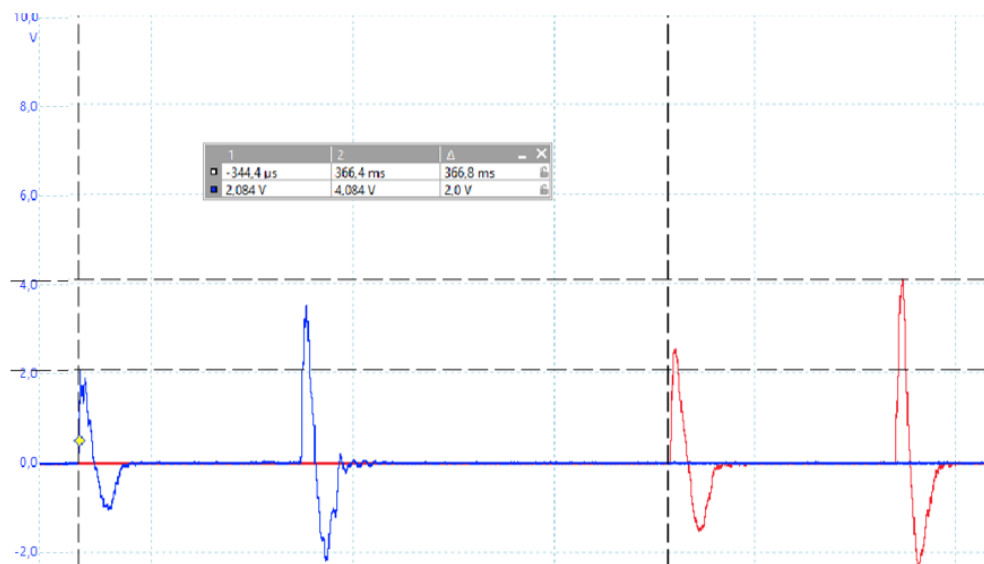


Fig. 52. Captured graphical result from a motorcycle with a speed of 40 km/h

The difference in analog voltage amplitudes from the rear and front tires was visible due to the different dimensions of the tires and the different air pressure in each tire. Moreover, the difference in voltage amplitudes was recognizable when comparing the car and motorcycle with the same speed. For example, the maximum voltage output from a car with a speed of 40 km/h was 5,995 V (Fig. 51), while a motorcycle's maximum analog generated voltage with the same speed was 4,084 V (Fig. 52). This difference is due to the different masses of the vehicles, as the car was heavier than a motorcycle, the load from a car to the sensors was higher than from a motorcycle. However, the pressure to the sensor applied decreases the voltage difference between lighter and heavier vehicles because the light motorcycle has narrow tires, and the pressure from that tire is relatively higher than the wider car tire. The same phenomena happened with the obtained voltages of the tractor, which are shown in Fig. 53.

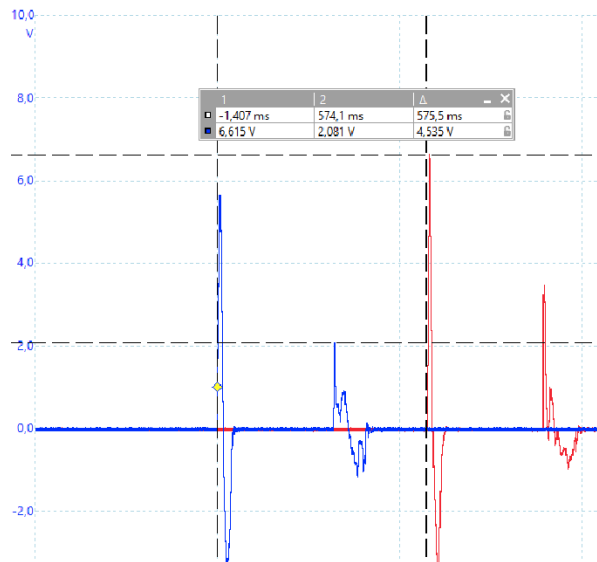


Fig. 53. Captured graphical result from a tractor with a speed of 25 km/h

The tractor's speed was low, only 25 km/h, but it generated higher voltage with narrow front tires than the car with 40 km/h due to its higher weight and narrow front tires. On the other hand, the rear tires were wide, and with low air pressure, the generated voltage from the tires to the piezoelectric sensor construction was low, about 2,081 V. However, all the analog voltages were above 1 V. Other obtained results from the vehicles are shown in Fig. 54.

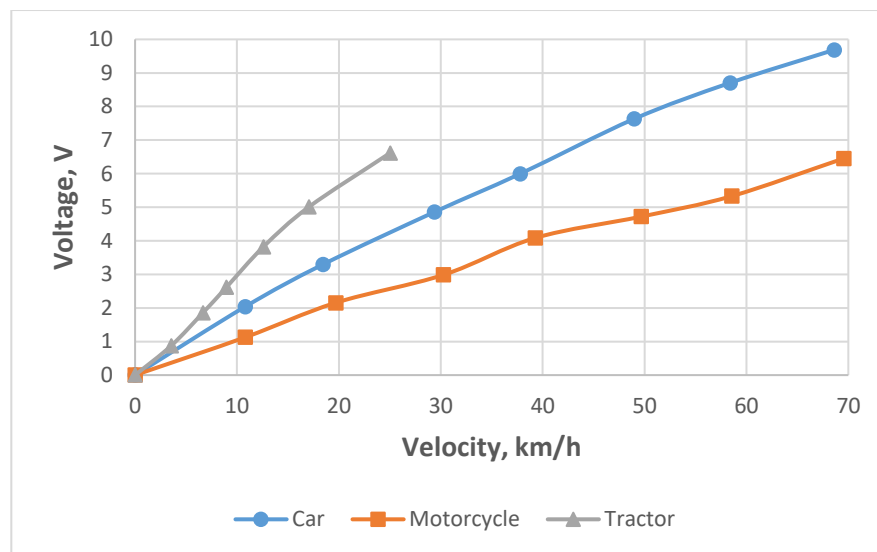


Fig. 54. Obtained results from experiments with vehicles, voltage versus velocity

The highest voltages from each experiment iteration were written in the obtained results graph. There are slight visible differences between the car and motorcycle speeds with the error because all the iterations of the speeds had to be equal to the given speed of 40 km/h. However, the calculated speed is approximately 37 – 39 km/h. This is due to the error of the speedometer, which is installed in the vehicle. Usually, speedometers show more speed than reached so drivers would not exceed the speed limit. Also, the error was due to the driver because it depended on the driver's experience to hold the exact needed speed of the vehicle. Therefore, obtained results validated the previously mentioned statement that the vehicle's weight impacts the output voltage increase. The tractor was the heaviest, and the motorcycle was the lightest, so heavy vehicles with low speed can create

the same amount of analog voltage as high-speed reached lightweight vehicles. In this case, the tractor moving at 25 km/h generated an above 6 V signal, while the motorcycle generated the same amount of voltage only at 70 km/h speed.

The voltage change at different speeds directly depends on the load a vehicle creates. The vehicle's load vector is created from two different vector components. One is a static component vector, and another is a dynamic component vector. The static component vector always has a constant load value and direction. The dynamic load component vector always has a variable meaning and variable direction. The sum of these vectors is the representative load from a vehicle. The mentioned load vectors are shown in Fig. 55. From the results graph (Fig. 54) was noticed that when the vehicle speed is meager, around 1 or 2 km/h, the obtained voltage values are around 0 V, which means that the representative load vector $\vec{a} + \vec{b}$ is only created from a static load component \vec{b} , in this case, the dynamic load component \vec{a} is equal to 0. As the speed of the vehicles was increased, the static load component \vec{b} was not changed, and it still had the maximum value. However, the dynamic load component \vec{a} increased as the vehicle's velocity increased, so the analog voltage signal was generated. This experiment proved that the obtained voltage values directly depend on the vehicle's speed.

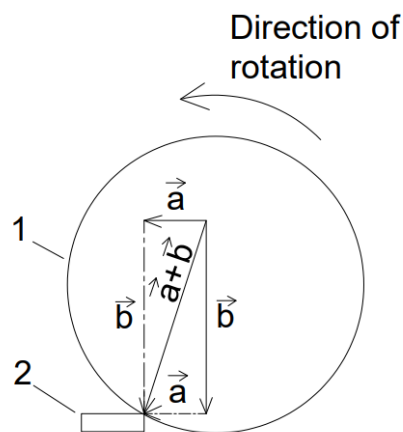


Fig. 55. Vector scheme. 1 – Vehicle tire, 2 – Piezoelectric sensor construction, \vec{a} – Dynamic load vector component, \vec{b} – Static load vector component, $\vec{a} + \vec{b}$ – Sum of load vector from a vehicle

3.1.8. Comparison of Designed Piezoelectric Sensor Construction Results with Other Authors

The research [18] designed a weigh-beam embedded in asphalt and used a PMN cement sensor underneath the construction. The vehicle with a mass of 10 t drove at 70 km/h with both tires per axle, and the generated voltage signal was only 0,3 V, which showed that sensitivity was low. The other researcher, C. Leung [20], embedded the piezoelectric cable into the pavement with plastic holders. As the vehicle passed through the sensor, the generated voltage was around 0,496 V, which was weak as the obtained signal. Another researcher [22] managed to reach 10 V of signal voltage. However, the piezo cable was installed on the road with cable protection, which is temporary and wears out fast, and as the cable was not protected with high-density material, such high sensitivity by the researcher [22] was obtained. In this study, the designed piezoelectric cable construction is reliable and can be embedded into the road surface. Piezo cable is protected adequately from mechanical wear from vehicle tires and still obtains high sensitivity from dynamic loads.

3.2. Selection of Electronic Components for the Speed Control System Prototype

Selecting electronic components is essential to operate a speed control system using designed piezoelectric sensor construction. This section of the chapter will present selected electronic components and their specifications for the speed control system prototype.

3.2.1. Selection of Analog Input / Digital Output Converter

As the vehicle drives through the piezoelectric sensor, it deforms the sensor, and the piezoelectric sensor's output generates analog amplitude voltage. The highest obtained analog voltage amplitude from an experiment on the road by a car was 9,18 V, where the vehicle speed was 70 km/h. Many industrial controllers can read analog voltage signals from 0 V to 10 V. However, the designed piezoelectric sensor construction might generate even more voltage when a car might exceed the speed of 100 km/h or even more. Accordingly, the generated output voltage could be from 10 V to 15 V, depending on the vehicle's velocity. Exceeded voltage output from the sensor would damage the industrial controller permanently. In order to protect the controller, it is essential to select an analog-to-digital converter that can accept higher analog voltage amplitude and convert it to a digitally decreased stable value which would be safe for the controller. The selected converter is an analog to digital converter PRECISION 4- 1/2 DIGIT, ADC (Fig. 56) from supplier Digi – Key Electronics [28].

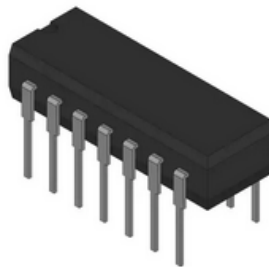


Fig. 56. PRECISION 4- 1/2 DIGIT, ADC analog to digital converter [28]

This converter can convert one analog signal with a maximum allowable amplitude of ± 18 V. Piezo cable, two contacts positive and negative wires must be connected to two converter pins. Also, it is essential to provide a direct current (DC) electric source for the converter to operate. Four pieces of piezo sensors will be used in the designed speed enforcement system, so four pieces of analog to digital converters will be used.

3.2.2. Selection of Traffic Light Element

The speed control system in this study will be equipped with traffic lights. On one side of the road will be installed one traffic light and another on the other side of the road (Fig. 22). For speed enforcement, other control systems use speed cameras, but in this study, the designed system will be only equipped with traffic lights because it is convenient to control this device of its simple operating principle. According to the law of Lithuania, “Approval of the Rules for the Installation of Road Traffic Lights” No. 3-81 [29], the traffic lights used on roads for vehicle traffic control must have three different color indicating lights, which are red, yellow, and green. Selected traffic light [31] is equipped with a 200 mm diameter, color-tinted lens, which can be seen from more than 500 m viewing distance. The supply voltage is from 100 to 240 V AC [30].

3.2.3. Selection of Relay Element for Traffic Light Lamp Switching

Since the selected traffic light supply voltage is 100 – 240 AC, it is essential to use the industrial relay, which, triggered from a lower amplitude voltage signal, could turn on and off the traffic light lamp. Furthermore, as the traffic light has three separate lamps, it is mandatory to use the relay for each. Therefore, the selected relay is an industrial [31] RV8H 1CO DC 24V 6A with a spring clamp terminal, as shown in Fig. 57.



Fig. 57. Industrial relay RV8H 1CO DC 24V 6A with spring clamp terminal [31]

The selected relay coil type is DC, meaning the relay's control signal must be a digital direct current signal. The coil voltage of DC is used 24 V, which is standard and can be triggered from the controller with a DC 24 V signal. The switching voltage is 250 V AC, which is acceptable for controlling the traffic light lamps with 240 V AC electric supply voltage. The maximum switching current is 6 A, which is also acceptable for the traffic light.

3.2.4. Selection of Control Unit Module

An analog-to-digital converter converts generated analog voltage signal from piezoelectric sensor construction to a digital signal. The input signals for programmable logic controllers are digital voltage type, so selecting the controller with at least four digital voltage inputs is essential because four piezoelectric sensors generate four independent signals. Moreover, the relays will be controlled by a digital voltage signal with 24 V voltage. For this reason, selecting the controller with at least six digital output pins is essential because the controller must control three lamps for one traffic light and another three for another.

There is no standard controller on the market as a standalone product with the needed input and output pins for this project, so it is decided to select a modular programmable logic controller (PLC), where needed modules are added for the PLC with the needed amount of input and output pins. The selected controller consists of four main modules: power supply module, central processing unit (CPU) module, digital input, and digital output modules (Fig. 58). Each module is selected from the supplier “SIEMENS” online configurator [32]. The selected power supply module is SIMATIC PM1207/1AC/24VDC/2.5A, which is compatible with CPU 1212C, 8DI/6DO/2AI. The selected CPU has eight digital inputs, six digital outputs, and two analog inputs. As there is a need for at least four digital inputs and at least six digital outputs, there is a selected digital input module Digital Input SM 1221, 8DI, 24V DC with eight digital inputs and also selected digital output module Digital Output SM1222, 8 DO, 24V DC with eight digital outputs.

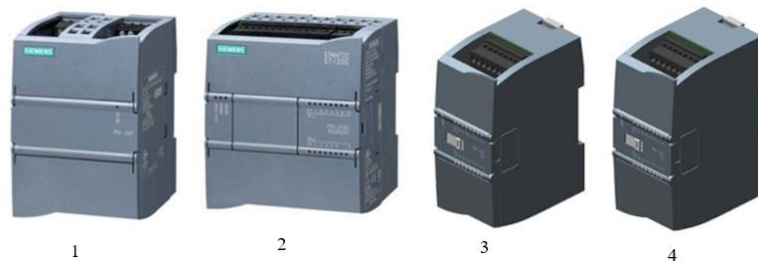


Fig. 58. Selected PLC modules. 1 – Power supply module, 2 – CPU, 3 – Digital input module, 4 – Digital output module [32]

Although selected Siemens Simatic S7-1200 PLC is a primary type of controller with this brand's lowest price, it would perfectly control the designed speed control system. Furthermore, these modules are manufactured for industrial use and can be used in wet environments because they have an IP 65 protection rating.

3.2.5. Circuit Prototype of Electronic Components

All previously selected electronic components would be connected with wires to ensure the closed circuit. The schematic view of the designed speed control system is shown in Fig. 59. Piezo sensors (1), (2), (3), and (4) are installed in the road pavement, traffic lights (5) and (6) are used for each of the traffic lines. In the controller box (7) are placed other smaller electronic components such as the PLC, analog-to-digital converters, and relays. The wiring in the scheme is provided with the dashed line, where analog data flows through four wires from one pair of piezo sensors (2) and (3) to the controller box (7). Another four wires are for the other two sensors (1) and (4). One phase AC, three wires, and one neutral wire are connected to one traffic light (5) by the road's path. Another traffic light (6) is also connected with one phase, three separate AC wires, and one neutral wire. However, these wires must be embedded in a narrow cut out through the asphalt to install the wires on the other side of the road. All the wires must be used with protective armor in order to protect wires from mechanical wear.

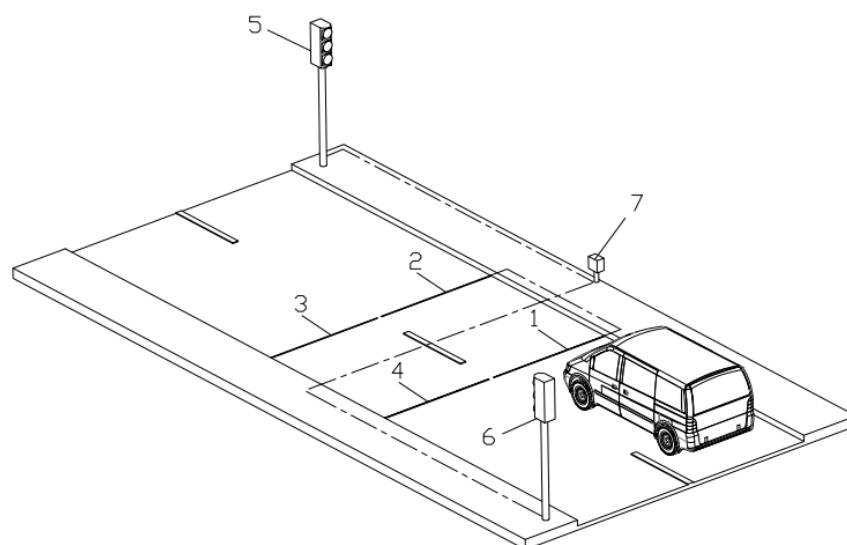


Fig. 59. Schematic view of the speed enforcement system electronic components and wiring (dashed line). 1 – Piezo sensor_1, 2 – Piezo sensor_2, 3 – Piezo sensor_3, 4 – Piezo sensor_4, 5 – Traffic light_1, 6 – Traffic light_2, 7 – Controller box

A detailed circuit prototype view of wired electronic components is shown in Fig. 60. The power supply is from an alternative current (AC) source, which only uses phase and neutral wires. Traffic lights (1) and PLC (3) have an AC power supply. The piezoelectric sensor (5) does not need a power supply because it generates an electric signal by itself and gives the analog signal to A / D converter (4). The converter (4) is supplied by direct current (DC) from PLC digital output, and the converted analog signal to digital is sent to the digital input module of the PLC (3). The PLC control relays (2) with digital output signals. According to the signal value, the relay switches on or off the AC power supply to the traffic light lamp (1). There also must be used a fuse in this electric circuit for protection. Also, grounding is essential for each electronic component to be connected directly to the ground to avoid high voltage because high voltages from energized metallic surfaces can be fatal for a human.

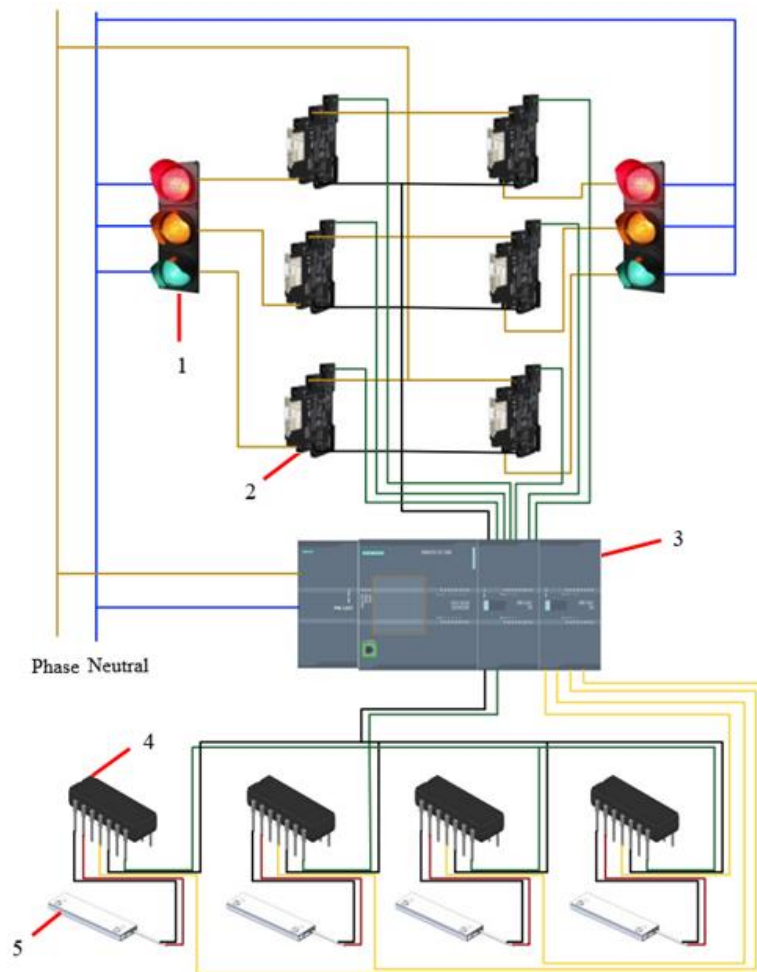


Fig. 60. Circuit prototype of the electronic components. 1 – Traffic light, 2 – Relay, 3 – PLC, 4 – Analog-to-digital converter, 5 – Piezo sensor. Wires: Brown – Phase, Blue – Neutral, Red – Analog signal terminal, Black – Ground, Yellow – Digital input, Green – Digital output.

3.3. Control Logic Evaluation for the Speed Enforcement System Prototype

The previous section of the chapter completed a selection of electronic components that could be used in a designed speed enforcement system. There is also an introductory section for evaluation of the control logic, in what sequence would all of the components be controlled so that the system would work properly. Finally, this section of the chapter will present the operation algorithm, a prototype of code in the Tinkercad environment.

3.3.1. Main Assumptions for the Speed Control System Logic

It is essential to define the distance between the piezoelectric cables and the distance between the piezoelectric sensors and traffic lights. In the investigation [22], the distance between the piezoelectric cables was set to 5 m. This distance ensured that the obtained analog signal voltages did not interfere with each other. If the cables were closer, for instance, 1 m, at higher vehicle speeds when the vehicle hit the piezo cable, the obtained signal would start to fluctuate over time. Subsequently, when another piezo cable was hit rapidly after, the first obtained signal would still generate voltage pulses, and the second signal would interfere with the first. As a result, the controller could receive incorrect data and struggle to perform accurate calculations. To avoid this problem, often is selected 5 m or 6 m. In order to save expenses on wires, it was selected to shorten the distance to 4 m because from the experiment obtained results, no interference between two piezoelectric sensors was detected with the highest 70 km/h speed. As the speed enforcement system prototype would be used in residential areas, where the speed restriction would be from 30 km/h to 40 km/h, using 4 m between the piezo cables is acceptable. A schematic view of the speed enforcement system is shown in Fig. 61. In the scheme, the distance between piezo sensors (2), (3), and (1), (4) is defined with the letter W .

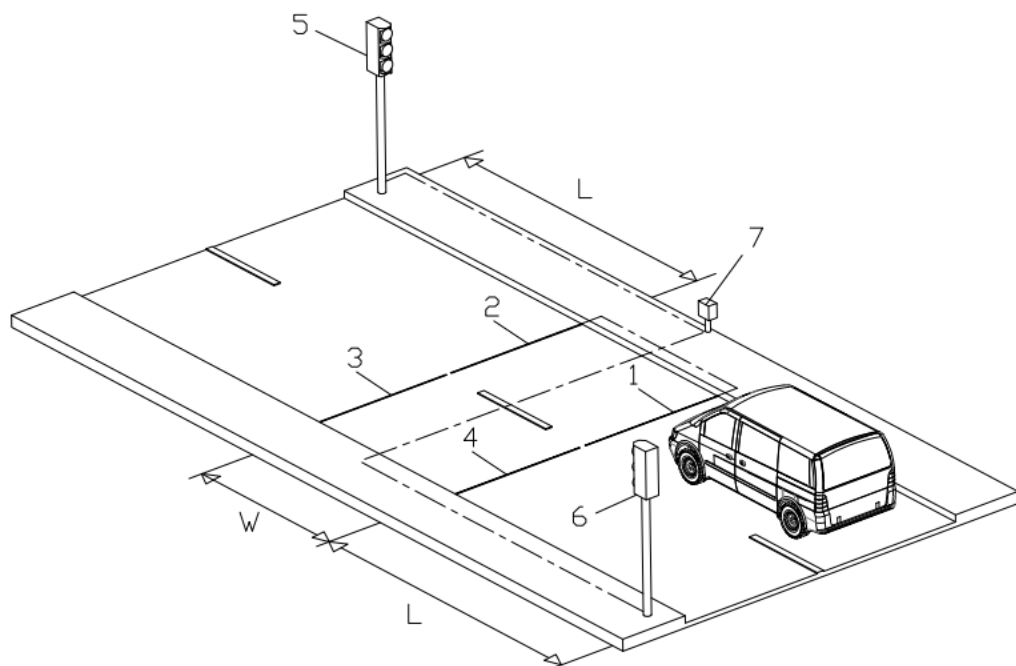


Fig. 61. Schematic view of the speed enforcement system prototype electronic components and wiring (dashed line). 1 – Piezo sensor_1, 2 – Piezo sensor_2, 3 – Piezo sensor_3, 4 – Piezo sensor_4, 5 – Traffic light_1, 6 – Traffic light_2, 7 – Controller box, W – is the distance between piezo sensors, L – is the distance between last piezo sensor and traffic light

According to the law of Lithuania, “Approval of the Rules for the Installation of Road Traffic Lights” No. 3-81 [29], the traffic lights must be visible at least 35 m distance when the speed limit is 50 km/h and 80 m when the speed limit is 70 km/h. In this case, the distance between the last piezo sensor and the traffic light should be 35 m because the speed limit is not higher than 50 km/h, and this distance in the schematic view is defined as L . However, in the same document [29] there is stated the operation time of each traffic light lamp. When the traffic light green lamp changes to yellow and red, it must blink twice for 3 s. After that, the green lamp is switched off, and the yellow

is turned on for 2 s and turned off. Before the red lamp is turned on, the sequence of green and yellow takes time of 5 s, which is essential to have in mind, because this is the time duration when the speed violator must stop before the traffic light. For this reason, it was decided that the distance L must be 100 m. If the speed limit is 40 km/h, it is enough time to stop before the traffic light because the 100 m to travel that distance around 40 km/h takes around 9 s. Even with the exceeded speed of 70 km/h, stopping is possible because traveling a 100 m distance with that speed takes around 5,3 s.

3.3.2. Operation Algorithm of the Speed Control System Prototype

The designed speed control system prototype does not measure the vehicle's speed directly. It just obtains signal pulses, which are converted to digital values. The speed evaluation principle is based on time evaluation. When the analog voltage signal is converted to the digital one from the piezo sensor, at that moment, there must be started time calculation. When the other piezo sensor is activated, the timer is turned off. The allowed time, which is set for the distance to pass between two piezo cables, is evaluated with obtained time from a vehicle. The operation algorithm simplified scheme is provided in Fig. 62.

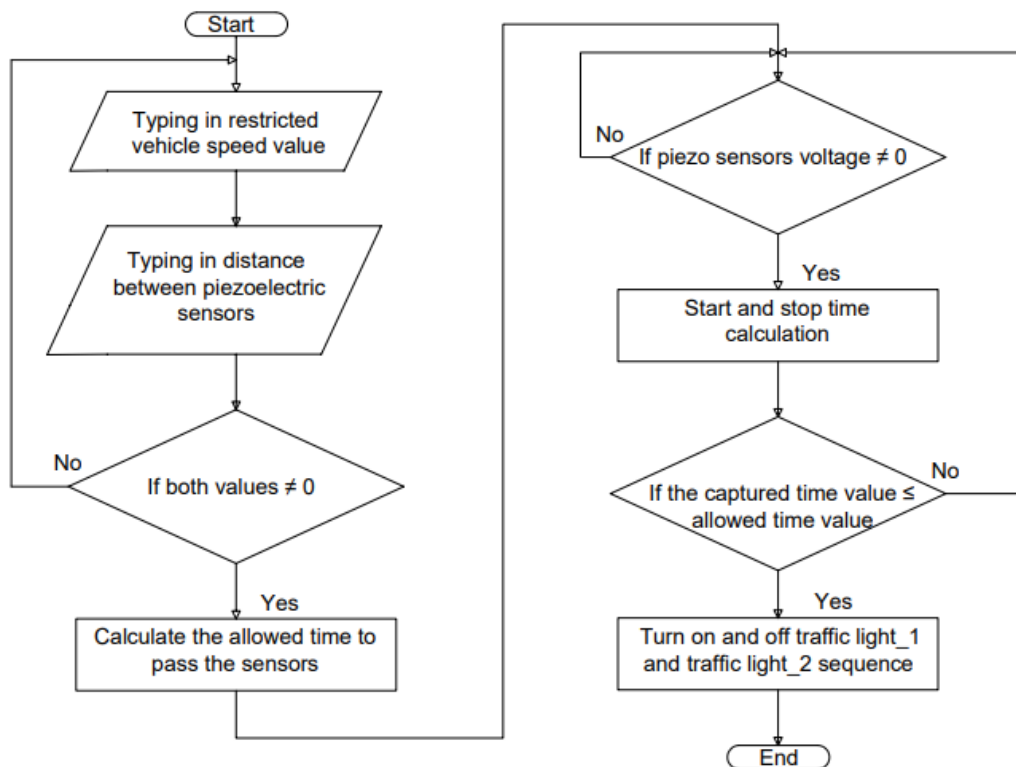


Fig. 62. Simplified scheme of operation algorithm

In the algorithm ellipse shape geometric form defines the beginning and end of the algorithm. The geometric parallelogram shape defines typed-in values, which an operator must set. The rhombus geometric shape defines the „IF“ statement, where the decision must be made. Finally, a rectangle geometric shape defines an action that must be performed. The simplified algorithm scheme at the beginning asks to type in restricted speed value and the distance between piezoelectric sensors. If both values are provided, there is a calculated time duration for passing through the sensors. After

that, piezo sensors are checked to see if any signal is captured. If yes, the time calculation is later stopped if the signal is captured from another piezo cable. This checking must be done for both sensor groups. After that, the time evaluation must be performed if captured time is less than allowed. If yes, then a traffic light sequence must be started. If not, then the check of the piezo sensors must be started again. A detailed scheme of the algorithm is provided in Appendix 1.

3.3.3. Simulation of Code in the Tinkercad Environment

In order to operate the speed enforcement system, it is essential to write code according to the provided algorithm. For the simulation of the logic for the speed enforcement system was used a Tinkercad simulation environment was used, where the circuit of the prototype is shown in Fig. 63. For the simulation of operation principle for a prototype was used Arduino Uno R3 microcontroller (1), LED lamps (2) and (3) to imitate both traffic lights, resistor (4) for each LED to protect from high currents and analog pushbuttons (5), (6), (7) and (8) to imitate the piezo sensors.

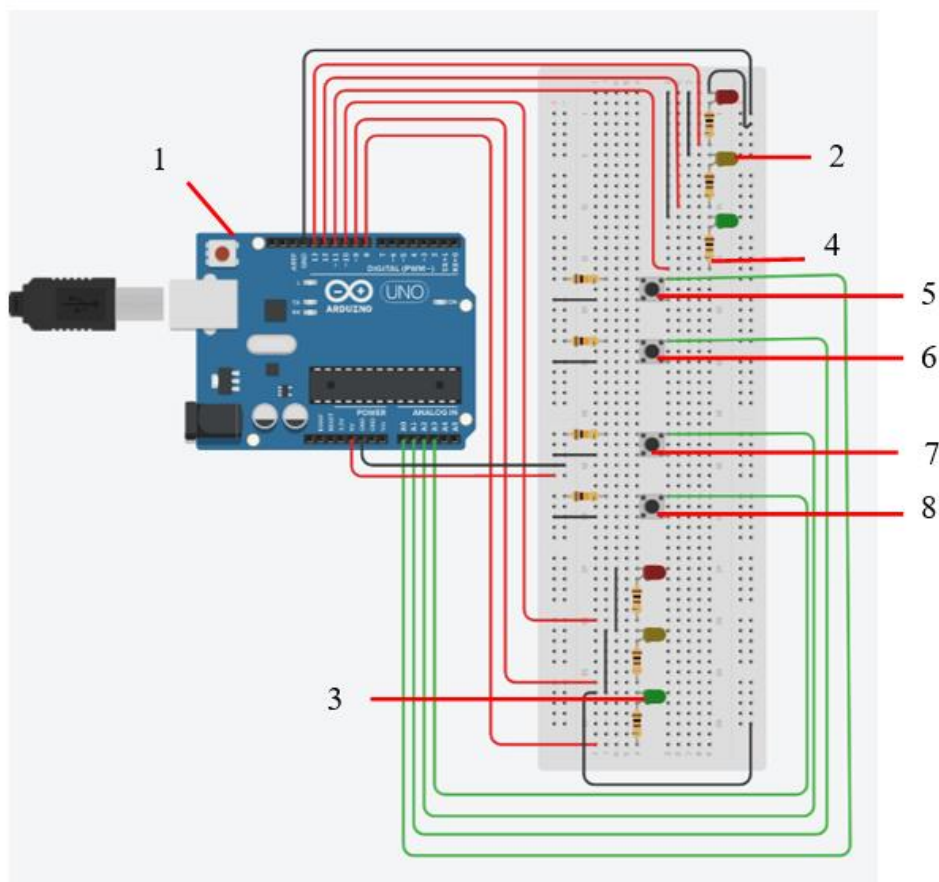


Fig. 63. Circuit of the prototype in Tinkercad environment. 1 – Arduino Uno R3, 2 – LED lamp as traffic light_1, 3 – LED lamps as traffic light_2, 4 – Resistor, 5 – Analog pushbutton as piezo sensor_1, 6 – Analog pushbutton as piezo sensor_2, 7 – Analog pushbutton as piezo sensor_3, 8 – Analog pushbutton as piezo sensor_4

The code is written in C++ language and is provided in Appendix 2. The electronic scheme of the speed control system prototype in the Tinkercad environment is shown in Appendix 3. The code is written following the operation algorithm. When pushbutton (5) is pressed, it sends a signal to the Arduino's analog input. The signal is sourced from the Arduino's 5V pin. Once the analog signal is received, the pushbutton trigger is activated, and the time starts counting for each cycle, with a time

refresh rate of 100 ms. When pushbutton (6) is pressed, the time counting is halted, and the captured time value is evaluated against the allowed time count value. If the captured time value is less than the allowed one, the traffic light sequence algorithm begins, and the red LED starts to glow. The same happens with the other group with pushbuttons and LEDs. With the provided control logic, the PLC with appropriate code language as ladder logic could operate.

3.4. Summary of the Chapter

Overall, this chapter focused on the design and experimentation of the piezoelectric sensor construction for a speed enforcement system. The experiments involved selecting the appropriate piezoelectric cable type, determining suitable spacer materials, testing the sensor's sensitivity to temperature and bending, and evaluating its performance on the road. The findings indicated that the PVDF copolymer cable had higher voltage sensitivity compared to the PVDF spiral wrap cable, and a two-wire cable with a thermo tube spacer provided optimal sensitivity. The sensor construction proved to be flexible, withstand a 10 t load, and generate sufficient voltage for operation under real road conditions. Additionally, in the chapter were outlined the main electronic components of the speed enforcement system, including piezoelectric sensors, an analog-to-digital converters, a programmable logic controller (PLC), and traffic lights. The system's logic was based on distance assumptions between sensors and traffic lights, with a specific time evaluation principle to determine the sequence of traffic lights based on the activation of piezo sensors.

4. Cost Estimation of the Speed Enforcement System

This chapter will calculate the total cost of each component used in the speed control system prototype. Therefore, will be calculated the labor cost, which will be directly dependent on the time spent.

4.1. The Cost Estimation of Each Component

The cost estimation was based on today's prices, and each component cost is evaluated in what is offered in the market today. The cost of each component is provided in Table 2.

Table 2. Cost of each component of the speed enforcement system

No.	Item	Cost, Eur
1	Piezoelectric copolymer cable 12 m	713,16
2	2 x Traffic signal docking lights	1077,24
3	4 x Analog to digital converter	17,96
4	4 x Industrial Relay RV8H	53,84
5	Simatic S7-1200 power module	168,98
6	Simatic S7-1200 CPU module	350,9
7	Digital input SM 1221 module	112,8
8	Digital output SM 1222 module	158,88
9	Siemens Simatic memory card	52
10	Rail for hanging the PLC modules	32,59
11	Siemens Simatic STEP 7 software	197,1
12	Cable of 5 wires 1,5 mm ² 216 m	278,64
13	Control box	105,59
14	Cable of 2 wires 1 mm ² 40 m	34,98
15	Fuse Eaton	5,69
16	Aluminum profile 28 m	260
17	Zinc pipe 108x2 mm 6 m	289,2
18	Cable protection 250 m	162,5
19	Cold asphalt mastic 25 kg	132,5
20	Anchors M5x40 3 packs	10,92
21	Bolts DIN7985 M4x6 3 packs	3,7
22	Nuts DIN934 M4 3 packs	3,3
23	Rivets DIN7337 3,2x6 3 packs	5,24
24	Thermo tube 12 m	5,4
25	Connectors 2 packs	21,39

There are 25 different components of this system, which are used for the system to operate correctly. The quantities are expressed in pieces, meters, packs, or kilograms. The approximate cost of all the components is 4255 Eur. The tools needed for building the speed enforcement system are not included because they can be rented, and rent prices differ in each dealer shop. The main tools

and machinery for rent would be a grinder with a disc for asphalt cutting and a mini excavator for digging in the ground for cables.

4.2. Labor Cost Estimation

Evaluating the approximate labor cost for the designed speed enforcement system prototype is essential because it takes time to build, design, manufacture and assemble the piezo cable construction and the whole speed enforcement system. Therefore, the labor cost of the speed enforcement system is calculated in Table 3.

Table 3. Labor cost for preparing the project and assembling

Operation	Time spent, h	Price, Eur
Cutting of profiles	1	25
Drilling	3	75
Assembling piezo sensors	4	100
Assembling the project	16	400
Modeling the project	10	250
Preparation of drawings	5	125
Programming	6	150

The one-hour labor price was assumed to be 25 Eur, and the total number of hours needed was approximately 45 h, so the estimated approximate labor price was 1125 Eur. This means that the total approximate cost of the designed speed enforcement system would cost 5380 Eur, including the cost of components and labor cost. However, this cost is without rented equipment and tools.

Evaluating the existing fixed speed camera cost just as a device starts from 14405 Eur [33]. This price is without the seller's suggested additional years of cloud data or assembling labor costs. Therefore, fixed-speed cameras are more than twice the price, and additional data management costs would exist. Moreover, the average speed camera systems cost even more because there are more cameras and more components. According to the article [34], in 2019, the average speed camera system cost was approximately 60000 Eur. With today's prices mentioned, systems now cost even more.

4.3. Summary of the Chapter

Overall, the chapter outlined the total cost estimation of the prototype speed control system by calculating the cost of each component required to build the system. The estimated cost of all the components used in the system was approximately 4255 Euros. Additionally, the chapter evaluated the labor cost needed to build, design, and assemble the piezo cable construction, estimated at around 1125 Euros. Therefore, the estimated cost of the designed speed enforcement system, including components and labor, was 5380 Euros. A fixed speed camera system costs twice as much as this study investigated a piezoelectric speed enforcement system. In contrast, an average speed camera system costs even more than current market prices. For these reasons, the designed speed enforcement system would be a more cost-effective solution than existing speed camera systems.

Conclusions

1. To design a speed enforcement system, road structural elements were developed, including piezoelectric cables and protective aluminum construction. Experiments showed that the PVDF copolymer cable had approximately 50% higher sensitivity than the PVDF spital tape cable. The two-wire cable and thermo tube spacers exhibited around 56% higher sensitivity than silicone and rubber spacers. Temperature tests revealed a sensitivity drop of approximately 72% at 60°C, but even under the lowest load impact, an acceptable analog signal voltage of 0,52 V was obtained. Flexural bending tests demonstrated the flexibility of the sensor construction for uneven pavement, while compression tests indicated it could withstand forces up to 98 kN, making it 9 times more robust than the stress from a fully loaded rubbish truck tire. On-road tests with vehicles (car, motorcycle, tractor) confirmed proper sensor operation, with the highest voltage of 9,18 V recorded from a car traveling at 70 km/h.
2. The speed enforcement system prototype required the selection of electronic components, and five main components were chosen: piezoelectric sensor, PLC, traffic light, relay, and analog-to-digital converter. An analog-to-digital converter with a ± 18 V range was selected to safeguard the PLC inputs from high voltages. The chosen PLC was modular, providing flexibility to accommodate modifications by combining different quantities of digital inputs and outputs. The traffic lights selected were designed for AC power supply, allowing them to be controlled by relays that were, in turn, controlled by the digital output signal from the PLC.
3. The control logic for the speed enforcement system was designed following the Lithuanian standard, specifying the sequence and duration of traffic light signals. The transition time from green to red light was set at 5 s. Based on this duration, it was determined that the distance between the traffic light and the piezoelectric sensor should be a minimum of 100 m. The control algorithm, presented in a flowchart format, compared the activation time of the piezo sensors with the allowed time. If the time difference between activations were shorter than the allowed threshold, the traffic light would turn red, indicating a speed violation. The code, written in C++, was simulated using LED lamps and analog pushbuttons in the Tinkercad environment.
4. The cost of the designed speed enforcement system was calculated based on current prices in the market, and each system component would cost 4255 Eur. In addition, the labor required for its implementation would amount to 1125 Eur. Therefore, the total cost of the system would be 5380 Eur. This price represented a significant cost advantage, being more than twice as affordable as fixed speed control cameras available in the market. Comparatively, the cost of an average speed control system exceeds 60000 Eur, making the designed system a highly cost-effective alternative to existing camera-based systems.

Recommendations

This research was completed with the tasks given to design speed enforcement system in residential areas. However, the completed research brought new questions which are worth to be investigated in further research. The recommendations for further research are listed below.

1. To investigate different geometry profiles for piezoelectric sensor construction. The designed protective profile should have less consisting parts. In that profile, an accurate installation groove for the piezoelectric cable should be used, which would not be necessary to use additional spacer materials.
2. To investigate protective aluminum profile properties in saline environments and to compare these properties with stainless steel material properties. As the piezoelectric sensor would be used in roads, in winter, roads usually have much salt on them to melt the snow on the roads. Therefore, this investigation would answer how reliable the aluminum material profile is in a saline environment.
3. To compose a speed enforcement system with wireless communications between the PLC and traffic lights. This would simplify the assembly process and would be a time-saving option. However, evaluating the changed estimated cost and reliability is necessary because the more electronic components in the system are used, the higher the probability of failing components might occur.
4. To conduct a sensitivity test of the designed piezoelectric road structural element when the sensor is embedded into the asphalt pavement and covered by cold asphalt mastics. The obtained voltage output results could be compared with obtained results in this study when the sensor was attached to the asphalt pavement. When the sensor is embedded into the road surface, there would be a potentially decreased risk of sensor damage if the vehicle brakes.

List of References

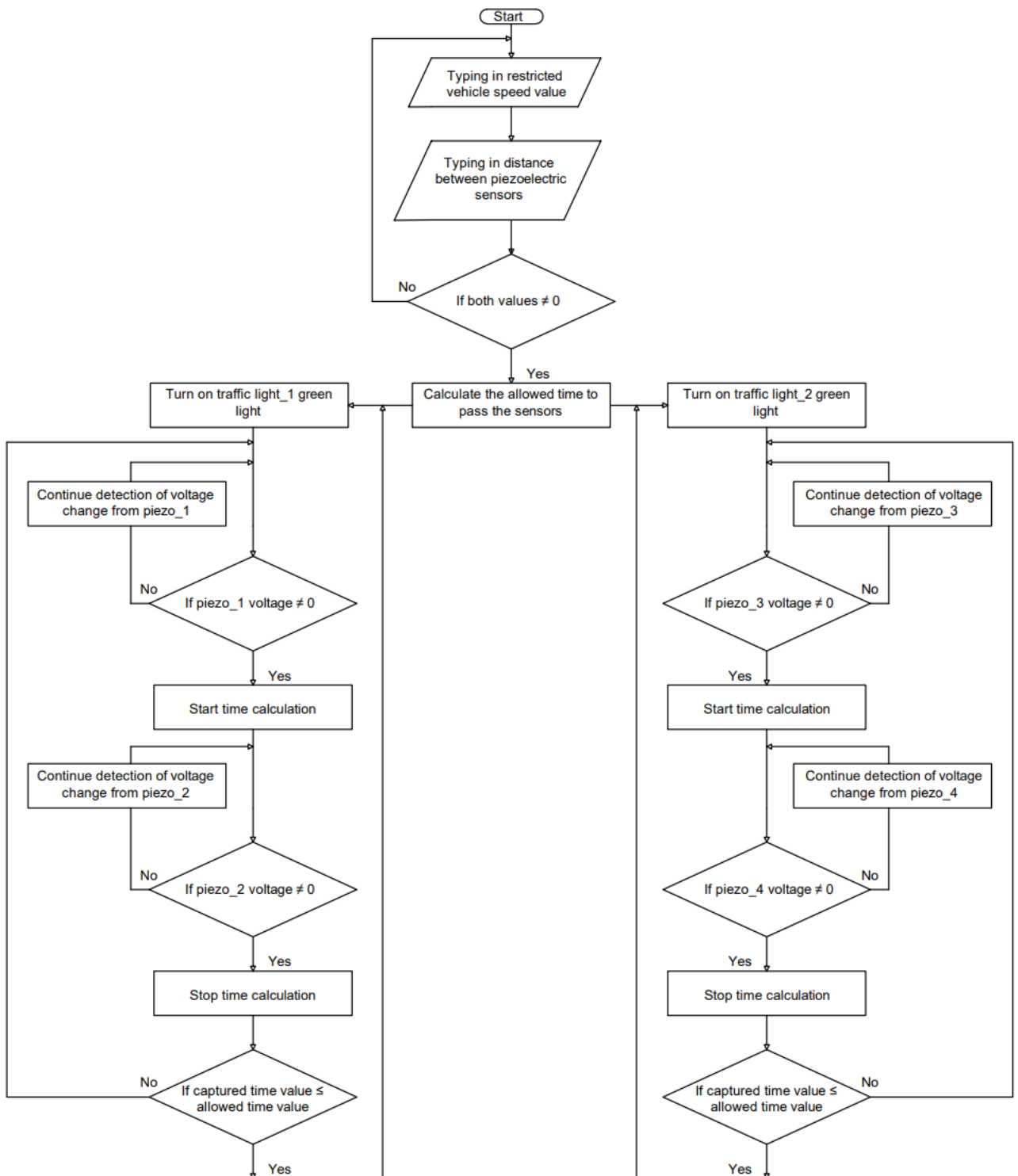
1. DISTEFANO, Natalia; LEONARDI, Salvatore. Evaluation of the effectiveness of traffic calming measures by SPEIR methodology: framework and case studies. *Sustainability*, 2022, 14.12: 7325.
2. GONZALO-ORDEN, Hernán, et al. Effects of traffic calming measures in different urban areas. *Transportation research procedia*, 2018, 33: 83-90.
3. SHAABAN, Khaled; MOHAMMAD, Anas; ELEIMAT, Ahid. Effectiveness of a fixed speed camera traffic enforcement system in a developing country. *Ain Shams Engineering Journal*, 2023, 102154.
4. KUNKLER, Jan; BRAUN, Maximilian; KELLNER, Florian. Speed Limit Induced CO₂ Reduction on Motorways: Enhancing Discussion Transparency through Data Enrichment of Road Networks. *Sustainability*, 2021, 13.1: 395.
5. HEO, Deokjae, et al. Triboelectric speed bump as a self-powered automobile warning and velocity sensor. *Nano Energy*, 2020, 72: 104719.
6. SINHA, Aditya, et al. Green energy generation from road traffic using speed breakers. *Materials Today: Proceedings*, 2021, 38: 160-168.
7. TUTUMLUER, Erol, et al. Sensing Infrastructure for Smart Mobility—Wireless Continuous Monitoring for I-ACT. *I-ACT-21-08*, 2022.
8. DISTEFANO, Natalia; LEONARDI, Salvatore. Evaluation of the benefits of traffic calming on vehicle speed reduction. *Civil Engineering and Architecture*, 2019, 7.4: 200-214.
9. GOENAGA, Boris; UNDERWOOD, Shane; FUENTES, Luis. Effect of speed bumps on pavement condition. *Transportation research record*, 2020, 2674.9: 66-82.
10. HO, Cheng-Yu; LIN, Huei-Yung; WU, Lu-Ting. Intelligent speed bump system with dynamic license plate recognition. In: *2016 IEEE International Conference on Industrial Technology (ICIT)*. IEEE, 2016. p. 1669-1674.
11. LAHRMANN, Harry Spaabæk, et al. Safety impact of average speed control in the UK. *Journal of transportation technologies*, 2016, 6.5: 312-326.
12. OLIVEIRA, Daniele Falci de, et al. Do speed cameras reduce speeding in urban areas?. *Cadernos de Saúde Pública*, 2015, 31: 208-218.
13. MARKEVICIUS, Vytautas, et al. Dynamic vehicle detection via the use of magnetic field sensors. *Sensors*, 2016, 16.1: 78.
14. MARKEVICIUS, Vytautas, et al. Vehicle speed and length estimation using data from two anisotropic magnetoresistive (AMR) sensors. *Sensors*, 2017, 17.8: 1778.
15. TUTUMLUER, Erol, et al. Sensing Infrastructure for Smart Mobility—Wireless Continuous Monitoring for I-ACT. *I-ACT-21-08*, 2022.
16. CAO, Yangsen, et al. Energy output of piezoelectric transducers and pavements under simulated traffic load. *Journal of Cleaner Production*, 2021, 279: 123508.
17. YANG, Hailu, et al. A preliminary study on the highway piezoelectric power supply system. *International Journal of Pavement Research and Technology*, 2018, 11.2: 168-175.
18. ZHANG, Jinrui, et al. A new smart traffic monitoring method using embedded cement-based piezoelectric sensors. *Smart Materials and Structures*, 2015, 24.2: 025023.

19. FINA, I.; MARTÍ, X.; CATALAN, G. Vehicle Classification System Based on Ferroelectric Materials. In: *2019 IEEE International Symposium on Applications of Ferroelectrics (ISAF)*. IEEE, 2019. p. 1-4.
20. LEUNG, Chung S.; HAO, Wei-Da; MONTIEL, Claudio M. Piezoelectric sensors for taxiway airport traffic control system. In: *2013 1st IEEE Conference on Technologies for Sustainability (SusTech)*. IEEE, 2013. p. 134-141.
21. HAUGEN, T., et al. INNOVATIVE USE OF PIEZOELECTRIC SPEED ENFORCEMENT SYSTEM FOR WEIGHT DATA COLLECTION. *ICWIM8*, 2019, 82.
22. GONZÁLEZ, Bernardino; JIMÉNEZ, Francisco J.; DE FRUTOS, José. A virtual instrument for road vehicle classification based on piezoelectric transducers. *Sensors*, 2020, 20.16: 4597.
23. APC International Ltd. 2023. Piezoelectric Charge Constants – American Piezo. [online] [Accessed 29 March 2023]. Available from: <https://www.americanpiezo.com/knowledge-center/piezo-theory/piezoelectric-constants.html>
24. Measurement Specialties. 2001. Properties of Piezo Cable. [online] [Accessed 29 March 2023]. Available from: https://www.metrolog.net/files/piezocable_properties_en_metrolog.pdf?fbclid=IwAR3g4wPNC Lf0S6NeEht6jYVNISvHwyrX-BUx6JJ_xKRGiUsb_-5c-MN9ahI
25. TECS. Bending Flexural Test. [online] [Accessed 13 April 2023]. Available from: <https://www.tec-science.com/material-science/material-testing/bending-flexural-test/>
26. Dr. Layla M. Hasan. Compression Test. [online] [Accessed 13 April 2023]. Available from: https://uomustansiriyah.edu.iq/media/lectures/5/5_2020_12_26!12_51_24_PM.pdf
27. Mascus Lietuva. Komercinis transportas. Gaisrinės ir kitos komunalinės paskirties transporto priemonės. Šiuokšliavežės. [online]. [Accessed 26 April 2023]. Available from: <https://www.mascus.lt/transportas/siuokshliavezes/man-tgs-26-330/lscyguhs.html>
28. Harris Corporation. Integrated Circuits (ICs). Data Acquisition. Analog to Digital Converters (ADC). [online]. [Accessed 26 April 2023]. Available from: <https://www.digikey.com/en/products/detail/rochester-electronics-llc/ICL8068CDD/12118866>
29. E-seimas. Lietuvos Respublikos susisiekimo ministro 2012 m. sausio 31 d. Nr. 3-81 įsakymas “Dėl kelių šviesoforo įrengimo taisyklių patvirtinimo”. [online]. [Accessed 26 April 2023]. Available from: <https://e-seimas.lrs.lt/portal/legalAct/lt/TAD/TAIS.418375>
30. Industrial supply. Lights To Go. Traffic Signal Docking Lights RYG (Red-Yellow-Green) [online]. [Accessed 26 April 2023]. Available from: <https://www.aoindustrialsupply.com/product/ryg-red-yellow-green-traffic-signal-docking-lights/>
31. Elfa distrelec. RV8H-S-D24 - Industrial Relay RV8H 1CO DC 24V 6A Spring Clamp Terminal, IDEC. [online]. [Accessed 28 April 2023]. Available from: https://www.distrelec.lt/lt/industrial-relay-rv8h-1co-dc-24v-6a-spring-clamp-terminal-idec-rv8h-d24/p/30221540?trackQuery=cat-DNAV_PL_05020201&pos=502&origPos=10&page=2&pageSize=50&origPageSize=50&track=true&filterapplied=filter_Coil+Voltage+++DC~~V%3D24
32. Siemens. Electrical products: Automatic cable dimensioning with smart control panel design in the TAI selection tool. [online]. [Accessed 28 April 2023]. Available from: <https://mall.industry.siemens.com/tst/#/Start>
33. Led lighting solutions. Guardian Pro Speed Radar Camera. [Accessed 29 April 2023]. Available from: <https://ledlighting-solutions.com/guardian-pro-speed-radar-camera.html>

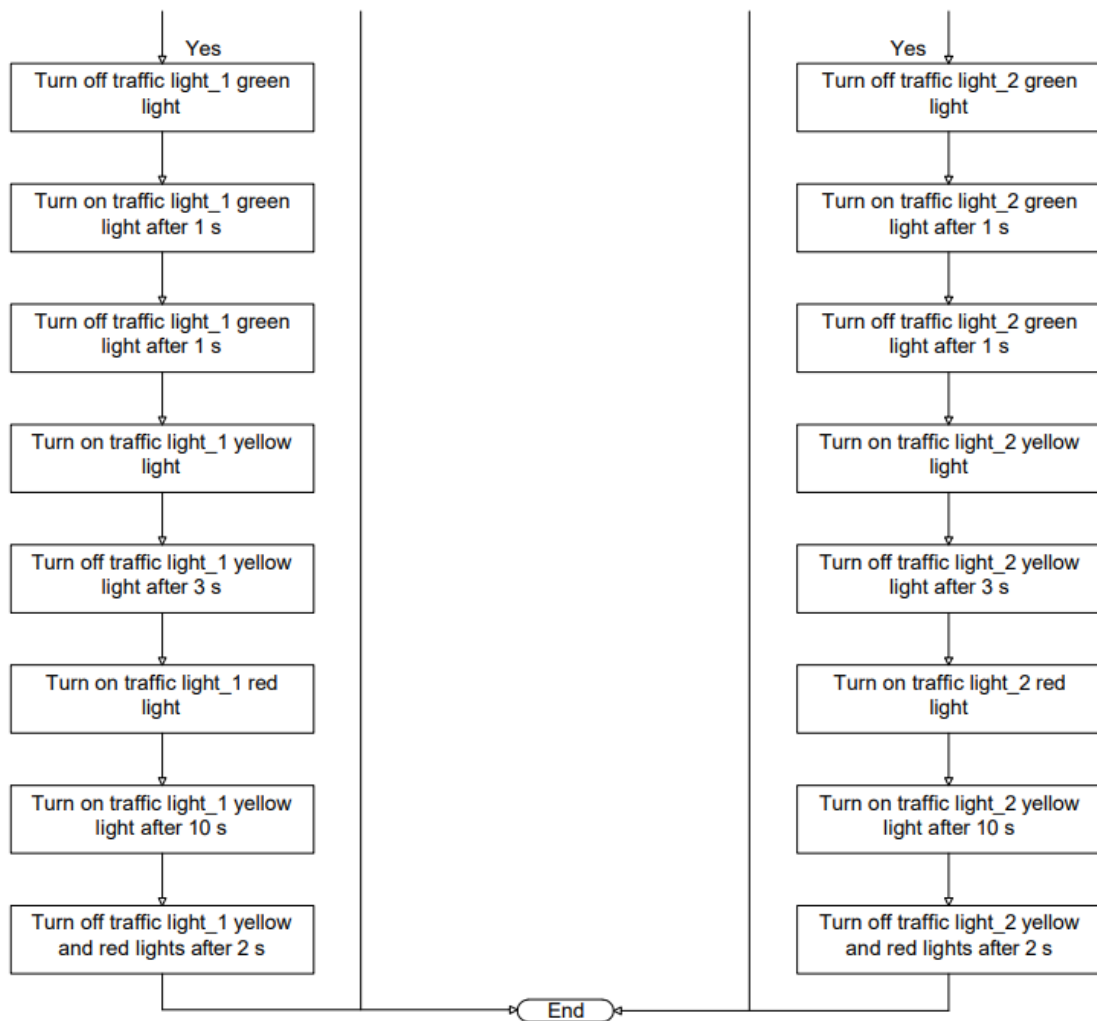
34. Naprys Ernestas. Brangus karas keliuose: jei „inkilas“– kaip butas, kiek kainuos sektoriniai matuokliai? [online]. [Accessed 28 April 2023]. Available from: <https://www.15min.lt/verslas/naujiena/finansai/brangus-karas-keliuose-jei-inkilas-kaip-butas-kek-kainuos-sektoriaus-matuokliai-662-1111326>

Appendices

Appendix 1. Detailed Scheme of the Algorithm



Appendix 2. Detailed Scheme of the Algorithm (continuation)



Appendix 3. C++ code

```
int buttonState = 0;
int buttonState2 = 0;
int buttonState3 = 0;
int buttonState4 = 0;
int button1trig = 0;
int button2trig = 0;
int countRight = 0;
int countLeft = 0;
const int knockSensor = A0;
const int knockSensor2 = A1;
const int knockSensor3 = A3;
const int knockSensor4 = A2;

void setup()
{
  pinMode(knockSensor, OUTPUT);
  pinMode(knockSensor2, OUTPUT);
  pinMode(knockSensor3, OUTPUT);
  pinMode(knockSensor4, OUTPUT);
  pinMode(13, OUTPUT);
  pinMode(12, OUTPUT);
  pinMode(11, OUTPUT);
  pinMode(10, OUTPUT);
  pinMode(9, OUTPUT);
  pinMode(8, OUTPUT);
  digitalWrite(11, HIGH);
  digitalWrite(8, HIGH);
  Serial.begin(9600);
}

void turnRed()
{
  digitalWrite(11, LOW);
  delay(300);
  digitalWrite(11, HIGH);
  delay(1000);
  digitalWrite(11, LOW);
  delay(300);
  digitalWrite(11, HIGH);
  delay(1000);
  digitalWrite(11, LOW);
  digitalWrite(12, HIGH);
  delay(3000);
  digitalWrite(12, LOW);
```

```

digitalWrite(13, HIGH);
delay(10000);
digitalWrite(12, HIGH);
delay(2000);
digitalWrite(11, HIGH);
digitalWrite(12, LOW);
digitalWrite(13, LOW);
}

void turnRed1()
{
  digitalWrite(8, LOW);
  delay(300);
  digitalWrite(8, HIGH);
  delay(1000);
  digitalWrite(8, LOW);
  delay(300);
  digitalWrite(8, HIGH);
  delay(1000);
  digitalWrite(8, LOW);
  digitalWrite(9, HIGH);
  delay(3000);
  digitalWrite(9, LOW);
  digitalWrite(10, HIGH);
  delay(10000);
  digitalWrite(9, HIGH);
  delay(2000);
  digitalWrite(8, HIGH);
  digitalWrite(9, LOW);
  digitalWrite(10, LOW);
}

void loop()
{
  // read the state of the pushbutton value
  buttonState = analogRead(knockSensor);
  buttonState2 = analogRead(knockSensor2);
  buttonState3 = analogRead(knockSensor3);
  buttonState4 = analogRead(knockSensor4);

  if (buttonState > 100) {
    button1trig = 1;
  }
  if (button1trig) {
    Serial.println("counting RIGHT LINE...");

```



```

    countRight++;
}
if (buttonState2 > 100) {
    Serial.println("took time RIGHT LINE");
    Serial.println(countRight);
    button1trig = 0;
    if (countRight <= 20 ) {
        Serial.println("turning RED because of RIGHT LINE!");
        turnRed();
    }
    countRight = 0;
}

if (buttonState3 > 100) {
    button2trig = 1;
}
if (button2trig) {
    Serial.println("counting LEFT LINE...");
    countLeft++;
}
if (buttonState4 > 100) {
    Serial.println("took time LEFT LINE");
    Serial.println(countLeft);
    button2trig = 0;
    if (countLeft <= 20 ) {
        Serial.println("turning RED because of LEFT LINE!");
        turnRed1();
    }
    countLeft = 0;
}

delay(100); // Delay a little bit to improve simulation performance
}

```

Appendix 4. Electronic Scheme from the Tinkercad Environment

